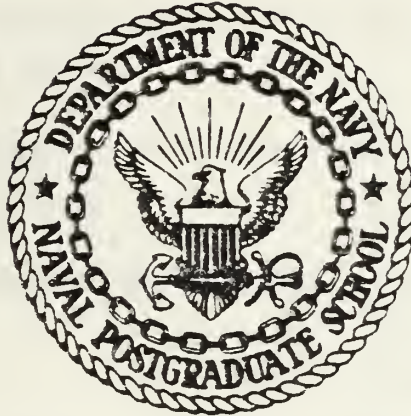


y Knox Library, NPS
rey, CA 93943

NAVAL POSTGRADUATE SCHOOL

Monterey, California



THESIS

AN IMPROVED MODEL FOR A ONCE-THROUGH COUNTER-
CROSS-FLOW WASTE HEAT RECOVERY UNIT

by

Steven L. Wesco

September 1983

Thesis Advisor:

P. F. Pucci

Approved for public release; distribution unlimited.

J210152

REPORT DOCUMENTATION PAGE

READ INSTRUCTIONS
BEFORE COMPLETING FORM

1. REPORT NUMBER	2. GOVT ACCESSION NO.	3. RECIPIENT'S CATALOG NUMBER
4. TITLE (and Subtitle) An Improved Model for a Once-Through Counter-Cross-Flow Waste Heat Recovery Unit		5. TYPE OF REPORT & PERIOD COVERED Master's Thesis; September 1983
7. AUTHOR(s) Steven L. Wesco		6. PERFORMING ORG. REPORT NUMBER
9. PERFORMING ORGANIZATION NAME AND ADDRESS Naval Postgraduate School Monterey, California 93943		8. CONTRACT OR GRANT NUMBER(s)
11. CONTROLLING OFFICE NAME AND ADDRESS Naval Postgraduate School Monterey, California 93943		10. PROGRAM ELEMENT, PROJECT, TASK AREA & WORK UNIT NUMBERS
14. MONITORING AGENCY NAME & ADDRESS (if different from Controlling Office)		12. REPORT DATE September 1983
		13. NUMBER OF PAGES 195
		15. SECURITY CLASS. (of this report)
		15a. DECLASSIFICATION/DOWNGRADING SCHEDULE
16. DISTRIBUTION STATEMENT (of this Report) Approved for public release; distribution unlimited.		
17. DISTRIBUTION STATEMENT (of the abstract entered in Block 20, if different from Report)		
18. SUPPLEMENTARY NOTES		
19. KEY WORDS (Continue on reverse side if necessary and identify by block number) Counter-Cross-Flow Heat Exchanger Waste Heat Recovery Unit (WHRU) RACER System		
20. ABSTRACT (Continue on reverse side if necessary and identify by block number) An improved model for a once-through counter-cross-flow waste heat recovery unit with a segmented fin-tube arrangement was developed. The model was coded in FORTRAN IV computer language for use on an IBM-3033 computer system, and was tested for various conditions of uniform and non-uniform gas flow distributions. Additional parameters varied were heat exchanger size, steam outlet pressure, steam outlet temperature and gas flow		

#20 - ABSTRACT - (CONTINUED)

rate. The effect of each variation on WHRU performance was evaluated and the interrelationship discussed. Results indicate the ideal design is a high steam temperature, low operating pressure, flow distribution controlled heat exchanger.

Approved for public release; distribution unlimited.

An Improved Model for a Once-Through Counter-
Cross-Flow Waste Heat Recovery Unit

by

Steven L. Wesco
Lieutenant Commander, United States Navy
B.S. in Applied Science, Miami University, 1973

Submitted in partial fulfillment of the
requirements for the degree of

MASTER OF SCIENCE IN MECHANICAL ENGINEERING

from the

NAVAL POSTGRADUATE SCHOOL

September 1983

W474

c.1

ABSTRACT

An improved model for a once-through counter-cross-flow waste heat recovery unit with a segmented fin-tube arrangement was developed. The model was coded in FORTRAN IV computer language for use on an IBM-3033 computer system, and was tested for various conditions of uniform and non-uniform gas glow distributions. Additional parameters varied were heat exchanger size, steam outlet pressure, steam outlet temperature and gas flow rate. The effect of each variation on WHRU performance was evaluated and the interrelationship discussed. Results indicate the ideal design is a high steam temperature, low operating pressure, flow distribution controlled heat exchanger.

TABLE OF CONTENTS

I.	INTRODUCTION -----	15
	A. BACKGROUND -----	15
	B. OBJECTIVES -----	17
II.	MODEL DESCRIPTION -----	19
	A. OVERVIEW -----	19
	B. INITIAL CALCULATIONS -----	24
	C. GEOMETRY -----	26
	D. SUPERHEATER NODAL ANALYSIS -----	29
	E. BOILING NODAL ANALYSIS -----	37
	F. HEATING NODAL ANALYSIS -----	44
	G. HEAT EXCHANGER SOLUTION PROCEDURE -----	46
III.	DISCUSSION OF RESULTS -----	49
	A. INITIAL TESTING -----	49
	B. EFFECT OF NON-UNIFORM DISTRIBUTIONS -----	52
	C. EFFECT OF HEAT EXCHANGER SIZE -----	55
	D. EFFECT OF STEAM OUTLET TEMPERATURE -----	57
	E. EFFECT OF HEAT EXCHANGER PRESSURE -----	58
	F. EFFECT OF GAS FLOW RATE ON HEAT EXCHANGER PERFORMANCE -----	60
	G. EFFECT OF NON-UNIFORM MASS DISTRIBUTION ON EXHAUST GAS TEMPERATURE -----	62
IV.	CONCLUSIONS -----	64
V.	RECOMMENDATIONS FOR FURTHER RESEARCH -----	66
	A. WHRU MODEL IMPROVEMENT AND EXPANSION -----	66

1. Fluid-Side Pressure Drop -----	67
2. Additional Geometries -----	67
3. Fouling -----	67
4. Alternate Working Fluids -----	67
5. Non-Uniform Temperature Distributions ---	68
APPENDIX A -----	121
LIST OF REFERENCES -----	194
INITIAL DISTRIBUTION LIST -----	195

LIST OF TABLES

I.	Normalized Flow Distribution -----	69
II-A.	Gas Flow Distributions ($\dot{m}_g = 121.8 \text{ lbm/s}$) -----	70
II-B.	Gas Flow Distributions ($\dot{m}_g = 99.1 \text{ lbm/s}$) -----	70
II-C.	Gas Flow Distributions ($\dot{m}_g = 77.4 \text{ lbm/s}$) -----	71
II-D.	Gas Flow Distributions ($\dot{m}_g = 66.7 \text{ lbm/s}$) -----	71
III.	Isentropic Power for Various Gas Flow Distributions, Gas Flow Rates and Steam Outlet Temperatures -----	72
IV.	Fluid Mass Flow Rate for Various Gas Flow Rates, Gas Flow Distributions and Steam Outlet Temperatures -----	73
V.	Power and Fluid Flow Rate for Various Size Heat Exchangers -----	74
VI.	Power and Fluid Flow Rate for Various Steam Operating Pressures -----	75

LIST OF FIGURES

1.	Waste Heat Recovery Unit Layout -----	76
2.	Heat Exchanger Nodal Arrangement -----	77
3.	Typical Nodal Gas and Fluid Flow -----	78
4.	Nodal Gas and Fluid Flow for End of Pass Condition -----	79
5.	Tube Fin Configuration -----	80
6.	Waste Heat Recovery Unit Tube Layout -----	80
7.	h_{TPf}/h_ℓ vs. Quality -----	81
8-A.	Uniform Flow Distribution -----	82
8-B.	Flow Distribution #1 -----	83
8-C.	Flow Distribution #2 -----	84
8-D.	Flow Distribution #3 -----	85
8-E.	Flow Distribution #4 -----	86
8-F.	Flow Distribution #5 -----	87
8-G.	Flow Distribution #6 -----	88
8-H.	Flow Distribution #7 -----	89
8-I.	Flow Distribution #8 -----	90
9-A.	Power vs. Gas Flow Rate (Distr.'s U, 1, 2) -----	91
9-B.	Power vs. Gas Flow Rate (Distr.'s U, 3, 4) -----	92
9-C.	Power vs. Gas Flow Rate (Distr.'s U, 5, 6) -----	93
9-D.	Power vs. Gas Flow Rate (Distr.'s U, 7, 8) -----	94
9-E.	Power vs. Gas Flow Rate (Composite) -----	95
10-A.	Fluid Flow Rate vs. Gas Flow Rate (Distr.'s U, 1, 2) -----	96

10-B.	Fluid Flow Rate vs. Gas Flow Rate (Distr.'s U, 3, 4) -----	97
10-C.	Fluid Flow Rate vs. Gas Flow Rate (Distr.'s U, 5, 6) -----	98
10-D.	Fluid Flow Rate vs. Gas Flow Rate (Distr.'s U, 7, 8) -----	99
10-E.	Fluid Flow Rate vs. Gas Flow Rate (Composite) --	100
11-A.	Power vs. No. of Heat Exchanger Passes ($\dot{m}_g = 121.8$ lbm/s) -----	101
11-B.	Power vs. No. of Heat Exchanger Passes ($\dot{m}_g = 99.1$ lbm/s) -----	102
11-C.	Power vs. No. of Heat Exchanger Passes ($\dot{m}_g = 77.4$ lbm/s) -----	103
11-D.	Power vs. No. of Heat Exchanger Passes ($\dot{m}_g = 66.7$ lbm/s) -----	104
11-E.	Fluid Flow Rate vs. No. of Heat Exchanger Passes ($\dot{m}_g = 121.8$ lbm/s) -----	105
11-F.	Fluid Flow Rate vs. No. of Heat Exchanger Passes ($\dot{m}_g = 99.1$ lbm/s) -----	106
11-G.	Fluid Flow Rate vs. No. of Heat Exchanger Passes ($\dot{m}_g = 77.4$ lbm/s) -----	107
11-H.	Fluid Flow Rate vs. No. of Heat Exchanger Passes ($\dot{m}_g = 66.7$ lbm/s) -----	108
12-A.	Power vs. Steam Outlet Temperature -----	109
12-B.	Fluid Mass Flow Rate vs. Steam Outlet Temperature -----	110
13-A.	Power vs. Heat Exchanger Operating Pressure ----	111
13-B.	Fluid Mass Flow Rate vs. Heat Exchanger Operating Pressure -----	112
14-A.	Fluid Temperature vs. Tube Length ($\dot{m}_g = 121.8$ lbm/s) -----	113
14-B.	Fluid Temperature vs. Tube Length ($\dot{m}_g = 99.1$ lbm/s) -----	114

14-C.	Fluid Temperature vs. Tube Length ($\dot{m}_g = 77.4 \text{ lbm/s}$) -----	115
14-D.	Fluid Temperature vs. Tube Length ($\dot{m}_g = 66.7 \text{ lbm/s}$) -----	116
14-E.	Fluid Temperature vs. Tube Length (Distr. 1, $\dot{m}_g = 121.8 \text{ lbm/s}$) -----	117
14-F.	Fluid Temperature vs. Tube Length (Distr.'s U, 1; $\dot{m}_g = 121.8 \text{ lbm/s}$) -----	118
15-A.	Gas Temperature Distribution (Uniform, $\dot{m}_g = 121.8 \text{ lbm/s}$) -----	119
15-B.	Gas Temperature Distribution (Distr. 1, $\dot{m}_g = 121.8 \text{ lbm/s}$) -----	120

NOMENCLATURE

English Letter Symbols

A	-	Area (ft^2)
A _b	-	Frontal Area Blocked by Tubes and Fins (ft^2)
A _{bt}	-	Bare Tube Area (ft^2)
A _f	-	Heat Exchanger Frontal Area (ft^2)
A _{fin}	-	Fin Area (ft^2)
A _{ff}	-	Cross Sectional Area for Fluid Flow (ft^2)
A _{ip}	-	Inside Heat Transfer Area Per Node (ft^2)
A _{min}	-	Minimum Cross Sectional Area for Gas Flow (ft^2)
A _{op}	-	Outside Heat Transfer Area Per Node (ft^2)
A _{ti}	-	Total Heat Exchanger Inside Area (ft^2)
A _{to}	-	Total Heat Exchanger Outside Area (ft^2)
C	-	Constant
C _{max}	-	Maximum Heat Capacity (BTU/hr-F)
C _{min}	-	Minimum Heat Capacity (BTU/hr-F)
C _f	-	Heat Capacity of Water/Steam (BTU/hr-F)
C _g	-	Heat Capacity of Gas (BTU/hr-F)
C _{pf}	-	Specific Heat of Water/Steam (BTU/lbm-F)
C _{pg}	-	Specific Heat of Gas (BTU/lbm-F)
d _f	-	Fin Outside Diameter (ft)
d _{fb}	-	Diameter of Fin Base (ft)
d _i	-	Inside Tube Diameter (ft)
d _o	-	Outside Tube Diameter (ft)

d_r	- Fin Root Diameter (ft)
G	- Flow Rate Per Unit Area (lbm/hr-ft ²)
h	- Fluid Enthalpy (BTU/lbm)
h_f	- Fluid-Side Heat Transfer Coefficient (BTU/hr-ft ² -F)
h_g	- Gas-Side Heat Transfer Coefficient (BTU/hr-ft ² -F)
h_{fg}	- Enthalpy Increment for Boiling (BTU/lbm)
h_ℓ	- Fluid-Side Heat Transfer Coefficient for Totally Liquid Flow (BTU/hr-ft ² -F)
h_{TPf}	- Heat Exchanger Inside Heat Transfer Coefficient in the Two-Phase Region (BTU/hr-ft ² -F)
j	- Heat Transfer Colburn j-factor
K_g	- Thermal Conductivity of Gas (BTU/hr-ft-F)
K_ℓ	- Thermal Conductivity of Steam/Water (BTU/hr-ft-F)
K_w	- Thermal Conductivity of Heat Exchanger Tube Wall (BTU/hr-ft-F)
ℓ	- Fin Height (ft)
ℓ_c	- Length of Cut from Fin Tip (ft)
L	- Tube Length Per Node (ft)
m	- Number of Heat Exchanger Passes
\dot{m}_f	- Steam/Water Mass Flow Rate (lbm/hr)
\dot{m}_g	- Gas Mass Flow Rate (lbm/hr)
n	- Number of Heat Exchanger Gas Paths
NTU	- Number of Transfer Units
N_f	- Number of Fins Per Inch
N_s	- Number of Segments in One Fin
$N_{t/r}$	- Number of Tubes Per Row
P	- Heat Exchanger Operating Pressure (psia)
Q	- Heat Transfer Rate (BTU/hr)

q''	- Heat Flux (BTU/hr-ft ²)
R_{th}	- Thermal Resistance (hr-ft ² -F/BTU)
R_o	- Heat Exchanger Outside Resistance (hr-ft ² -F/BTU)
S_n	- Tube Spacing Normal to Gas Flow (ft)
S_p	- Tube Spacing Parallel to Gas Flow (ft)
T_f	- Fluid Temperature (F)
T_g	- Gas Temperature (F)
T_{fB}	- Fluid Bulk Temperature (F)
T_{gB}	- Gas Bulk Temperature (F)
T_{gf}	- Gas-Side Film Temperature (F)
T_{wo}	- Average Outside Wall Temperature (F)
U_{oi}	- Overall Heat Transfer Coefficient (BTU/hr-ft ² -F)
w_s	- Fin Segment Width (ft)
x	- Steam Quality
x	- Average Steam Quality Per Node

Dimensionless Groups

Nu	- Nusselt Number
Pr	- Prandtl Number
Re	- Reynolds Number
St	- Stanton Number

Greek Letter Symbols

ϵ	- Effectiveness
μ_l	- Viscosity of Fluid (lbm/ft-hr)
μ_v	- Viscosity of Vapor (lbm/ft-hr)
η_f	- Fin Efficiency

- ρ - Density (lbm/ft)
- ρ_{ℓ} - Density of Saturated Water (lbm/ft)
- ρ_v - Density of Saturated Vapor (lbm/ft)

I. INTRODUCTION

A. BACKGROUND

Since the introduction of the DD-963 class ships into the fleet, the U.S. Navy has become firmly committed to gas turbine propulsion plants. Currently, besides the DD-963 class, there are four additional ship classes which are, or will be, gas turbine powered. These are the Patrol Hydrofoil Missile (PHM's), the Oliver Hazard Perry FFG-7 class, the Ticonderoga CG-47 class and the soon to be built DDG-51 class.

This commitment to gas turbine propulsion has stimulated great interest in the concept of converting the waste heat from the gas turbine engines into useful shaft power. In December 1979 the Naval Sea Systems Command awarded contracts for development of a conceptual design of a new generation of waste heat recovery systems. The goal of the design was to provide a system which would realize a 25 percent minimum improvement in ship propulsion fuel consumption and increase the ship's operating range by 1000 nautical miles. The outgrowth of the effort has been the RAnkine Cycle Energy Recovery (RACER) system. As conceived, the RACER system will be an unfired waste heat recovery system designed to convert waste heat from the exhaust of the main propulsion gas turbine engines into useful shaft horsepower. Such a system has

commonly been called a COGAS or Combined Gas And Steam system. The hot exhaust gases of the main propulsion turbine are passed through a Waste Heat Recovery Unit (WHRU), where steam of the desired temperature and pressure is generated. The steam is used to drive a steam turbine which operates in parallel with the propulsion gas turbine through a common reduction gear.

Numerous papers have been written concerning the RACER system. Halkola, Cambell and Jung [Ref. 1] discussed the conceptual design for the system. Mattson [Ref. 2] presented a plan for designing reliability and maintainability into the RACER system and Combs [Ref. 3] developed a computer model of a COGAS system which designs a waste heat recovery unit and allows comparison of system performance by variation of system parameters.

References 1, 2 and 3 all agree that the desired goal of fuel conservation must not come as a result of increased maintenance, manpower, or main propulsion system down-time. The design philosophy dictates that the system have high reliability, be inherently safe, have low maintenance requirements and be essentially automatic in operation.

Reference 1 states that the waste heat recovery unit paces the design of the system. The majority of effort by Combs [Ref. 3] was to create a WHRU design model which would simulate the performance characteristics of a physical boiler. Since great expense is involved in the design, fabrication

and operation of prototype systems, it is of primary importance to achieve a realistic mathematical simulation first. To this end, Combs devised a model which designs a WHRU when given feedwater inlet temperature, steam outlet temperature, operating pressure, inlet and outlet gas conditions and gas flow rate.

In this study, the initial model of Combs was considered and an improved computer model of the waste heat recovery unit was developed. A once-through counter-cross-flow heat exchanger was selected because of the advantages of lower initial cost, faster response, compactness and low operating cost. The improvement in the model is that the heat exchanger is discretized into individual "nodes" much in the manner done by Shu and Kuo [Ref. 4]. This procedure treats smaller physical pieces of the overall heat exchanger as individual small heat exchangers to attain a better understanding of the temperature distributions within the WHRU. The improved model allows an analysis of the effect of non-uniform velocity distributions on the performance of the WHRU, and ultimately, the RACER system.

B. OBJECTIVES

There were five main objectives for this thesis.

1. Devise an improved computer model for the once-through WHRU. This model was to predict the performance of various size WHRU's given feedwater inlet temperature, steam outlet

temperature, WHRU operating pressure, inlet gas mass flow distribution and inlet gas temperature distribution.

2. Enable the designer to establish a design WHRU size based on the performance of the model with various input conditions.

3. Evaluate the design WHRU utilizing various uniform and non-uniform inlet gas distributions for both on-design and off-design conditions.

4. Re-evaluate the WHRU utilizing the same uniform and non-uniform gas distributions into the WHRU, but with different steam outlet temperatures.

5. Provide a framework for future studies involving a development of a three dimensional model of a WHRU and a detailed, complete COGAS system cycle analysis and optimization.

di
n

II. MODEL DESCRIPTION

A. OVERVIEW

The waste heat recovery unit chosen was a once-through counter-cross-flow heat exchanger. A computer program was written to model this type heat exchanger for analysis of the effect of uniform and non-uniform inlet gas mass distributions. Variation of other parameters, other than the gas distribution, provides a thorough understanding of the operation of the heat exchanger in a multitude of conditions. The model was written for incorporation into a RACER system analysis, but it is not limited to that application.

Figure 1 shows a three dimensional representation of a typical layout of a marine gas turbine waste heat recovery unit. The unit is headered on the fluid inlet and exit and designed to be installed in the gas turbine exhaust gas duct. The exhaust gas entering the bottom of the WHRU provides the energy for transfer to the fluid-side of the system. The fluid (feedwater) enters at the upper header of the WHRU and flows alternately back and forth through the unit until exiting as steam at the lower header. The U-bends shown in Figure 1 at the ends of the tube passes allow each tube to enter and exit the heat exchanger as a continuous path for fluid flow. As a tube makes one horizontal traverse across the WHRU it is referred to as a pass. Therefore, the number

of times a tube passes through the gas flow defines the vertical size of the heat exchanger as a 15, 20, 25, etc., pass heat exchanger.

A gas flow distribution is depicted as entering the WHRU in Figure 1. The gas flow is shown oriented along the tube pass as a non-uniform distribution. Additionally, the gas flow may be non-uniform in the direction into the heat exchanger, i.e., along the axis of the headers as shown in Figure 1. This two dimensional gas flow distribution may be non-uniform in both mass and temperature. The nature of the heat exchanger, by virtue of the cross flow of the fluid, decrees that, even if the mass and temperature distributions entering the heat exchanger were uniform in both directions, these distributions can become distorted and non-uniform as the gas passes through the heat exchanger in the third dimension. This distortion can be caused by the variation of the heat transfer characteristics along the tube. The problem of analysis becomes more complicated if cross mixing of the gas is considered.

The model of Combs [Ref. 3] treated the gas distribution as a uniform and constant value in one direction. Combs assumed the mass and temperature of the gas along the axis of the tube was everywhere the same for a complete pass. The model yielded results which were close to the results attained by other studies and gave a reasonable estimate of the overall heat transfer characteristics of the heat

exchanger. The model, however, could not predict the effect of non-uniformity of the gas distribution on the performance of the WHRU. This study discretizes the dimension along the axis of the tube pass and enables the designer to evaluate the effects of variations in mass flow rate and temperature. It is assumed, however, that the distributions along the axis of the headers are all the same as the outer distribution. The concept of discretization and "nodal" arrangement is shown in Figure 2. The representation shows a matrix arrangement where the number of rows corresponds to the number of passes in the heat exchanger, and the number of columns corresponds to the number of gas paths in the discretization. The number of passes is a user defined input to the model but the number of gas paths is fixed in the model at ten.

Use of the model requires that the user provide the following conditions. First, the number of passes that a particular water/steam tube is to make through the heat exchanger must be specified. This parameter will physically size the heat exchanger in the vertical direction. The mass flow rate of the gas turbine exhaust gas, (\dot{m}_g) , for each of ten exhaust gas paths through the heat exchanger must be entered. For a uniform distribution, this is simply the total exhaust gas mass flow divided by ten. A simplifying assumption of the model is that there is no cross mixing of flow as the gas passes through the heat exchanger; therefore,

the mass entering a particular gas path is constant through the heat exchanger.

Next, the temperature of the gas entering each gas path is entered. For this study the temperature distribution of the gas was considered uniform for all runs; however, the model is not constrained to uniform temperature distributions.

The gas was assumed to be at atmospheric pressure entering the heat exchanger and gas side pressure drops were not considered in the calculations.

The user next enters the feedwater inlet temperature, the steam outlet temperature and the fluid-side operating pressure. These parameters are used in the initial calculations to determine a first "guess" mass flow rate on the fluid-side of the heat exchanger. The minimum allowed exhaust gas temperature is entered. This value is a user desired constraint and is specified as the minimum acceptable temperature the user can accept to prohibit hot side corrosion. The model is not constrained to maintain the exhaust gas temperature above the user specified temperature.

The number of feet in length, per node, is entered. This parameter is based on the physical size of the heat exchanger being analyzed in the horizontal direction. For all runs in this study, an assumed tube row length of ten feet divided by ten gas paths yielded a tube length per node of one foot. There is no constraint on the length parameter, within reasonable limits.

The heat exchanger model was written as a two dimensional analysis, i.e., all parameters in the third dimension were assumed uniform. The next parameter entered is the number of tubes per row, which is used to size the heat exchanger in the third dimension. Figure 1 shows a three dimensional representation of the heat exchanger design. Each particular tube enters at the top of the heat exchanger and passes alternately back and forth below itself until exiting the heat exchanger at the bottom. The tubes in each subsequent plane, behind the first, enter and exit in the same manner, but alternate slightly up and down to give a staggered tube arrangement. The nodes are numbered in standard matrix format with the upper left being node (1,1), and counting across row one as (1,2), (1,3), etc., to (1,10); then node (2,1) is directly below node (1,1), and so on, to the bottom of the matrix. Figure 2 shows the nodal arrangement of the heat exchanger. The fluid may enter from either side of the heat exchanger. If the heat exchanger has an even number of passes, the fluid will enter on the same side as the steam exit, and on the opposite side for an odd number of passes. Each tube is continuous from entry to exit.

The final user entry is the geometric scaling factor which is used in the geometry portion of the model to scale all the physical dimensions of the tube, with the exception of the length, up or down.

Two additional simplifications were assumed in the model. First, the fluid side pressure drop was not considered. Lastly, even though the tube passes were discretized to determine the temperature distributions, the tube length within a node still has a significant length for a temperature gradient. For analysis, the gas temperature at any node was assumed to be uniform across the length of the node at both the entry and exit.

B. INITIAL CALCULATIONS

The WHRU is essentially analyzed in three sections; superheating, boiling and heating. Given an inlet gas distribution, water/steam inlet and outlet temperatures, and an operating pressure, there is a unique fluid-side mass flow rate which will satisfy all boundary conditions. The model attempts, through iteration, to determine the resultant fluid-side mass flow rate. The analysis is also greatly affected by the number of passes (i.e., the physical size) of the heat exchanger. There are clearly combinations of parameters for which no solution is possible, or the solution is trivial in that the mass flow rate of the fluid is so small as to be meaningless.

For calculations, variable assignment is as follows:

- (1) $\dot{m}_g(m,n)$ = gas flow rate through gas path n at tube pass m ;
- (2) $T_g(m,n)$ = gas temperature into node (m,n) . The gas temperature out of node (m,n) will be the gas temperature into node $(m-1,n)$;

(3) $T_f(m,n)$ = fluid temperature into node (m,n). The fluid temperature out node (m,n) will equal the fluid temperature into node (m,n+1) if the fluid is flowing to the right (see Fig. 3), or the fluid temperature out of node (m,n) will equal the fluid inlet temperature of node (m,n-1) if the fluid is flowing to the left.
 At the end of a fluid pass the fluid out of a node will equal the fluid temperature into the node directly below, i.e., $T_f(m,n) = T_f(m+1,n)$;

(4) \dot{m}_f = fluid-side mass flow rate

Figures 3 and 4 are representations of typical nodes depicting the above explanation of fluid and gas flow.

After all entries are made the program initializes by summing the individual $\dot{m}_g(NR,n)$ elements to find $\dot{m}_{g \text{ total}}$, then the $T_g(NR,n)$ elements are averaged. The $T_g(NR,n)$ elements are averaged by multiplying each element by the corresponding fraction of the total gas mass that is passing through each gas path. These "weighted" temperatures are summed and the result is divided by the number of gas paths. The result is then the average temperature of the gas into the heat exchanger. An average gas temperature is determined using the user specified minimum gas temperature out and the average gas temperature into the heat exchanger. Then:

$$Q = \dot{m}_{g \text{ total}} C_{pg} (T_{g \text{ avg in}} - T_{g \text{ avg out}})$$

where C_{pg} is evaluated at the heat exchanger gas bulk temperature. Now, a first "guess" fluid mass flow rate is calculated from an energy balance

$$\dot{m}_f = \frac{Q}{h_{f \text{ out}} - h_{f \text{ in}}}$$

where $h_{f \text{ in}}$ and $h_{f \text{ out}}$ are the fluid inlet and outlet enthalpies at the user specified feedwater inlet temperature and steam outlet temperature.

C. GEOMETRY

The geometry portion of the model is nearly identical to that used by Combs [Ref. 3]. A fin-tube with helically curved extended surfaces on circular tubes is assumed for this model. The fins are segmented and the tubes are configured in banks of one row each with the rows staggered. The base tube surface is taken from Weirman, Taborek and Marner [Ref. 5]. The description of the finned tubes is as follows:

d_i	= tube inside diameter	= 1.86 in.
d_o	= tube outside diameter	= 2.00 in.
d_r	= fin root diameter	= 2.00 in.
N_f	= fins per inch	= 5.94
ℓ	= fin height	= 1.015 in.
ℓ_c	= length of cut from fin tip	= 0.82 in.
d_f	= fin outside diameter	= 4.03 in.
t_f	= fin thickness	= 0.048 in.
w_s	= fin segment width	= 0.17 in.
N_s	= number of segments in 360 degrees	= 38

The finned tube configuration is shown in Figure 5. The tube length, L , and the number of tubes per row, $N_{t/r}$, are the user specified entries. The tube layout is shown in Figure 6. The center to center tube spacing in the transverse direction is 4.50 inches. The equilateral, staggered tube arrangement used in this model leads to a spacing normal to the gas flow, s_n , of 4.50 inches and a spacing parallel to the gas flow, s_p , of 3.90 inches, as shown in Figure 6. The heat exchanger height is established by the number of WHRU passes (rows) and the tube spacing parallel to the gas flow, s_p .

In order to establish the minimum gas flow cross-sectional area the total "blocked" frontal area, A_b , of the heat exchanger must be calculated from

$$A_b = N_{t/r} L d_o + L N_f N_{t/r} 2 t_f ,$$

and the minimum gas flow area is

$$A_{min} = A_f - A_b$$

where A_f is the total frontal area of the heat exchanger exposed to gas flow. The total inside area available for heat transfer per pass is

$$A_{ip} = \pi d_i L N_{t/r} .$$

The gas-side surface area available per pass for heat transfer is the sum of the fin surface area and the bare tube surface area per pass. The fin surface area per tube is calculated from

$$A_{fin} = N_f L [N_s (2 \ell_c w_s + 2 t_f \ell_c + w_s t_f) + \frac{\pi}{2} (d_{fb}^2 - d_o^2)]$$

where $d_{fb} = d_f - 2\ell_c$. The bare tube area per tube is

$$A_{bt} = \pi d_o L - \pi d_o t_f N_f L.$$

Therefore, the total outside area per pass available for heat transfer is

$$A_{op} = N_{t/p} (A_{fin} + A_{bt}).$$

The cross sectional area for fluid flow is calculated from

$$A_{ff} = \frac{\pi}{4} d_i^2 N_{t/p}.$$

With the mass flow rates, terminal temperatures and heat exchanger geometry established, the remainder of the model may be solved by nodal analysis for the unique fluid mass flow rate and the location of the beginning of the boiling and superheating regimes.

D. SUPERHEATER NODAL ANALYSIS

In the heat exchanger there is only one node where two conditions are initially known, and that is at the node where the steam is exiting. At this node, both the gas inlet mass flow rate and temperature and the fluid outlet temperature have been specified by the user. Using the initial values of the fluid mass flow rate from the estimated overall energy balance and the desired superheater steam outlet temperature, the heat exchanger is analyzed in the reverse direction through the superheater, through the boiler and through the heater to arrive at the feedwater inlet. For the given geometry and flow conditions, the model will calculate the water inlet temperature consistent with the assumed estimated mass flow rate. If the temperature arrived at by analysis as the inlet to the first node does not match the user specified feedwater inlet temperature, then the fluid-side mass flow rate is adjusted up or down and the entire process is begun again.

To begin, at the final node the gas inlet temperature and mass flow rate are known. Also, the fluid outlet temperature and a first "guess" fluid mass flow rate are known. It is then assumed that the bulk (average) fluid and gas temperatures for the node are equal to these known temperatures. All fluid and gas properties for a node are evaluated at the bulk temperatures.

The gas-side Reynolds number for the node is calculated using the bulk temperature. With the Reynolds number, a

j-factor is obtained from a polynomial fit to the data for tube layout number 5 in Ref. 5 (Fig. 6). By definition, the j-factor is related to the heat transfer coefficient, h_g , by

$$j = S_t \text{Pr}^{2/3} .$$

By introducing

$$St = \frac{Nu}{Re \text{Pr}} ,$$

the previous expression can be written as

$$j = \frac{Nu}{Re_g \text{Pr}_g} \text{Pr}^{2/3} = \frac{Nu}{Re_g \text{Pr}_g^{1/3}} ,$$

and

$$Nu = j Re_g \text{Pr}_g^{1/3}$$

where

$$Nu = \frac{h_g d_o}{K_g}$$

and K_g = the thermal conductivity of the gas. Therefore, a relationship may be written for the heat transfer coefficient as follows:

$$h_g = j \frac{K_g}{d_o} Re_g Pr_g^{1/3} .$$

In the superheat region, the water-side heat transfer coefficient is calculated by using the Dittus-Boelter correlation

$$h_f = 0.023 \frac{K_f}{d_i} Re_f^{0.8} Pr_f^{0.4}$$

where all properties are obtained at the bulk temperature of the steam in the node. Using the tube wall resistance together with h_g and h_f , the overall heat transfer coefficient for the node can be written as

$$U_{oi}(m,n) = \frac{1}{\frac{1}{h_f} + \frac{A_{ip} \ln(d_o/d_i)}{2\pi K_w N_{t/p} L} + \frac{A_{ip}}{A_{op}} \frac{1}{\eta_t h_g}}$$

where:

$$\eta_t = 1 - (1 - \eta_f) \frac{A_{fin}}{A_{op}} .$$

The fin efficiency, η_f , is calculated from the expression

$$\eta_f = \frac{\tanh ML}{ML}$$

where

$$M = \sqrt{h_g P/KA}$$

and, if the fin is approximated by a set of rectangular strips extending from the tube wall,

$$L = \frac{d_f - d_o}{2} .$$

Now, the cross-sectional area, A , of a rectangular strip may be written as

$$A = w_s t_f$$

and the perimeter is

$$P = 2(w_s + t_f) .$$

So, using known geometric parameters and the thermal conductivity of the fin metal, the parameter ML may be expressed as

$$ML = C \sqrt{h_g}$$

where

$$C = \left(\frac{d_f - d_o}{2} \right) \sqrt{\frac{2(w_s + t_f)}{w_s t_f K}}$$

Now,

$$\eta_t = \left[1 - \left(1 - \frac{\tanh C\sqrt{h_g}}{C\sqrt{h_g}} \right) \frac{A_{fin}}{A_{op}} \right] .$$

The pass effectiveness is calculated using the effectiveness-NTU method. The correlation for the effectiveness for a single pass, cross flow heat exchanger with both fluids unmixed is taken from Incropera and DeWitt [Ref. 6]

$$\epsilon_p = 1 - \exp\left[\left(\frac{1}{C_r}\right) (NTU)^{0.22} \{\exp[-C_r (NTU)^{0.78}] - 1\}\right]$$

where:

$$C_r = \frac{C_{\min}}{C_{\max}}$$

$$NTU = \frac{U_{oi(m,n)} A_{ip}}{C_{\min}} .$$

C_{\min} is the lesser of C_f and C_g where

$$C_f = C_{pf} \dot{m}_f$$

and

$$C_g = C_{pg} \dot{m}_g(m,n)$$

and C_{\max} is the greater of the two. All fluid and gas properties are again evaluated at the bulk temperature.

Two equations must be satisfied to find the solution to a node. These are the rate equation

$$Q = \epsilon C_{\min} (T_{gin} - T_{fin})$$

and the energy equation

$$Q = \dot{m}_f C_{pf} (T_{f \text{ out}} - T_{f \text{ in}}) .$$

In the two equations the only unknown is $T_{f \text{ in}}$. Equating the two and solving for $T_{f \text{ in}}$ yields

$$T_{f \text{ in}} = \frac{\epsilon C_{\min} T_{g \text{ in}} - \dot{m}_f C_{pf} T_{f \text{ out}}}{\epsilon C_{\min} - \dot{m}_f C_{pf}} .$$

Now, Q for the node is

$$Q = \dot{m}_f C_{pf} (T_{f \text{ out}} - T_{f \text{ in}})$$

and

$$T_{g \text{ out}} = T_{g \text{ in}} - \frac{Q}{\dot{m}_g C_{pg}} .$$

Next, new bulk temperatures for the node are calculated as

$$T_{g \text{ bulk}} = (T_{g \text{ in}} + T_{g \text{ out}}) / 2$$

and

$$T_{f \text{ bulk}} = (T_{f \text{ out}} + T_{f \text{ in}}) / 2 .$$

An average outside tube wall temperature is calculated from

$$T_{wo} = T_{g \text{ bulk}} - \frac{U_{oi} A_{ti}}{h_g A_{to}} (T_{gB} - T_{fB})$$

where A_{ti}/A_{to} are total inside/outside areas for the node and T_{gB}/T_{fB} are the new node bulk temperatures. The expression for T_{wo} is derived from the following formulation for heat transfer in the node

$$Q = \frac{T_{gB} - T_{fB}}{\sum R_{th}} = \frac{T_{gB} - T_{wo}}{R_o}$$

which reduces to

$$T_{wo} = T_{gB} - \frac{R_o}{\sum R_{th}} (T_{gB} - T_{fB})$$

where

$$R_o = \frac{1}{\eta_t h_g A_{to}}$$

and

$$\sum R_{th} = \frac{1}{U_{oi} A_{ti}} .$$

The gas-side film temperature is

$$T_{gf} = \frac{T_{gB} + T_{wo}}{2} .$$

This gas-side film temperature is now introduced at the beginning of the calculations for the node as the new gas bulk temperature.

The assumed bulk temperatures, at the beginning of the calculations, were obviously too high since the gas inlet and fluid outlet temperatures were used. This assumption, however, allowed a solution for the node to be found. The model stores the result of this first pass and returns to the beginning utilizing the new bulk temperatures to calculate a new solution to the node. At the end of the second pass through, the result of the calculation for $T_{g\ out}$ is compared to the result obtained the first time. If $T_{g\ out}$ has changed, then the new result is stored and the process is repeated. When $T_{g\ out}$ no longer changes, the process has converged to a good solution for the node.

A check is made to determine if the fluid inlet temperature is less than or equal to the saturation temperature for the pressure specified. If the temperature is higher than the saturation temperature, the model proceeds to the next node of the superheater and repeats the entire process.

If the fluid temperature equals the saturation temperature, superheating has theoretically begun at the interface between this and the final node of the boiling portion of the model. If this condition exists, the model proceeds to the boiling nodal analysis.

As mentioned previously, the model works through the heat exchanger in the direction opposite to fluid flow. When it is determined that the fluid temperature into a node is below the saturation temperature, the node is "split" to determine the physical location in the node where superheating begins.

To split the node the \dot{m}_g quantity into the node and the physical length, L , are halved. The geometry is recomputed as if the node were only half as large. The solution process is reinitiated and, when a solution is achieved, the saturation temperature check is redone. If the temperature into the node is still below the saturation temperature, \dot{m}_g and the length are halved again and the process is repeated. This procedure is continued until the temperature into the node is found to equal the saturation temperature or be above it. If the temperature is above the saturation temperature, then the \dot{m}_g and L parameters are changed to a value halfway between the current and previous values, and the process is continued until the temperature into the partial node exactly equals the saturation temperature. The values for Q , $T_{g\ out}$, $T_{f\ in}$ and U_{oi} are stored to be used later to develop weighted averages with the boiling portion parameters.

The remainder of the node is solved in the boiling portion of the model.

E. BOILING NODAL ANALYSIS

Nodes in the boiling section are solved by the same iterative scheme developed in the superheating section. The

correlations utilized to determine the solution are different since flow in the boiling regime will involve two phases on the fluid-side. In two phase flow the inside heat transfer coefficient will change with quality, x , and the heat flux, q'' . The correlation selected for this model is the same as that used by Combs [Ref. 3] which was recommended by Tong [Ref. 7] for both nucleate boiling and forced convection. The analysis presented by Combs is presented here.

The equation for the two-phase flow heat transfer coefficient was given by Schrock and Grossman in Tong [Ref. 7] as

$$\frac{h_{TPf}}{h_l} = B \left[\frac{q''}{G h_{fg}} + A \left(\frac{1}{x_{tt}} \right)^n \right] .$$

The constants are given by Wright [Ref. 7]: $B = 6.70 \times 10^3$, $A = 3.5 \times 10^{-4}$, and $n = 0.66$. The heat transfer coefficient, assuming a totally liquid flow is

$$h_l = 0.023 \frac{K_l}{d_i} \left[\frac{d_i G (1-x)}{\mu_l} \right]^{0.8} \left[\frac{C_{p\ell} \mu_l}{K_l} \right]^{0.1}$$

and the Martinelli parameter is

$$\frac{1}{x_{tt}} = \left[\frac{x}{1-x} \right]^{0.9} \left[\frac{\rho_l}{\rho_v} \right]^{0.5} \left[\frac{\mu_v}{\mu_l} \right]^{0.1}$$

The limits of the data for this correlation are:

quality: 0.05--0.57

heat flux: 6.0×10^4 -- 1.45×10^6 BTU/hr-ft²,

In this model, heat flux in the boiling section will be at levels considerably below 6×10^4 BTU/hr-ft² and the full range of quality must be considered. Therefore, in order to predict the performance of the Schrock and Grossman correlation at lower heat flux and quality above 0.57, a plot was made (Fig. 7), of the ratio h_{TPF}/h_L vs. quality where h_L is the heat transfer coefficient from the Dittus-Boelter correlation for water at saturated liquid conditions. The correlation of Dengler and Addoms, as given in Tong [Ref. 7], indicates that low heat flux and high water-vapor mixture velocity favor the forced convection mechanism. After a review of the information available in Tong, it is not entirely clear whether the forced convection or the nucleate boiling mechanism is dominant for the relatively low flow velocities and low heat flux of this model. In any case, the Schrock and Grossman correlation applied at low heat flux represents a type of compromise between the entirely forced convection assumptions of Dengler and Addoms and the "mixed" assumption of Schrock and Grossman.

A simplification assumed in the model is that the quality in the node is the average quality for the entire length of the node. Also, to expedite the numerical procedure, it is assumed that the node effectiveness is 0.25, initially. The effectiveness rarely attains a value higher than this for this type heat exchanger, so the assumption is valid. The value of the effectiveness is adjusted to the "true" value in the iterative process. In a process involving

a change of phase the fluid is isothermal. In actuality, there is a slight temperature change through the boiling regime but for purposes of analysis this change is neglected. For this reason the fluid bulk temperature in any node in the boiling portion is equal to the fluid saturation temperature. Therefore, to determine the amount of energy absorbed by the fluid in a node, the change in fluid enthalpy between the inlet and outlet is calculated.

In the first node in the boiler, which is the node immediately before the superheater or a partial node if the node was split, the gas bulk temperature is again set equal to the gas inlet temperature. The gas-side heat transfer coefficient is calculated using the same procedure as delineated in the superheater nodal analysis. Next, a Q for the node is calculated from

$$Q = \epsilon \dot{m}_g C_{pg} (T_{g \text{ in}} - T_{f \text{ in}})$$

where the effectiveness, ϵ , is initially assumed to be 0.25 and $T_{f \text{ in}}$ is equal to the fluid saturation temperature. A fluid inlet enthalpy is derived from

$$h_{f \text{ in}} = h_{f \text{ satv}} - (Q/\dot{m}_f)$$

where $h_{f \text{ satv}}$ = enthalpy of the fluid at saturated vapor. The fluid bulk enthalpy is

$$h_{fB} = (h_{fin} + h_{fsatv})/2 .$$

The average quality for the node is calculated from

$$x_{avg} = \frac{h_{fB} - h_{fsatl}}{h_{fsatv} - h_{fsatl}}$$

where h_{fsatl} is the enthalpy of the fluid at a saturated liquid condition. The Martinelli parameter is determined from

$$\frac{1}{x_{tt}} = \left[\frac{x_{avg}}{1-x_{avg}} \right]^{0.9} \left[\frac{\rho_l}{\rho_v} \right]^{0.5} \left[\frac{\mu_v}{\mu_l} \right]^{0.1}$$

where ρ_l/ρ_v are the liquid/vapor densities at the saturation temperature and μ_v/μ_l are the liquid/vapor viscosities at the saturation temperature. Now the heat transfer coefficient for totally liquid flow is calculated

$$h_l = 0.023 \frac{K_l}{d_i} \left[\frac{d_i G (1-x_{avg})}{\mu_l} \right]^{0.8} \left[\frac{C_{pl} \mu_l}{K_l} \right]^{0.1} .$$

From this the heat transfer coefficient is calculated for two-phase flow

$$h_{TPf} = h_l \left[B \left\{ \frac{Q}{G h_{fg}} + A \left(\frac{1}{x_{tt}} \right)^n \right\} \right]$$

where $h_{fg} = h_{fsatv} - h_{fsatl}$ and the constants A, B and n have the aforementioned values and G is the mass flow rate

per unit area. Finally, the node overall heat transfer coefficient is calculated from

$$U_{oi} = \frac{1}{\frac{1}{h_{TPf}} + \frac{A_{ip} \ln(d_o/d_i)}{2\pi K_w N_{t/p} L} + \frac{A_{ip}}{A_{op}} \frac{1}{h_g \eta_t}} .$$

Whenever two phase flow is involved, the heat capacity of the fluid is assumed infinite. For this reason, within the boiling regime, C_{min} will always equal the heat capacity of the hot side, so,

$$C_{min} = \dot{m}_g C_{pg}$$

and the Number of Transfer Units, NTU, is

$$NTU = \frac{U_{oi} A_{ip}}{C_{min}} .$$

The node effectiveness is

$$\epsilon = 1 - \exp(-NTU) .$$

Now, a revised Q for the node is calculated from

$$Q = \epsilon C_{min} (T_{gin} - T_{fin}) .$$

From this Q a revised gas outlet temperature is calculated

$$T_{g \text{ out}} = T_{g \text{ in}} - (Q/C_{\min}) .$$

With this gas temperature out, a new film temperature is calculated in the same manner as for the superheating section.

The gas outlet temperature is stored and the film temperature is used to repeat the process for the node. At the end of the second time through, the gas outlet temperature derived is compared with the result from the first. If equality exists, a solution for the node has been found and the model proceeds to the next node. If inequality exists, the result of the current iteration is stored for comparison with the results of the following iteration.

When a final solution is attained, the enthalpy of the fluid at the inlet to the node is checked against the enthalpy of saturated water at the heat exchanger pressure. If the inlet enthalpy is greater than or equal to the enthalpy of saturated water, the model proceeds to the next node and begins the solution process again. If the inlet enthalpy is less than the enthalpy of saturated water then the model proceeds to a node splitting routine similar to that used when transitting from the superheating regime to the boiling regime.

The node splitting is again accomplished by halving the mass flow rate on the gas-side and halving the physical length, L , of the node. The remaining geometric parameters are recomputed and the solution process is reinitiated. The

mass and length adjustment procedure is continued until the inlet enthalpy is equal to the enthalpy of saturated water. When this is achieved, the values of $T_{g\ out}$, U_{oi} and Q are stored to be recombined as weighted averages with the heating portion of the node to give the overall nodal values.

The remainder of the node is solved in the heating portion of the model.

F. HEATING NODAL ANALYSIS

The procedure for analyzing a node in the heating portion of the model is identical to that used in the superheating portion. Each node is analyzed in an iterative process, and it makes no difference if the first node was a split node. The first node in the heating section will have a gas inlet temperature equal to the gas outlet temperature of the node directly below. The fluid outlet temperature will equal the fluid saturation temperature for the specified pressure.

An outline of the calculations is as follows:

1. Calculate the gas-side heat transfer coefficient using the node gas inlet temperature as the gas bulk temperature.
2. Calculate the fluid-side heat transfer coefficient initially using the fluid saturation temperature as the fluid bulk temperature.
3. Calculate the overall heat transfer coefficient using the effectiveness-NTU method.

4. Determine the node fluid inlet temperature from

$$T_{f \text{ in}} = \frac{\epsilon C_{\min} T_{g \text{ in}} - \dot{m}_f C_{pf} T_{f \text{ out}}}{\epsilon C_{\min} - \dot{m}_f C_{pf}}$$

5. Calculate a first "guess" for Q for the node from

$$Q = \dot{m}_f C_{pf} (T_{f \text{ out}} - T_{f \text{ in}})$$

6. Calculate the node gas outlet temperature from

$$T_{g \text{ out}} = T_{g \text{ in}} - (Q / \dot{m}_g C_{pg}) .$$

7. Calculate $T_{g \text{ bulk}} = (T_{g \text{ in}} + T_{g \text{ out}}) / 2$

8. Calculate a node average film temperature from

$$T_{gf} = (T_{gB} + T_{wo}) / 2$$

9. Store the result of the first pass through the model and iterate until procedure converges to solution, utilizing gas outlet temperature for comparison at each pass.

All properties of the gas and fluid are evaluated at the respective bulk temperatures for the node. The process is repeated node by node until the node at the fluid inlet to the heat exchanger is completed. The final node is either

node (1,1) for an odd number of passes, or node (1,10) for an even number of passes in the heat exchanger.

G. HEAT EXCHANGER SOLUTION PROCEDURE

When the procedure of the heating section has arrived at a solution for the final node of the heat exchanger, the fluid inlet temperature for the node is compared to the user specified feedwater inlet temperature. If equality exists, the model proceeds to an output routine where the matrices of water/steam temperatures, exhaust gas temperatures, overall heat transfer coefficients and individual heat transfer per node are printed. Additionally, the fluid-side mass flow rate, minimum pinch point temperature difference, total Q for the heat exchanger and isentropic steam turbine power are calculated and printed.

The pinch point temperature difference is defined in this model as the minimum difference in the heat exchanger between the gas inlet temperature and the fluid inlet temperature to any node. Consideration of the effect of a pinch point below approximately 25 deg. F is cause for concern only if the low pinch point is coupled with a low gas temperature. This combination is non-prohibitive to hot side corrosion. If the final node fluid inlet temperature is not equal to the user specified feedwater inlet temperature, then the fluid mass flow rate that was "guessed" at the beginning is adjusted and the entire model is run again. If the solution

temperature is too high the "guessed" fluid mass flow rate is lowered. With less mass going through the heat exchanger the flow velocity is decreased. A lower flow velocity through the heat exchanger enables more energy from the gas-side to be transferred to the fluid-side. A larger Q will increase the temperature differential between the fluid inlet and outlet which will yield a lower solution fluid inlet temperature the second time through the model. The process is opposite, i.e., mass is added, if the fluid inlet temperature to the first node is found to be too low.

The model will continue to adjust the mass after each iteration in smaller amounts until an exact match is made to the user specified feedwater inlet temperature. When equality is achieved, the model proceeds to the output routine where the above mentioned parameters are printed.

Included, as Appendix A, are sample outputs of the model for the uniform distribution, distribution 1 and distribution 5 for all four of the selected gas mass flow rates. The run numbers at the top of the first page of each output were utilized for accounting purposes. The uniform distribution was used for runs 1, 10, 19 and 28; distribution 1 was used for runs 2, 11, 20 and 29; and distribution 5 was used for runs 6, 15, 24 and 33. The first page of the output shows the inter-active questions asked by the model and the user responses. The following pages show the matrices developed by the model in the solution process. Comparison of the

matrices for the uniform and non-uniform distributions demonstrates the serious impact of the non-uniformity on the performance. The non-uniform distribution profiles can be seen as projected profiles on the results of each of the matrices. The final page of the output is a listing of additional parameters which are calculated by the model including the fluid mass flow rate, Q based on the individual matrices, location of the beginning of boiling and superheating within the WHRU and the isentropic horsepower.

III. DISCUSSION OF RESULTS

A. INITIAL TESTING

The foregoing model was coded in FORTRAN IV and applied in a computer simulation on an IBM-3033 computer.

To properly test the model and develop an understanding of the operation of the WHRU several runs were made utilizing a uniform gas distribution with a total mass flow rate and temperature corresponding to a gas turbine horsepower rating for approximately a 20 kt. speed. The conditions presupposed usage of a General Electric LM2500 Gas Turbine Engine, and gas mass and temperature data was taken from [Ref. 8]. Initially, the model was run with attention to pinch point temperatures. The number of passes was varied to find the largest heat exchanger which could be used and still maintain a pinch point in excess of 25 degrees fahrenheit. Under conditions of non-uniform flow distributions the model definition of pinch point is misleading since small gas mass flow rates through a particular gas path may yield a nearly zero pinch point when the overall performance of the heat exchanger is not affected. Inspection of the model output for the non-uniform distributions will demonstrate this result. The preliminary runs allowed selection of a 23 pass heat exchanger with a 29.4 deg. F pinch point. Therefore, the 23 pass heat exchanger became the "design." The performance data tabulated for the LM2500 engine [Ref. 8] was utilized to select four gas mass flow

rates and inlet temperatures which correspond closely to data points on a cubic power curve. The four combinations of mass and temperature chosen were:

$$\dot{m}_g = 121.8 \text{ lbm/s}, \quad T_{g \text{ in}} = 844^\circ \text{ F}, \quad \text{SHP} = 17500, \quad \text{NPT} = 3000 \text{ rpm}$$

$$\dot{m}_g = 99.1 \text{ lbm/s}, \quad T_{g \text{ in}} = 755^\circ \text{ F}, \quad \text{SHP} = 10000, \quad \text{NPT} = 2400 \text{ rpm}$$

$$\dot{m}_g = 77.4 \text{ lbm/s}, \quad T_{g \text{ in}} = 702^\circ \text{ F}, \quad \text{SHP} = 5000, \quad \text{NPT} = 1800 \text{ rpm}$$

$$\dot{m}_g = 66.7 \text{ lbm/s}, \quad T_{g \text{ in}} = 694^\circ \text{ F}, \quad \text{SHP} = 3000, \quad \text{NPT} = 1200 \text{ rpm}$$

Each of these was run in the model as uniform and various non-uniform distributions.

To develop the non-uniform distributions, a normalized flow distribution table was constructed and is presented as Table I. This table shows the fraction of the total mass flow rate which is passing through each individual gas path for each of nine different flow distributions. The flow distributions were arbitrarily derived in an attempt to develop a spectrum of distributions that may enter the heat exchanger. A graphical display of each of the flow distributions is shown in Figures 8A-8I. The total mass flow rate used was multiplied by each entry in the normalized flow distribution table to arrive at the mass flow rate through each of the ten gas paths for any of the nine distributions. This procedure allowed a comparison of the effects of non-uniform distributions on the performance of the heat exchanger. All nine distributions were run for each of the

four chosen mass and temperature combinations. The actual mass flow distributions used are shown in Tables II-A--II-D. The combination of nine distributions and four different total gas flow rates yielded 36 runs. For the runs, the remaining parameters were:

- | | |
|---|--------------|
| a) feedwater inlet temperature | = 200 deg. F |
| b) desired steam temperature | = 650 deg. F |
| c) steam operating pressure | = 400 psia |
| d) minimum allowed gas outlet temperature | = 300 deg. F |
| e) node length | = 1.0 ft. |
| f) number of tubes per row | = 32 |
| g) geometric scaling factor | = 1.0 |

The model calculates the isentropic horsepower that would be developed by an ideal steam turbine. This power can also be viewed as the maximum power available from the developed superheated steam exhausting to a fixed condenser pressure. The method of calculation is to determine the enthalpy of the steam at the outlet pressure and temperature and then subtract the enthalpy of the steam after isentropic expansion to a condenser pressure of 2 psia. The difference in enthalpy was multiplied by the fluid mass flow rate, with the appropriate conversions, to arrive at a horsepower value. The horsepower calculated for each run is tabulated in Table III. The table lists the results of each run of the model for all 36 runs for each of 5 different steam outlet temperatures. Table IV is a similar table showing the solution values of

the fluid mass flow rates derived in each run. The two tables demonstrate the variation of fluid mass flow rate and power which is attained by varying the desired steam outlet temperature; and the effect of the non-uniform distributions on performance.

B. EFFECT OF NON-UNIFORM DISTRIBUTIONS

The data from column 1 of Table III was plotted and is shown in Figures 9A-9E as power vs. gas flow rate. Figure 9A shows the comparison of the uniform distribution with distributions 1 and 2. Figure 9B shows the comparison of the uniform distribution with distributions 3 and 4, etc. From the graphs it can be seen that the distribution inflicting the most serious impact on the heat exchanger performance is distribution 1 (see Figure 8-B). Distribution 1 is highly center concentrated and utilizes the area available for heat transfer the least efficiently. For comparison, distribution 3 is a nearly uniform distribution and it inflicts a relatively minor impact on the performance. Distributions 2 and 4 are ranked next in order of impact. These are also distributions where the mass is centrally concentrated, but to a lesser degree than distribution 1. Distributions 5 and 6 are mirror images of one another and also have a zero mass flow rate through two of the gas paths. A zero mass flow rate indicates that the flow through that particular pass has no velocity. In a real situation there will be a transient heat transfer

from the still mass of gas surrounding the tubes by natural convection until the gas temperature reaches the tube wall or fluid temperature. In any case, the amount of heat transferred in such a node is negligible compared to the nodes experiencing a gas flow rate. For the model, a zero gas flow rate in a node will be treated as having zero heat transfer, i.e., a "dead node," therefore, the Q for the node was set to zero, the fluid inlet temperature and fluid outlet temperature were set equal and the gas outlet temperature was set equal to the gas inlet temperature. In reality, the gas temperature in a "dead node" will attain the temperature of the fluid in the node but for pinch point calculation purposes the original gas inlet temperature was maintained. Also, since the model assumes no cross-mixing of the gas between gas paths as the distribution passes through the heat exchanger, this assumption ignores the potential tendency of the gas mass distribution to become uniform during passage. Distributions 5 and 6 are skewed to the left and right, respectively. The combination of the null gas flow paths and the skewedness of these distributions caused the second most detrimental effect on the heat exchanger. It should be noted, however, that whether the distribution was skewed to the right or left side had relatively no effect; that is, the results for distribution 5 are nearly identical to those for distribution 6. The same result was true for distributions 7 and 8, which are also mirror images of each other with left and

right skewedness. The effect of distributions 7 and 8 were very nearly the same as those for distribution 4. Figure 9E is a composite which demonstrates the effect of all the distributions. The ranking as to effect yields:

1. the uniform distribution gives the best performance
2. distr. 3, nearly uniform
3. distr. 4, least center concentrated, nearly same as distr.'s 7 and 8
4. distr. 2, intermediately center concentrated
5. distr.'s 5 and 6, skewed with null flow paths
6. distr. 1, highly center concentrated

The ranking can be viewed as a measure of the efficiency of the distribution in utilizing the area available in the heat exchanger for heat transfer. As the amount of distortion of the flow increases, the quantity of energy transferred decreases.

Figures 10A-10E are graphical representations of the solution fluid mass flow rates vs. the gas mass flow rates for each of the distributions; exactly as was done to develop Figures 9A-9E. As was to be expected, the results for Figures 10A-10E are identical to those for power vs. gas flow rate, since power is directly proportional to the fluid mass flow rate.

After these preliminary results, it was decided to conduct the remaining runs utilizing only the uniform distributions and the worst of the non-uniform distributions; i.e.,

distribution 1. It was assumed that results for the remaining distributions would fall between the values of these two.

C. EFFECT OF HEAT EXCHANGER SIZE

Next, an analysis was done to determine the effect on output power and fluid mass flow rate by varying the number of heat exchanger passes. Using the four chosen gas mass flow rates, runs were conducted for heat exchangers of 20, 21, 23 and 25 passes. All runs were for 650 deg. F outlet steam at 400 psia operating pressure. Therefore, the runs for the 23 pass heat exchanger were the "design" runs and the runs for 20, 21 and 25 passes were the "off-design" runs provided for comparison. The results of these runs are tabulated in Table V and graphically presented in Figures 11A-11H as power and fluid mass flow rate, respectively, vs. the number of heat exchanger passes. Again, because of the relationship between power and fluid mass flow rate, the graphical results are similar in contour. The results show that as the size of the heat exchanger is increased, so will the power out. To provide the increased power the mass flow rate of the fluid must increase since for the different sized heat exchangers the inlet and outlet enthalpies of the fluid is not changing. The limit to the increase in size is the available energy in the gas. Increasing the heat exchanger size to the point where sufficient energy is transferred from the gas to the fluid to attain the minimum

acceptable exhaust gas temperature is the maximum size possible.

The curves display an interesting result concerning the differences between the uniform distribution and the non-uniform distribution. As the size of the heat exchanger increases, the two curves are converging with the difference in power (or fluid mass flow rate) being less for the larger heat exchanger than for the smaller. From the data of Table V, it can be seen that, for the 121.8 lbm/s gas flow rate, the power from distribution 1 is 89% of the power attained from the uniform distribution for a 20 pass heat exchanger. This increases to approximately 91% for the 25 pass heat exchanger. The more rapid increase in power for the non-uniform distribution is caused by the mass concentration in the center gas paths. For a particular size heat exchanger, the paths with a small gas mass flow will attain the temperature of the fluid, usually in the boiling region. From that point on, these paths contribute little, or not at all, to the total heat transfer. The high concentration of mass in the center paths, however, contribute greatly to the total heat transfer because of the high velocity of the flow and the high heat transfer coefficients. These paths of high concentration will contribute until the gas exits the heat exchanger. By adding more passes to the heat exchanger it is as if the "dead areas" in the low mass flow paths were placed in the path of the high mass flows. The effect is a

significant increase in the heat transfer. The high heat transfer coefficients, mass velocity and temperature differentials all contribute to a greater percentage increase per pass than is achieved by the uniform distribution. As additional passes are added, the performance of the non-uniform distribution improves, but it will never attain the level of the uniform distribution. For two heat exchangers of equal size, the uniform distribution gives the most efficient use of the available area for heat transfer.

D. EFFECT OF STEAM OUTLET TEMPERATURE

Each distribution, uniform and distributions 1-8, was run at each of the four gas flow rates for five specified steam outlet temperatures. The power and fluid mass flow calculated by the model are presented in Tables III and IV. The results are also presented graphically in Figures 12-A and 12-B for the uniform distribution and distribution 1 at each of the four gas flow rates.

Both the tabular and graphical data shows a nearly uniform increase in fluid mass flow rate with the linear decrease in steam outlet temperature. The tabular data for power demonstrates a non-linear result, showing initially a decrease in power with a decrease in steam outlet temperature, and then increasing to attain a power higher than that for a 650 deg. F steam outlet temperature.

The non-linearity of the power is caused by the non-linearity of the steam enthalpy as the steam outlet temperature

decreases. The combination of the change in enthalpy and the change in the fluid mass flow rate results in a misleading impression of attaining a higher power at a lower steam temperature. The total power does increase but the specific power decreases. The increase in fluid mass flow between a 650 deg. F steam outlet temperature and a 550 deg. F steam outlet temperature is approximately 7%. The increase in power at the lower steam outlet temperature is less than 0.2%. The penalty to utilize a lower steam temperature and maintain an equivalent power output is a water/steam system which must be able to circulate 7% more fluid in the same time period. This result may have serious impact in the design when condenser size, circulating pump size, valves, piping and the steam turbine are taken into consideration. The steam turbine must also be considered with respect to the lower steam temperature having a lower quality through the latter stages of the expansion. The effects of overly "wet" steam can be disastrous to many turbines. The end result is that the sacrifice in power at the higher steam temperature is justified by the decrease in fluid flow required and higher end point quality.

E. EFFECT OF HEAT EXCHANGER PRESSURE

The uniform distribution and distribution 1 were run for each of the four gas flow rates with three different specified heat exchanger operating pressures. The pressures were the "design" pressure of 400 psia and then 500 psia and 600

psia. The tabulated results of these runs are presented in Table VI, and graphically presented in Figures 13-A and 13-B for power and fluid mass flow rate, respectively, vs. heat exchanger pressure. Again, because of the direct correlation between fluid mass flow rate and power, the contours of the graphical results are similar.

The curves show a decrease in power and fluid mass flow rate as heat exchanger pressure is increased. As the pressure is increased by 50% above the design level, there is a 4% drop in the system fluid mass flow rate and a 7.5% loss in power. Clearly, the benefits derived from the decrease in system fluid mass flow rate does not justify the sacrifice in system power. With respect to the analysis of the previous section, a compromise must be reached to achieve the maximum power from the system within the confines of a maximum acceptable fluid mass flow rate.

The graphical results also show the effect of the non-uniform distribution for each of the four gas flow rates. As the gas flow rate decreases, the penalty for non-uniformity has a lesser effect. The percentage loss for the four flow rates are approximately 9, 8, 7 and 6 percent, respectively, from highest flow rate to lowest. The loss is approaching zero as the flow rate approaches zero. The loss in power is directly related to the decrease in fluid mass flow rate determined in the solution; and the decrease in fluid flow rate is a result of the ineffectiveness of the non-uniformity on the operation of the heat exchanger.

F. EFFECT OF GAS FLOW RATE ON HEAT EXCHANGER PERFORMANCE

The data from the matrix of water/steam temperatures for the four gas flow rates as uniform distributions was plotted as a function of tube length. The curves are shown in Figures 14-A--14-D. Figure 14-E is a plot of the water/steam temperatures as a function of tube length for distribution 1 with a gas mass flow rate of 121.8 lbm/s. Figure 14-F is a superposition of Figure 14-E on Figure 14-A.

Analysis of Figures 14-A through 14-D shows the effect of the decrease in gas flow rate on the rate of heat transfer as the fluid passes through the heat exchanger. The higher the gas flow, the steeper is the slope of the curve in the superheat region. A steeper slope is indicative of a shorter tube length required to attain the desired superheat temperature. The effect, as the gas flow rate is decreased, is that more of the heat exchanger is dedicated to superheating. The length of the tube required to raise the water from a saturated liquid to a saturated vapor condition is nearly the same for all gas flow rates with only a "left shift" on the plots caused by the superheat conditions. The slope of the curves in the heating region is the opposite of that of the superheat. As the gas flow rate decreases the slope of the curve in the heating region increases.

Since, for all conditions, the feedwater inlet temperature and steam outlet temperature are the same, all tubes

are continuous and of the same length, the difference in the curves is attributable to the rate of heat transfer and the total amount of energy transferred. The rate equation is

$$Q = \epsilon C_{\min}(T_{g \text{ in}} - T_{f \text{ in}})$$

and this must equal the energy balance equation

$$\begin{aligned} Q &= \dot{m}_g C_{pg}(T_{g \text{ in}} - T_{g \text{ out}}) \\ &= \dot{m}_f C_{pf}(T_{f \text{ out}} - T_{f \text{ in}}) \end{aligned}$$

The change in gas mass flow rate will obviously decrease the total amount of energy transferred since less gas in means less energy into the heat exchanger. If the curves were plotted in a third dimension with Q , the smallest Q would occur with the smallest gas flow rate. The forced equality with the rate equation means that, as the gas flow rate decreases, the rate of heat transfer must decrease. The figures show the total effect on the profile operation of the heat exchanger is of little consequence. The similarity of the curves is an indication of the "physical operation" of the heat exchanger under varying conditions. For the test runs, a decrease in gas flow rate was coupled with a decrease in gas inlet temperature. The two parameters changing and the similarity of the curves emphasizes the physical constancy of the design.

Figure 14-E is the plot for distribution 1. The "ripple" effect in the heating and superheating regions is a result of the non-uniformity of the gas mass distribution, but the superposition shown in Figure 14-F demonstrates the obliviousness of the physical properties of the heat exchanger to a variation of input.

G. EFFECT OF NON-UNIFORM MASS DISTRIBUTION ON EXHAUST GAS TEMPERATURE

For all runs of the model the temperature distribution of the exhaust gas entering the heat exchanger was assumed uniform. To determine the effects of a non-uniform gas mass distribution on the exhaust gas temperature profile, a plot was made of the gas temperatures across several of the heat exchanger passes. The matrix of exhaust gas temperatures was used and data was plotted for both a uniform distribution and distribution 1. The gas mass flow rate was 121.8 lbm/s. Figures 15-A and 15-B show the results.

Figure 15-A demonstrates that with a uniform mass and temperature distribution at the inlet to the heat exchanger, the distribution is virtually undistorted by passage through the WHRU. This result must be considered ideal with respect to the assumption of no cross-mixing of the gas during passage. There is a smooth transition of energy from inlet to outlet which accounts for the best performance of the heat exchanger under this condition. The effect of the non-uniformity is clearly seen in Figure 15-B. The temperature distribution is

rapidly distorted to become almost a replica of the gas flow distribution. This is a result of the disparity of heat transferred and heat transfer rates from node to node in the WHRU. A slight smoothing effect is seen in the boiling portion, but distortion is again accentuated in the heating section. In a real situation there will be some non-uniformity of temperature as it enters the heat exchanger. The analysis shows that the condition will be worsened to the degree of the mass non-uniformity with the subsequent loss of performance in the WHRU.

The distortion of the exhaust gas temperature distribution forces consideration of pinch point. When the temperature differential between the exhaust gas and the tube becomes less than approximately 25 deg. F coupled with a gas temperature less than approximately 300 deg. F, the WHRU may experience localized hot-side corrosion due to sulphur products in the exhaust gas. It should be noted that this condition will exist only near the top of the heat exchanger near the exhaust gas exit. If the degree of flow distortion is severe and maintained for a long period, the effects can be disastrous.

IV. CONCLUSIONS

The waste heat recovery unit is a practical method of recouping thermal energy from gas turbine engine exhaust gases for fuel economy improvement. In the design and installation of a RACER system several factors must be taken into consideration.

1. Mass Flow Distribution. The performance of a waste heat recovery unit is adversely affected by a non-uniform gas mass distribution; and the degradation is directly proportional to the degree of non-uniformity. To ensure acceptable results, the system should have flow distribution control devices installed between the gas turbine and the WHRU.

2. Operating Pressure. The operating pressure of the system affects the power output inversely. A higher pressure system requires less fluid to deliver the same power but the percent reduction in fluid required does not justify the percent loss in power. Since the system is not a main propulsion system requiring a large volume of fluid, the model suggests using a low pressure system.

3. Steam Outlet Temperature. Reducing the outlet temperature required forces an increase in fluid mass flow rate to maintain the same power out. High temperature steam, however, has a greater wear effect on system components such as valves, seals and piping. The model suggests a steam temperature as high as practical should be used, within material constraints.

4. Heat Exchanger Size. Power and fluid mass flow rate are directly related to heat exchanger size. The size of the WHRU should be as large as the available space and weight constraints allow, or as large as necessary to produce the power required. Consideration must be given to the system as a whole since, as the heat exchanger becomes larger, so does the piping, valves, pumps and condenser necessary to operate.

5. Speed. Power developed is a function of the energy available in the exhaust gas flow. At higher gas turbine speeds more horsepower is available from the WHRU to assist the main propulsion system. Utilizing the latest NAVSEA speed profile, the heat exchanger should be sized in accordance with the ship speed most commonly used.

All data suggests a WHRU as large as physically possible, operated at a low steam pressure, high steam temperature, and with flow distribution control devices installed provides the best performance.

V. RECOMMENDATIONS FOR FURTHER RESEARCH

A. WHRU MODEL IMPROVEMENT AND EXPANSION

The control imposed on the WHRU model in this study was adjustment of the steam flow rate to maintain a user specified steam outlet temperature. This forces the steam system to respond to a variation of gas inlet conditions by "throttling" the feedwater system to maintain the required steam temperature.

This is only one of several types of control systems which may be used in a RACER system installation. Two possible alternative systems are: one which maintains a constant steam flow rate while allowing the steam temperature to fluctuate, and one in which pressure is allowed to "float" with steam demand. In this second type system, the flow resistance of the system is used, and as the fluid mass flow rate decreases (steam demand decreases), the pressure required decreases. Knowing the inter-relationship will yield a "floating" $T_{f\ out}$ as well. Investigation into the performance of a WHRU with these types of control could lead to an improved output. The investigation of all types of control should consider the effects on the entire system because, the type of control may dictate the type steam turbine which must be used.

To expand the understanding of the effects of non-uniform gas distributions on the WHRU performance, the current

model could be enlarged to allow a variation of the input in an additional dimension. A two dimensional non-uniform input will yield a three dimensional picture of the temperature distributions as the gas passes through the heat exchanger. An analysis of this type would help design the flow distribution control devices to eliminate severe trouble spots contributing to hot side corrosion and to maximize the WHRU performance.

In addition to the expansion to a three dimensional analysis, the current model could be improved by including the following items.

1. Fluid-Side Pressure Drop

The water/steam-side pressure drop may be a significant percentage of the system operating pressure. Calculation of the pressure drop and its effect on system performance should be included.

2. Additional Geometries

Additional fin-tube configurations should be considered for possible improvement of the heat transfer characteristics and the weight and space requirements of the WHRU.

3. Fouling

Consideration of inside and outside heat transfer surface fouling should be given when investigating possible fin-tube configurations.

4. Alternate Working Fluids

Working fluids, other than water, should be investigated for possible enhanced thermodynamic characteristics at

a minimum cost in system maintainability, while maintaining safety to operating personnel.

5. Non-Uniform Temperature Distributions

The current model could be utilized to determine the effects of non-uniform temperature distributions. The gas is at a uniform temperature as it exits the gas turbine, but it probably is not uniform at the inlet to the WHRU. Investigation into the effects of non-uniformity of both gas mass and temperature should be accomplished.

The model should be incorporated into a complete RACER system analysis, including models of the steam turbine, condenser and circulating pump. Variations of gas distribution input can then be analyzed to determine total system effect. Understanding the total system effect and the inter-relationship of the variables could then be used to optimize the system.

TABLE I

NORMALIZED FLOW DISTRIBUTION

NORMALIZED FLOW DISTRIBUTION										
DIST. NO.	GAS PATH									
	1	2	3	4	5	6	7	8	9	10
U	.010	.010	.010	.010	.010	.010	.010	.010	.010	.010
1	.017	.049	.068	.112	.254	.254	.112	.068	.049	.017
2	.031	.044	.086	.133	.206	.206	.133	.086	.044	.031
3	.080	.090	.100	.110	.120	.120	.110	.100	.090	.080
4	.025	.063	.105	.140	.165	.165	.140	.105	.065	.025
5	.100	.224	.192	.153	.131	.096	.064	.030	.000	.000
6	.000	.000	.030	.064	.096	.131	.163	.192	.224	.100
7	.127	.194	.157	.124	.086	.073	.067	.066	.064	.043
8	.043	.064	.066	.067	.073	.086	.124	.157	.194	.127

TABLE II-A

GAS FLOW DISTRIBUTIONS ($\dot{m}_g = 121.8 \text{ LBM/S}$)

GAS MASS FLOW RATE = 121.8 LBM/S

GAS TEMPERATURE AT HEAT EXCHANGER INLET = 844 DEG. F

CASE 575 (REF 8) SHP = 17500 NPT = 3000

DIST. NO.	GAS PATH									
	1	2	3	4	5	6	7	8	9	10
U	12.18	12.18	12.18	12.18	12.18	12.18	12.18	12.18	12.18	12.18
1	2.07	5.97	8.28	13.54	30.94	30.94	13.64	8.28	5.97	2.07
2	3.78	5.36	10.47	16.20	25.09	25.09	16.20	10.47	5.36	3.78
3	9.74	10.96	12.18	13.40	14.62	14.62	13.40	12.18	10.96	9.74
4	3.05	7.92	12.79	17.05	20.10	20.10	17.05	12.79	7.92	3.05
5	12.18	27.28	23.29	19.35	15.96	11.69	7.80	3.65	0.00	0.00
6	0.00	0.00	3.65	7.80	11.69	15.96	19.85	23.29	27.28	12.18
7	15.47	23.63	19.12	15.10	10.47	8.89	8.11	8.04	7.75	5.24
8	5.24	7.75	8.04	8.11	8.89	10.47	15.10	19.12	23.63	15.47

TABLE II-B

GAS FLOW DISTRIBUTIONS ($\dot{m}_g = 99.1 \text{ LBM/S}$)

GAS MASS FLOW RATE = 99.1 LBM/S

GAS TEMPERATURE AT HEAT EXCHANGER INLET = 755 DEG. F

CASE 561 (REF 8) SHP = 10000 NPT = 2400

DIST. NO.	GAS PATH									
	1	2	3	4	5	6	7	8	9	10
U	9.91	9.91	9.91	9.91	9.91	9.91	9.91	9.91	9.91	9.91
1	1.68	4.85	6.74	11.10	25.17	25.17	11.10	6.74	4.85	1.68
2	3.08	4.36	8.52	13.18	20.41	20.41	13.18	8.52	4.36	3.08
3	7.92	8.92	9.91	10.90	11.90	11.90	10.90	9.91	8.92	7.92
4	2.48	6.44	10.41	13.37	16.35	16.35	13.87	10.41	6.44	2.48
5	9.91	22.20	19.03	16.15	12.99	9.51	6.35	2.97	0.00	0.00
6	0.00	0.00	2.97	6.35	9.51	12.99	16.15	19.03	22.20	9.91
7	12.59	19.23	15.56	12.29	8.52	7.23	6.60	6.54	6.31	4.26
8	4.26	6.31	6.54	6.50	7.23	8.52	12.29	15.56	19.23	12.59

TABLE II-C

GAS FLOW DISTRIBUTIONS ($\dot{m}_g = 77.4$ LBM/S)

GAS MASS FLOW RATE = 77.4 LBM/S

GAS TEMPERATURE AT HEAT EXCHANGER INLET = 702 DEG. F

CASE 553 (REF 8)

SHP = 5000

NPT = 1800

DIST. NO.	GAS PATH									
	1	2	3	4	5	6	7	8	9	10
U	7.74	7.74	7.74	7.74	7.74	7.74	7.74	7.74	7.74	7.74
1	1.31	3.80	5.26	8.67	19.66	19.66	8.67	5.26	3.80	1.31
2	2.41	3.41	6.65	10.29	15.94	15.94	10.29	6.65	3.41	2.41
3	6.19	6.97	7.74	8.51	9.29	9.29	8.51	7.74	6.97	6.19
4	1.94	5.03	8.13	10.83	12.77	12.77	10.83	8.13	5.03	1.94
5	7.74	17.34	14.86	12.61	10.15	7.43	4.96	2.32	0.00	0.00
6	0.00	0.00	2.32	4.96	7.43	10.15	12.61	14.86	17.34	7.74
7	9.83	15.02	12.15	9.60	6.65	5.65	5.15	5.11	4.93	3.33
8	3.33	4.93	5.11	5.15	5.65	6.65	9.60	12.15	15.02	9.83

TABLE II-D

GAS FLOW DISTRIBUTIONS ($\dot{m}_g = 66.7$ LBM/S)

GAS MASS FLOW RATE = 67.7 LBM/S

GAS TEMPERATURE AT HEAT EXCHANGER INLET = 694 DEG. F

CASE 545 (REF 8)

SHP = 3000

NPT = 1200

DIST. NO.	GAS PATH									
	1	2	3	4	5	6	7	8	9	10
U	6.77	6.77	6.77	6.77	6.77	6.77	6.77	6.77	6.77	6.77
1	1.15	3.32	4.60	7.58	17.20	17.20	7.58	4.60	3.32	1.15
2	2.11	2.98	5.82	9.00	13.94	13.94	9.00	5.82	2.98	2.11
3	5.41	6.10	6.77	7.44	8.13	8.13	7.44	6.77	6.10	5.41
4	1.70	4.40	7.11	9.47	11.17	11.17	9.47	7.11	4.40	1.70
5	6.77	15.17	13.00	11.03	8.88	6.50	4.34	2.03	0.00	0.00
6	0.00	0.00	2.03	4.34	6.50	8.88	11.03	13.00	15.17	6.77
7	8.60	13.14	10.63	8.40	5.82	4.94	4.50	4.47	4.31	2.91
8	2.91	4.31	4.47	4.50	4.94	5.82	8.40	10.63	13.14	8.60

TABLE III

ISENTROPIC POWER FOR VARIOUS GAS FLOW DISTRIBUTIONS,
GAS FLOW RATES AND STEAM OUTLET TEMPERATURES

	RUN NO.	DISTR. NO.	STEAM TEMPERATURE				
			650	625	600	575	550
GAS MASS 121.8 LBM/S	1	U	6944	6943	6933	6946	6956
	2	1	6286	6315	6295	6317	6348
	3	2	6550	6570	6550	6580	6598
	4	3	6924	6925	6910	6927	6939
	5	4	6692	6708	6691	6713	6730
	6	5	6397	6419	6415	6420	6434
	7	6	6390	6382	6407	6431	6464
	8	7	6754	6742	6722	6727	6750
	9	8	6715	6733	6744	6763	6762
GAS MASS 99.1 LBM/S	10	U	4484	4489	4488	4500	4510
	11	1	4123	4123	4153	4155	4183
	12	2	4276	4277	4292	4296	4323
	13	3	4475	4477	4479	4489	4501
	14	4	4356	4358	4368	4375	4395
	15	5	4161	4187	4203	4222	4227
	16	6	4165	4194	4187	4220	4245
	17	7	4365	4395	4387	4392	4399
	18	8	4379	4373	4379	4408	4417
GAS MASS 77.4 LBM/S	19	U	2948	2957	2957	2967	2974
	20	1	2756	2779	2779	2801	2809
	21	2	2840	2857	2853	2872	2882
	22	3	2943	2953	2953	2962	2970
	23	4	2882	2897	2898	2910	2919
	24	5	2770	2793	2812	2833	2837
	25	6	2773	2795	2811	2821	2842
	26	7	2891	2901	2914	2918	2921
	27	8	2890	2906	2901	2918	2933
GAS MASS 67.7 LBM/S	28	U	2515	2522	2522	2530	2536
	29	1	2365	2389	2393	2411	2417
	30	2	2434	2451	2451	2462	2471
	31	3	2512	2519	2519	2527	2533
	32	4	2465	2479	2480	2490	2498
	33	5	2377	2405	2418	2435	2437
	34	6	2388	2406	2416	2425	2442
	35	7	2476	2481	2492	2496	2499
	36	8	2469	2487	2482	2496	2507

TABLE IV

FLUID MASS FLOW RATE FOR VARIOUS GAS FLOW RATES, GAS FLOW DISTRIBUTIONS AND STEAM OUTLET TEMPERATURES

	RUN NO.	DISTR. NO.	STEAM TEMPERATURE				
			650	625	600	575	550
GAS MASS 121.8 LBM/S	1	U	12.33	12.54	12.75	12.97	13.20
	2	1	11.17	11.41	11.58	11.79	12.04
	3	2	11.63	11.87	12.05	12.28	12.52
	4	3	12.30	12.51	12.71	12.93	13.17
	5	4	11.89	12.12	12.31	12.53	12.77
	6	5	11.36	11.59	11.80	11.99	12.21
	7	6	11.35	11.53	11.78	12.01	12.27
	8	7	12.00	12.18	12.36	12.56	12.81
	9	8	11.93	12.16	12.40	12.63	12.83
GAS MASS 99.1 LBM/S	10	U	7.96	8.11	8.25	8.40	8.56
	11	1	7.32	7.46	7.64	7.76	7.94
	12	2	7.60	7.72	7.89	8.02	8.20
	13	3	7.95	8.09	8.24	8.38	8.54
	14	4	7.74	7.87	8.03	8.17	8.34
	15	5	7.39	7.56	7.74	7.88	8.02
	16	6	7.40	7.58	7.70	7.88	8.05
	17	7	7.75	7.94	8.07	8.20	8.35
	18	8	7.78	7.90	8.05	8.23	8.38
GAS MASS 77.4 LBM/S	19	U	5.24	5.34	5.44	5.54	5.64
	20	1	4.90	5.02	5.11	5.23	5.33
	21	2	5.04	5.16	5.26	5.36	5.47
	22	3	5.23	5.33	5.43	5.53	5.64
	23	4	5.12	5.23	5.33	5.43	5.54
	24	5	4.92	5.05	5.17	5.29	5.38
	25	6	4.93	5.05	5.17	5.27	5.39
	26	7	5.14	5.24	5.36	5.45	5.54
	27	8	5.13	5.25	5.34	5.45	5.56
GAS MASS 67.7 LBM/S	28	U	4.47	4.56	4.64	4.72	4.81
	29	1	4.20	4.32	4.40	4.50	4.59
	30	2	4.32	4.43	4.51	4.60	4.69
	31	3	4.46	4.55	4.63	4.72	4.81
	32	4	4.38	4.48	4.56	4.65	4.74
	33	5	4.22	4.34	4.45	4.55	4.62
	34	6	4.24	4.35	4.44	4.53	4.63
	35	7	4.40	4.48	4.58	4.66	4.74
	36	8	4.39	4.49	4.56	4.66	4.76

TABLE V. POWER AND FLUID FLOW RATE
FOR VARIOUS SIZE HEAT EXCHANGERS

	DISTR.	NUMBER OF HEAT EXCHANGER PASSES				UNITS
		20	21	23	25	
GAS MASS 121.8 LBM/S	U	6748	6820	6944	7043	HP
	1	6010	6110	6286	6433	HP
	U	11.99	12.11	12.31	12.51	LBM/S
	1	10.67	10.85	11.17	11.43	LBM/S
GAS MASS 99.1 LBM/S	U	4370	4414	4484	4538	HP
	1	3964	4020	4123	4211	HP
	U	7.76	7.84	7.96	8.06	LBM/S
	1	7.04	7.14	7.32	7.48	LBM/S
GAS MASS 77.4 LBM/S	U	2884	2908	2948	2978	HP
	1	2654	2693	2756	2809	HP
	U	5.12	5.17	5.24	5.29	LBM/S
	1	4.71	4.78	4.90	4.99	LBM/S
GAS MASS 66.7 LBM/S	U	2466	2485	2515	2537	HP
	1	2281	2312	2365	2408	HP
	U	4.38	4.41	4.47	4.51	LBM/S
	1	4.05	4.11	4.20	4.28	LBM/S

TABLE VI. POWER AND FLUID FLOW RATE FOR VARIOUS
STEAM OPERATING PRESSURES

	DISTR.	OPERATING PRESSURE			UNITS
		400	500	600	
GAS MASS 121.8 LBM/S	U	6944	6672	6423	HP
	1	6286	6041	5821	HP
	U	12.33	12.06	11.82	LBM/S
	1	11.17	10.92	10.71	LBM/S
GAS MASS 99.1 LBM/S	U	4484	4245	4027	HP
	1	4123	3904	3697	HP
	U	7.96	7.67	7.41	LBM/S
	1	7.32	7.05	6.80	LBM/S
GAS MASS 77.4 LBM/S	U	2948	2749	2569	HP
	1	2756	2571	2398	HP
	U	5.24	4.97	4.73	LBM/S
	1	4.90	4.65	4.41	LBM/S
GAS MASS 66.7 LBM/S	U	2515	2339	2179	HP
	1	2365	2208	2055	HP
	U	4.47	4.23	4.01	LBM/S
	1	4.20	3.99	3.78	LBM/S

LAYOUT OF MARINE GAS TURBINE WASTE-HEAT STEAM GENERATOR: ONCE-THROUGH,
COUNTER-CROSS FLOW HEAT EXCHANGER

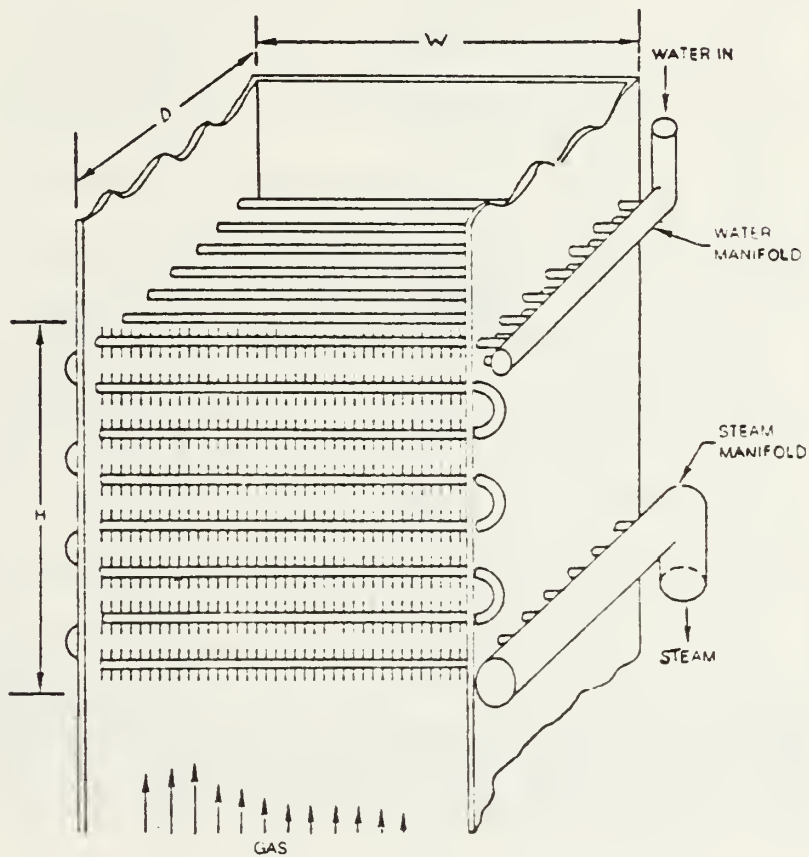



Figure 1. Waste Heat Recovery Unit Layout

NR = Number of Heat Exchanger Passes

 = General Node (m,n)

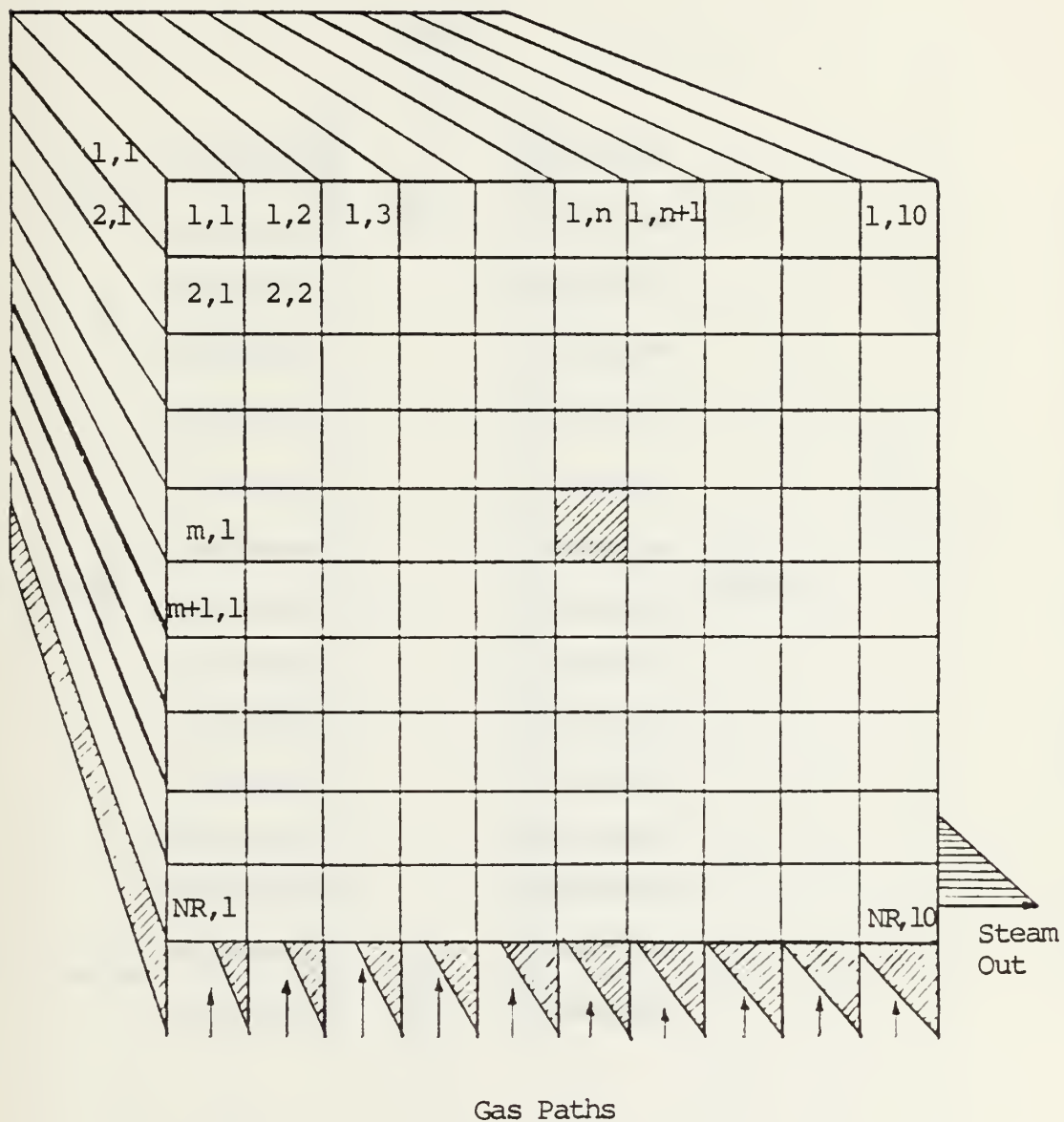


Figure 2. Heat Exchanger Nodal Arrangement

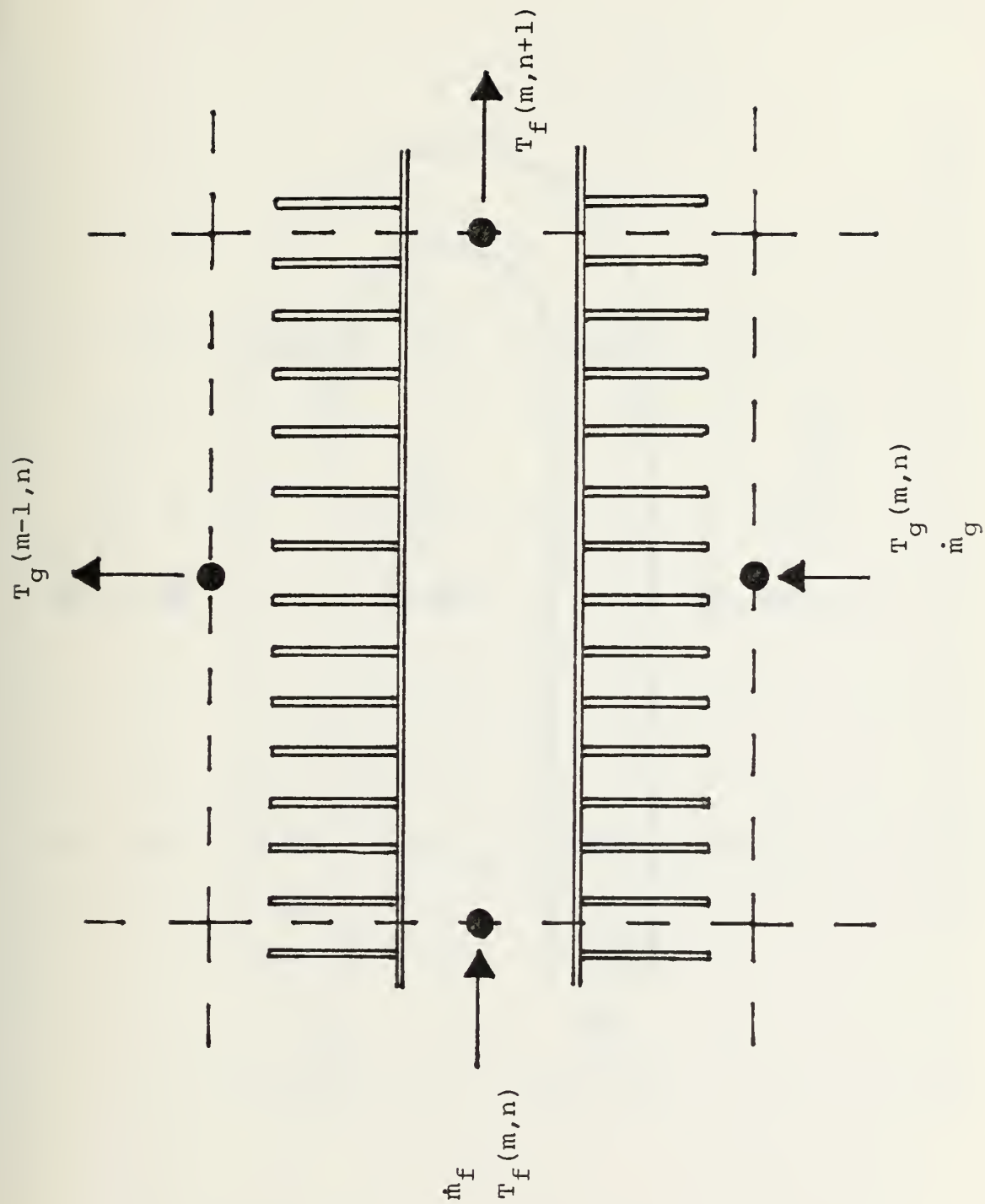


Figure 3. Typical Nodal Gas and Fluid Flow

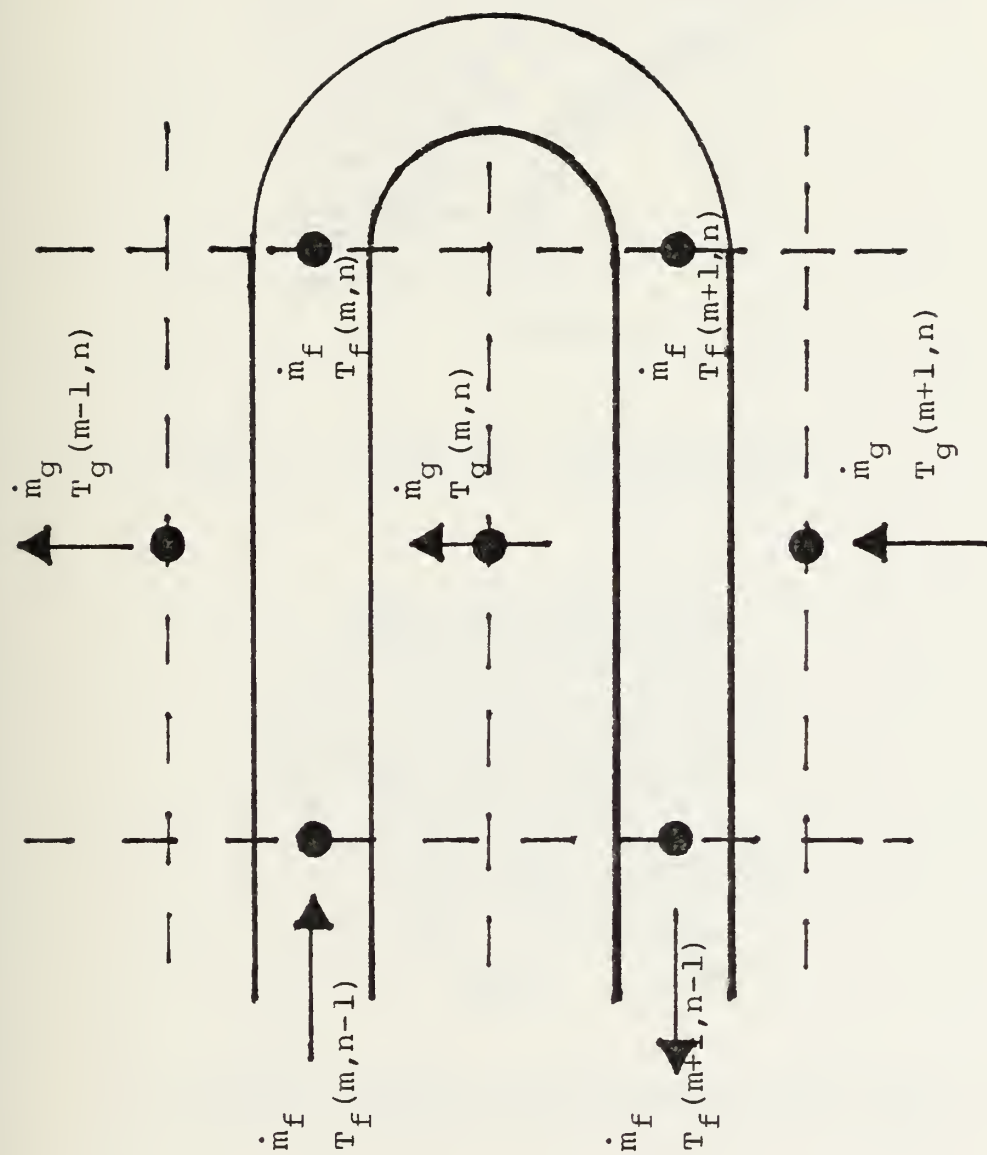


Figure 4. Nodal Gas and Fluid Flow for End of Pass Condition

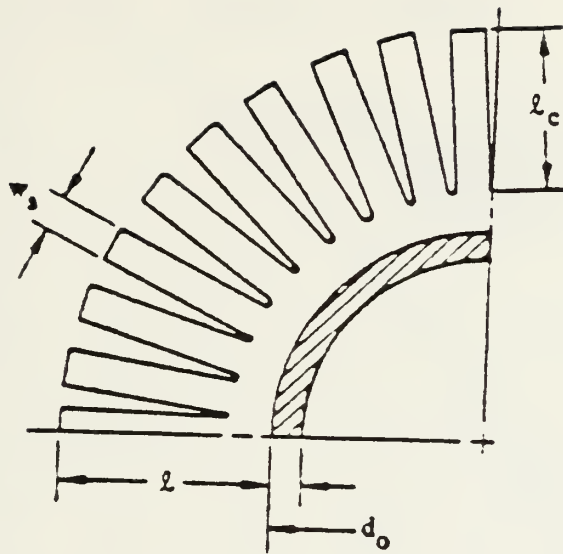


Figure 5. Tube Fin Configuration

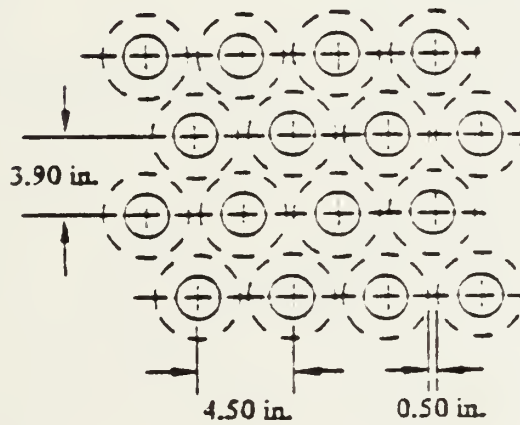


Figure 6. Waste Heat Recovery Unit Tube Layout

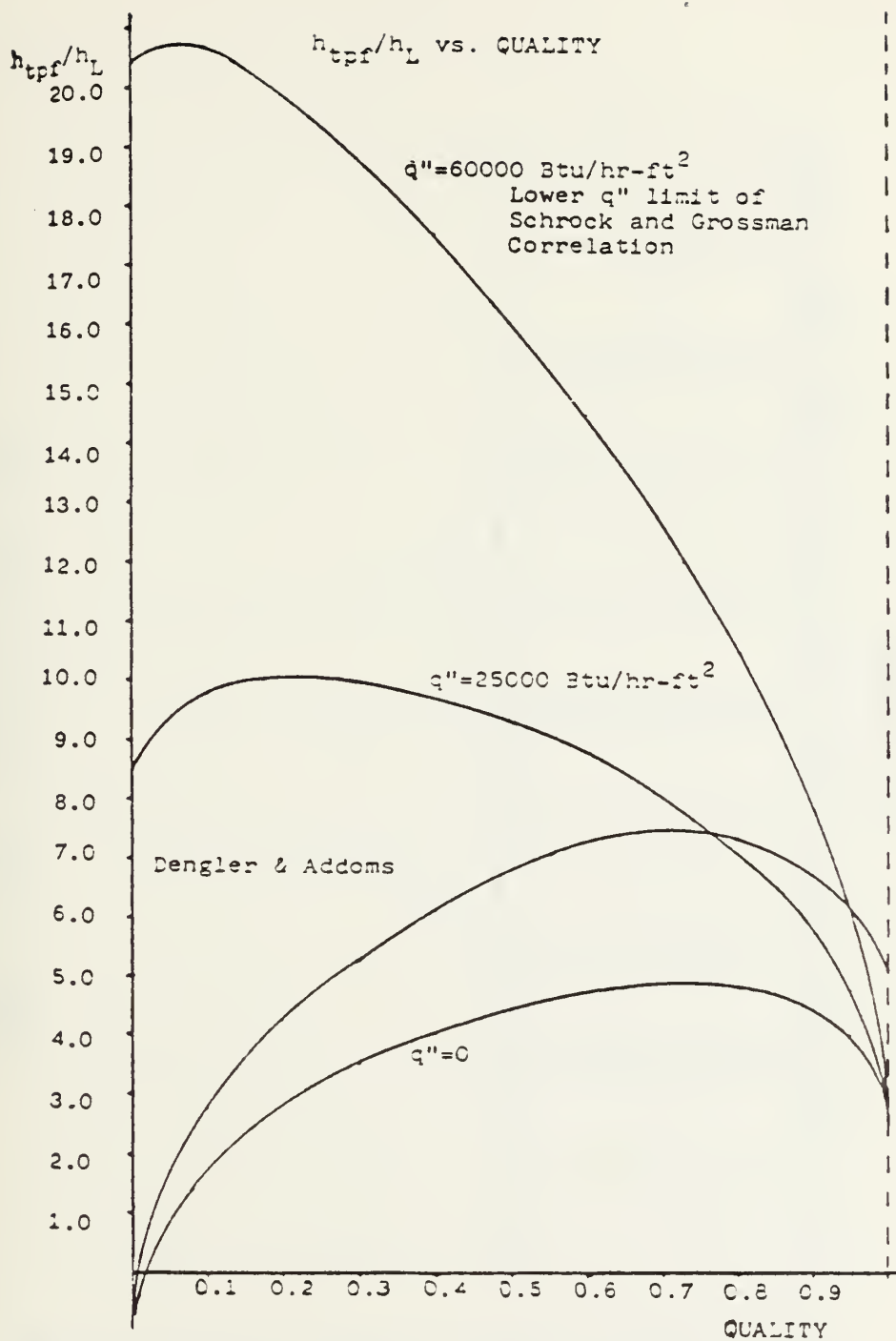


Figure 7. h_{TPf}/h_L vs. Quality

GAS FLOW DISTRIBUTION

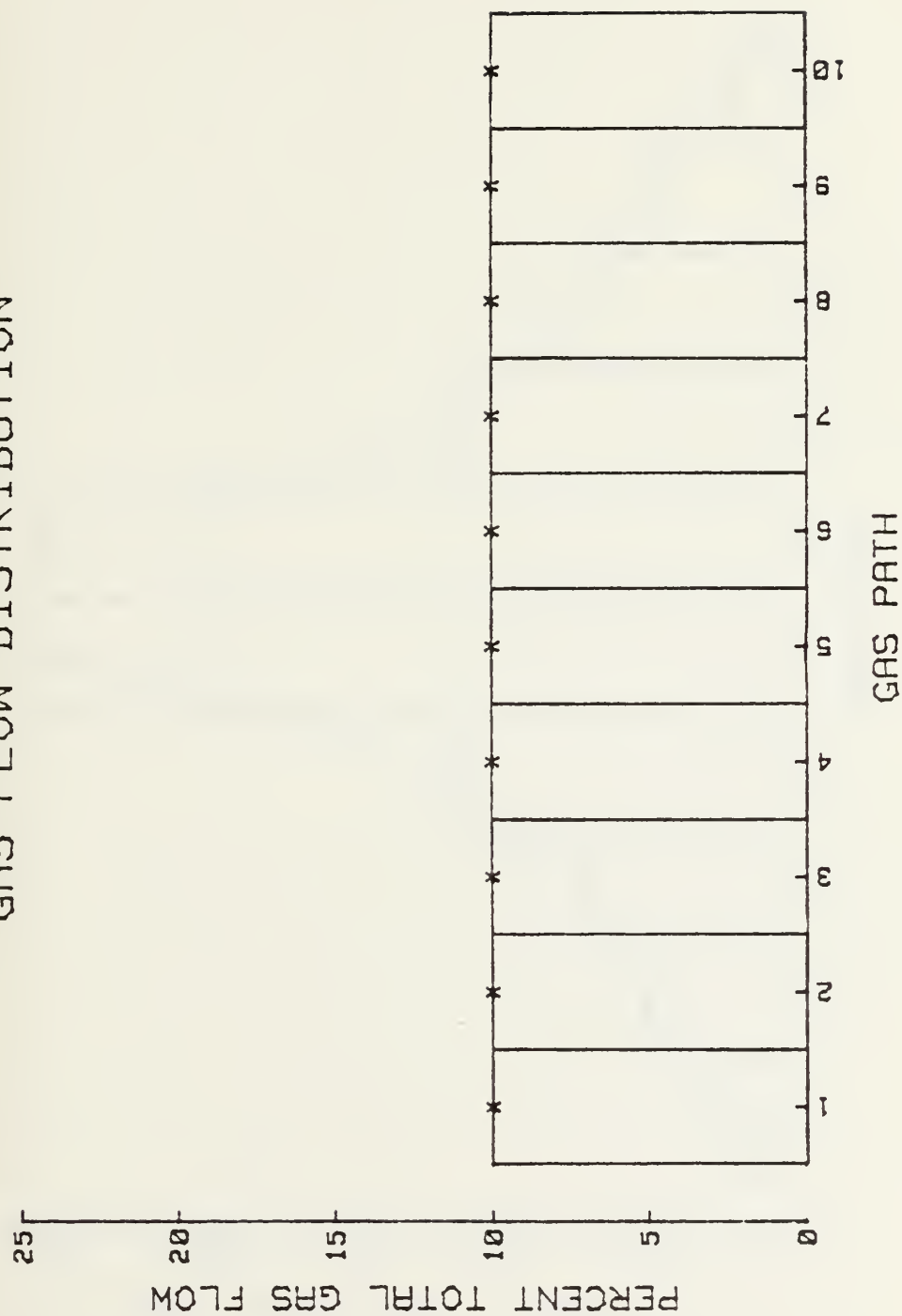


Figure 8-A. Uniform Flow Distribution

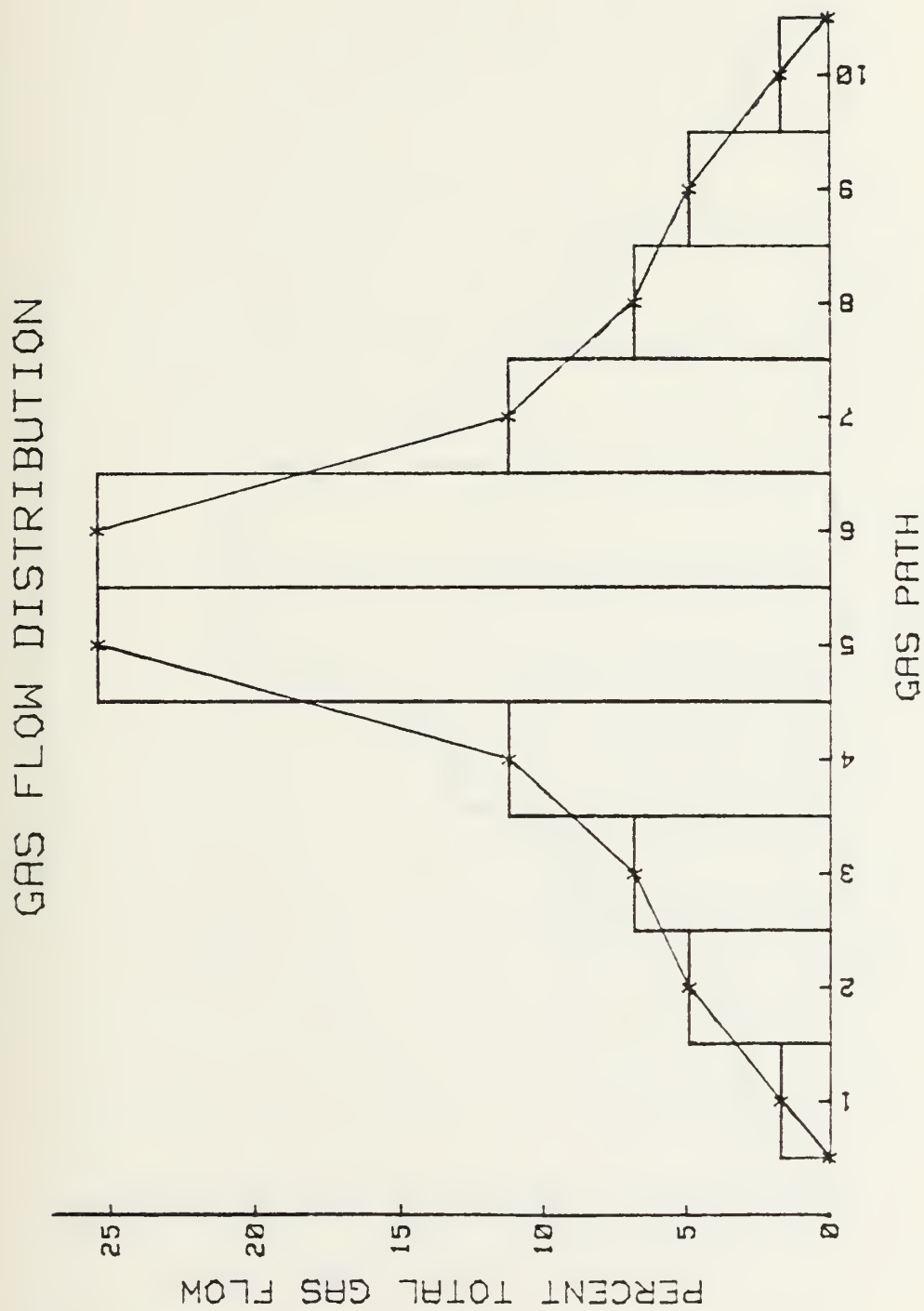


Figure 8-B. Flow Distribution #1

GAS FLOW DISTRIBUTION

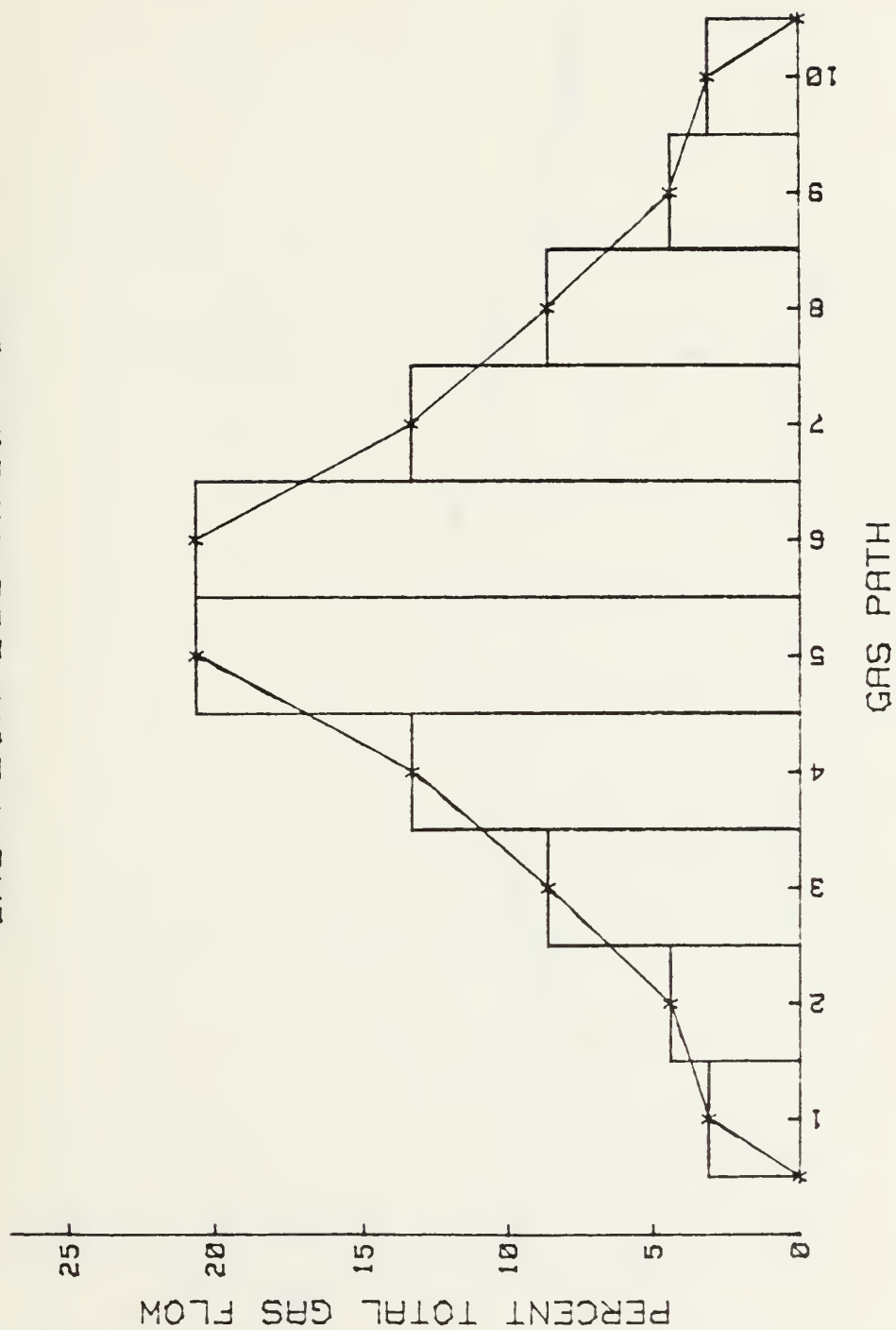


Figure 8-C. Flow Distribution #2

GAS FLOW DISTRIBUTION

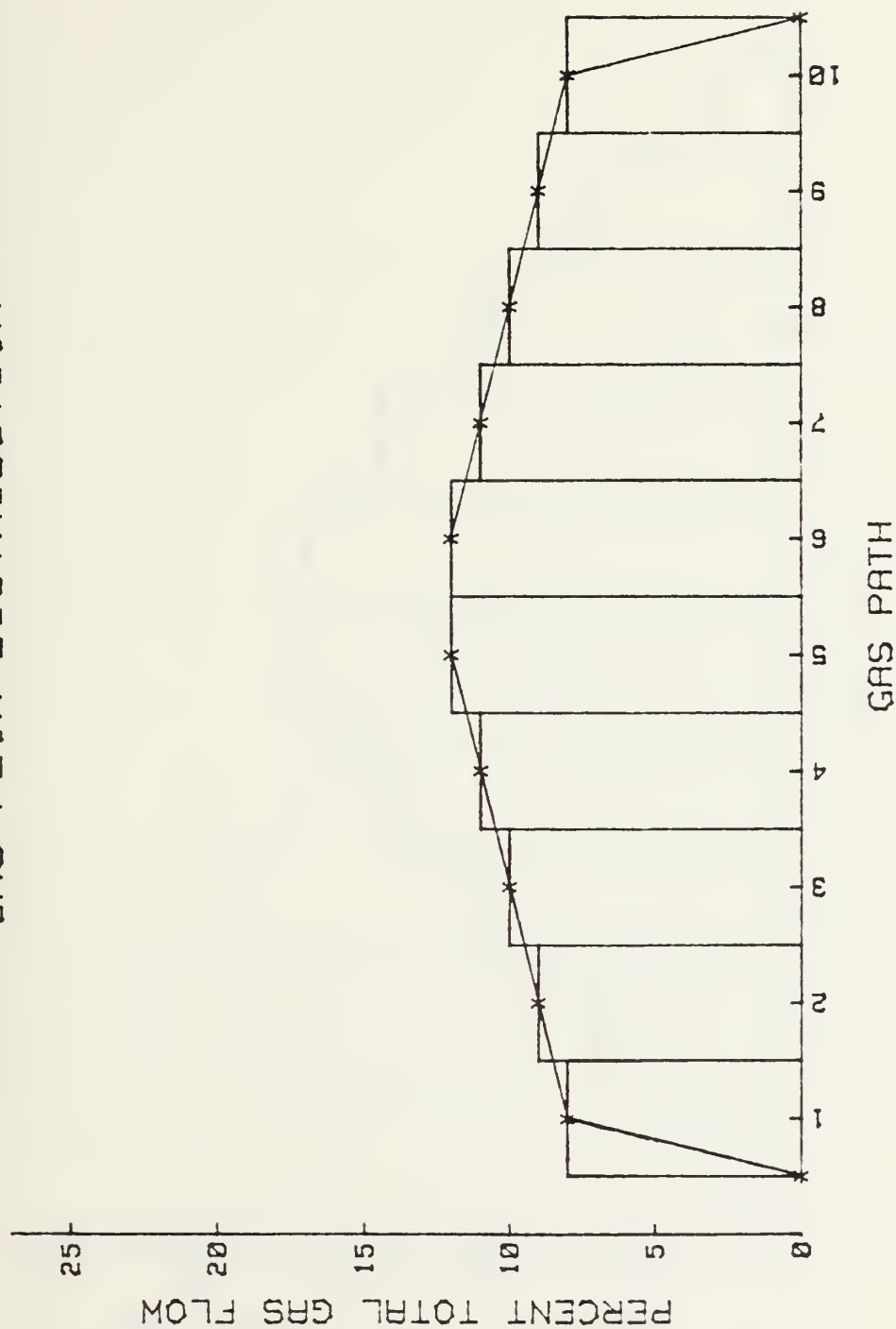


Figure 8-D. Flow Distribution #3

GAS FLOW DISTRIBUTION

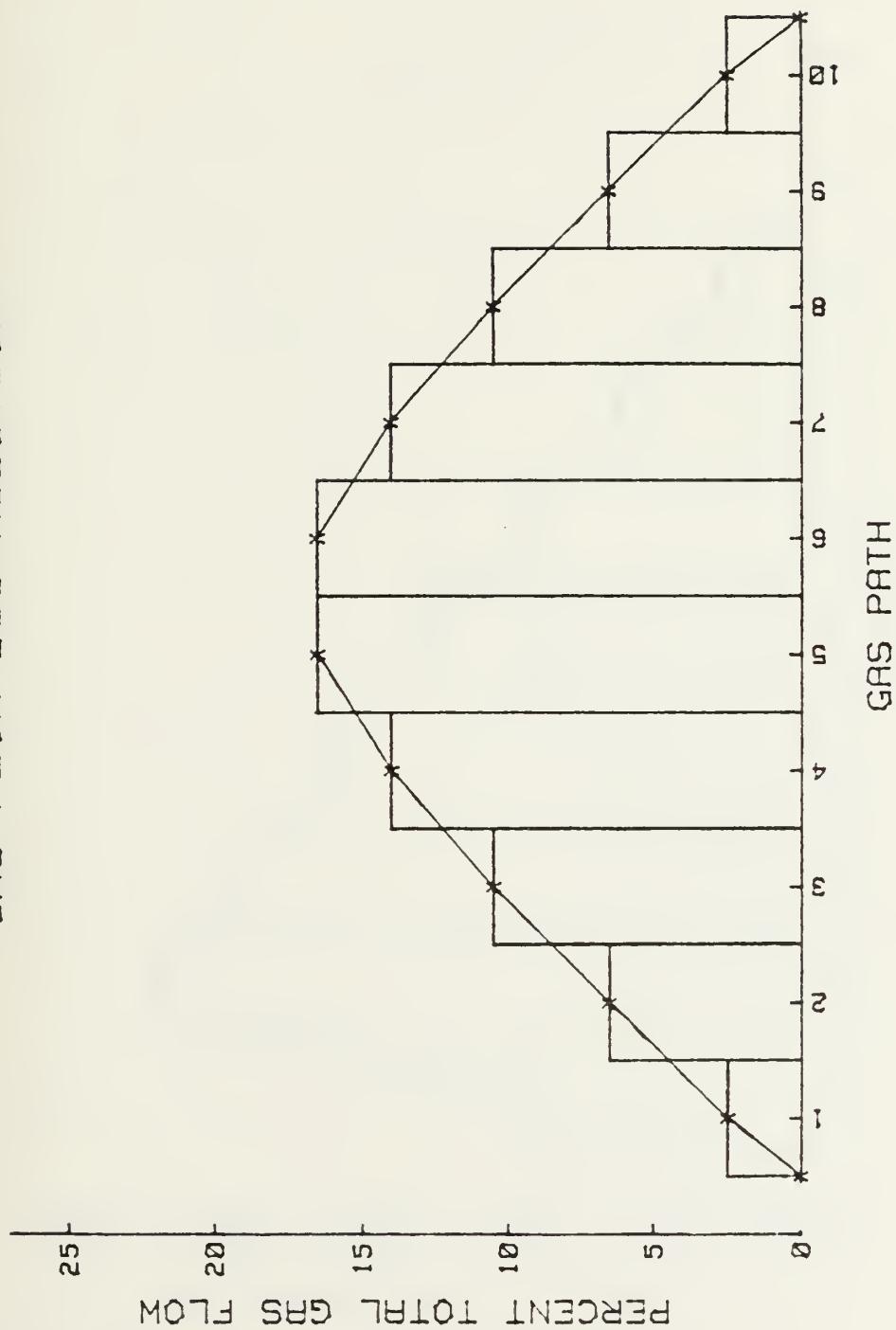


Figure 8-E. Flow Distribution #4

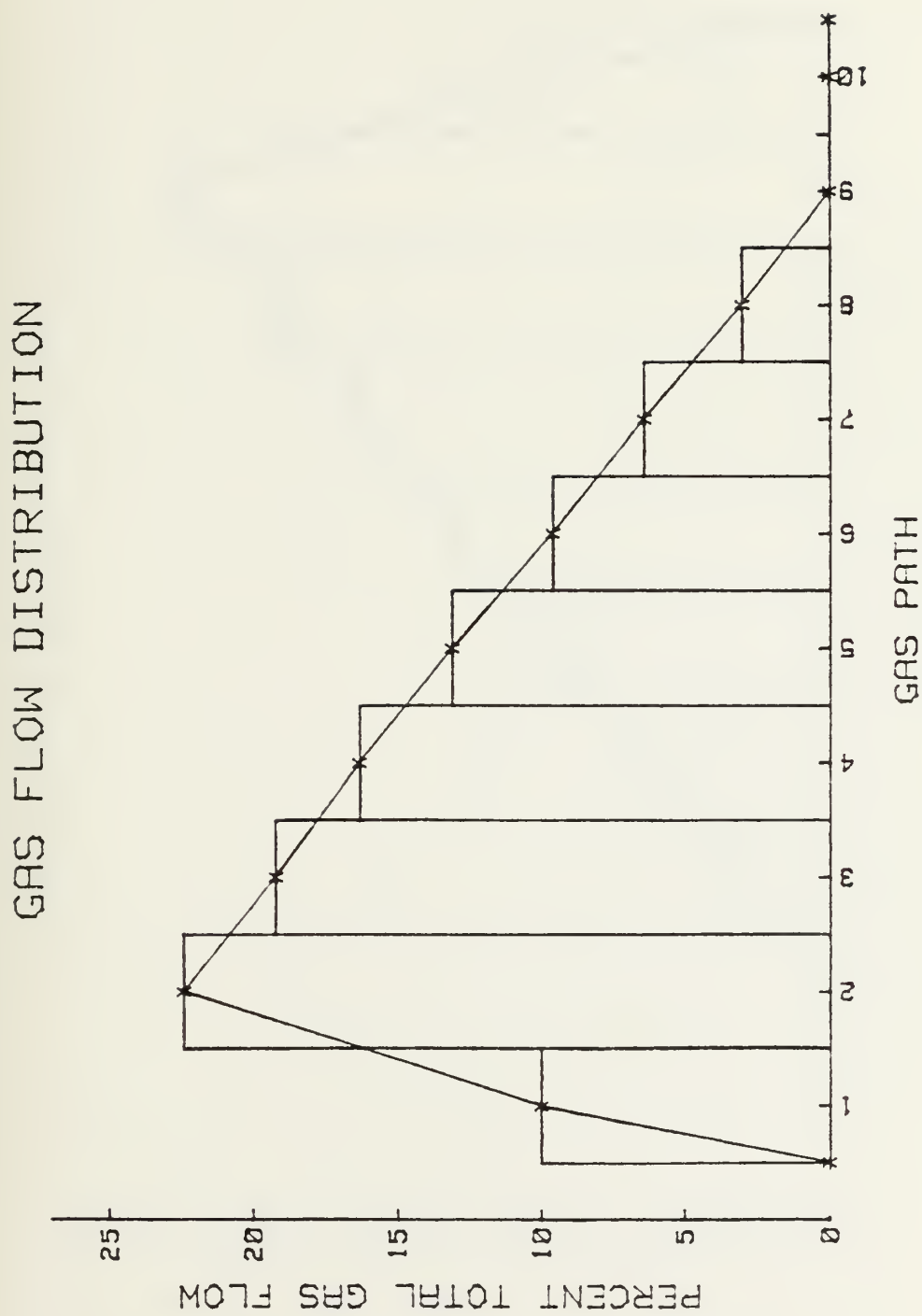


Figure 8-F. Flow Distribution #5

GAS FLOW DISTRIBUTION

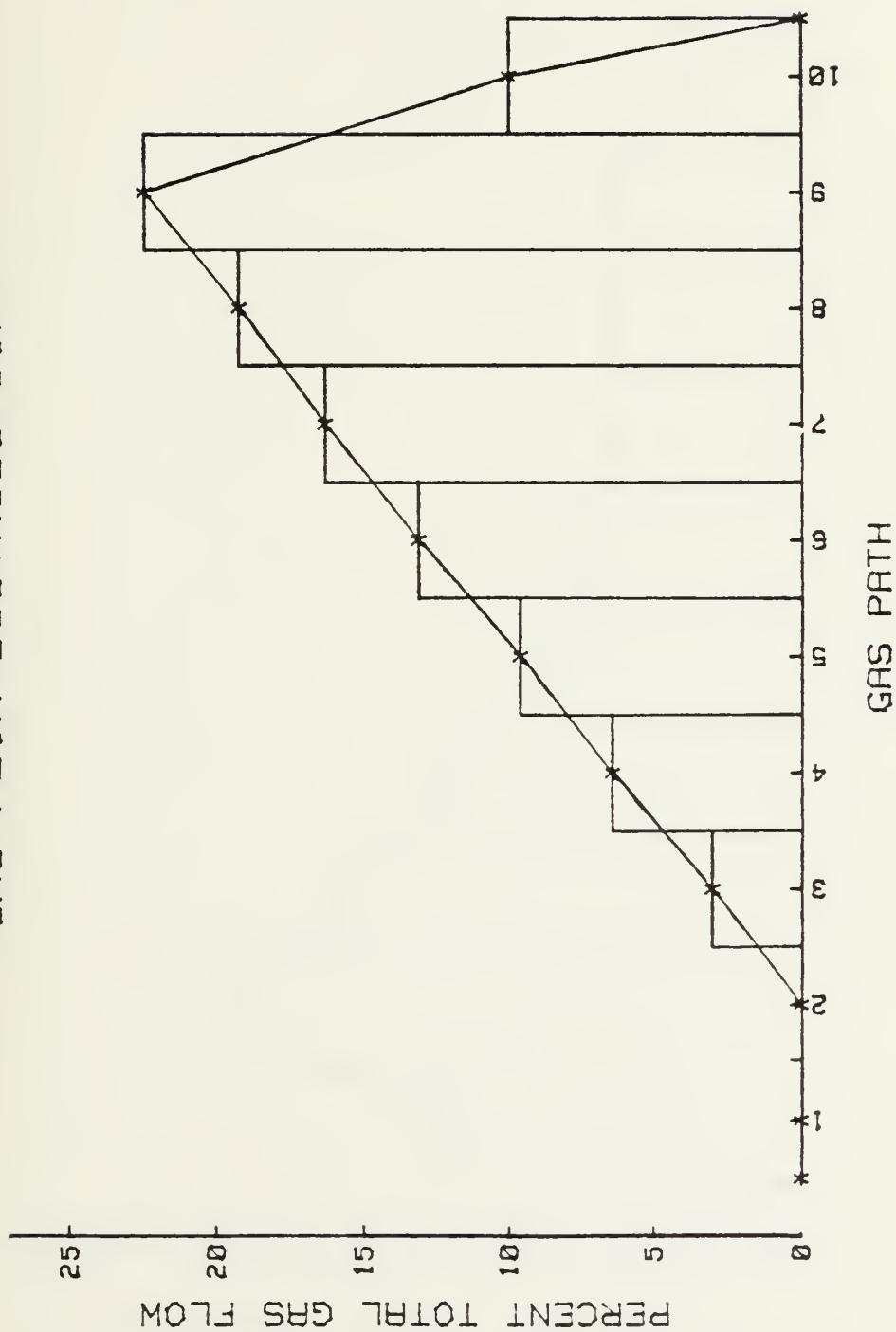


Figure 8-G. Flow Distribution #6

GAS FLOW DISTRIBUTION

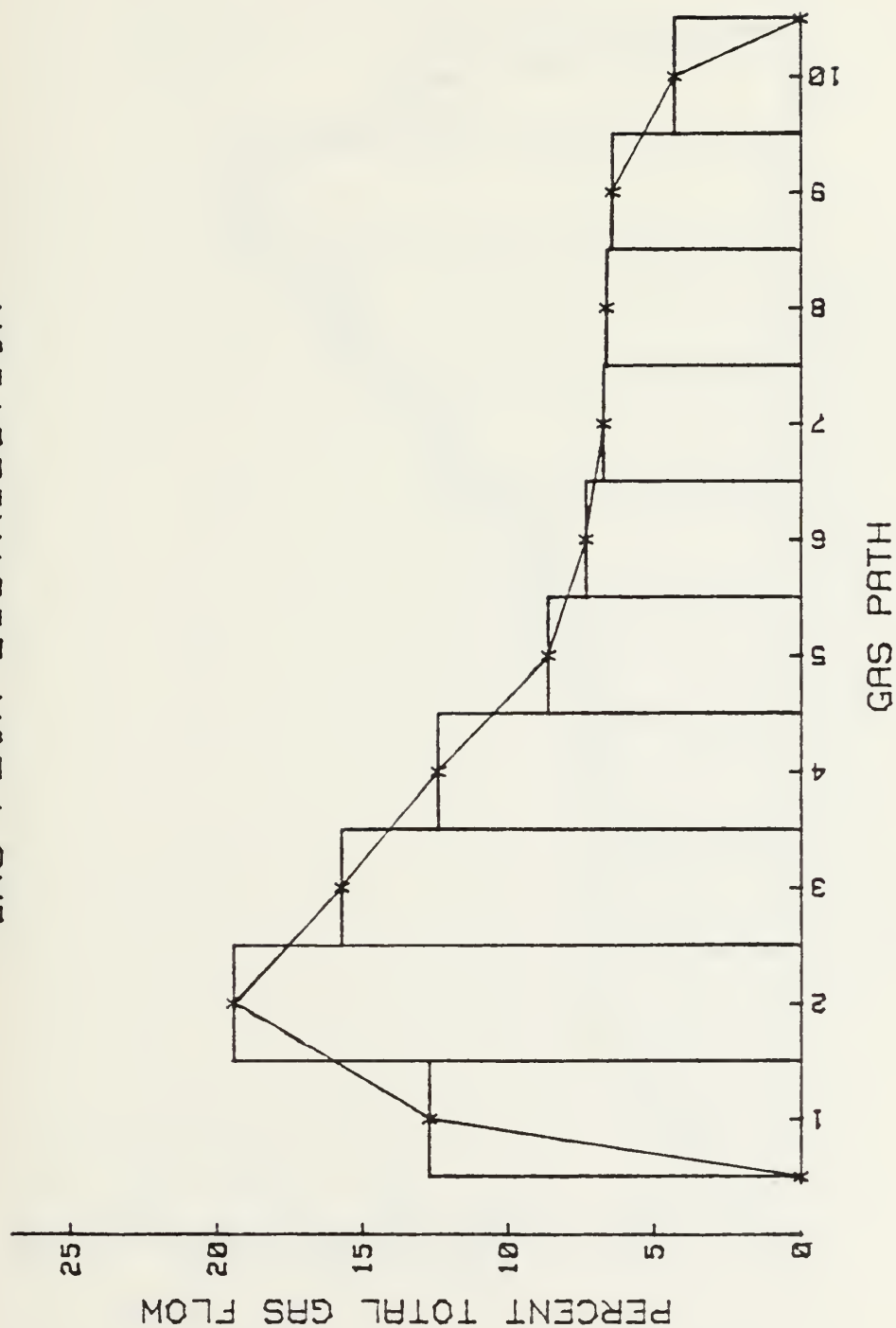


Figure 8-H. Flow Distribution #7

GAS FLOW DISTRIBUTION

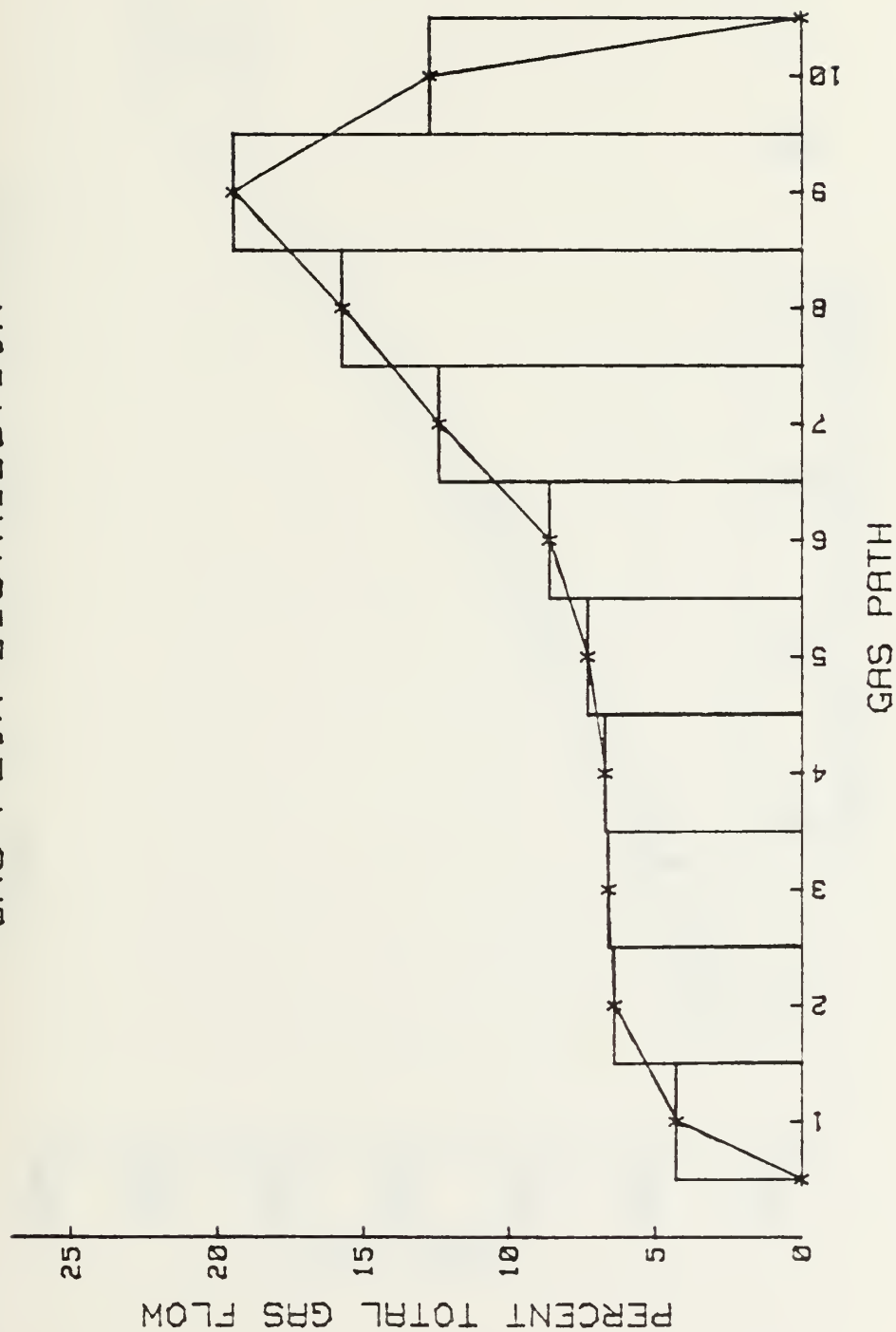


Figure 8-1. Flow Distribution #8

POWER VS. GAS MASS FLOW RATE

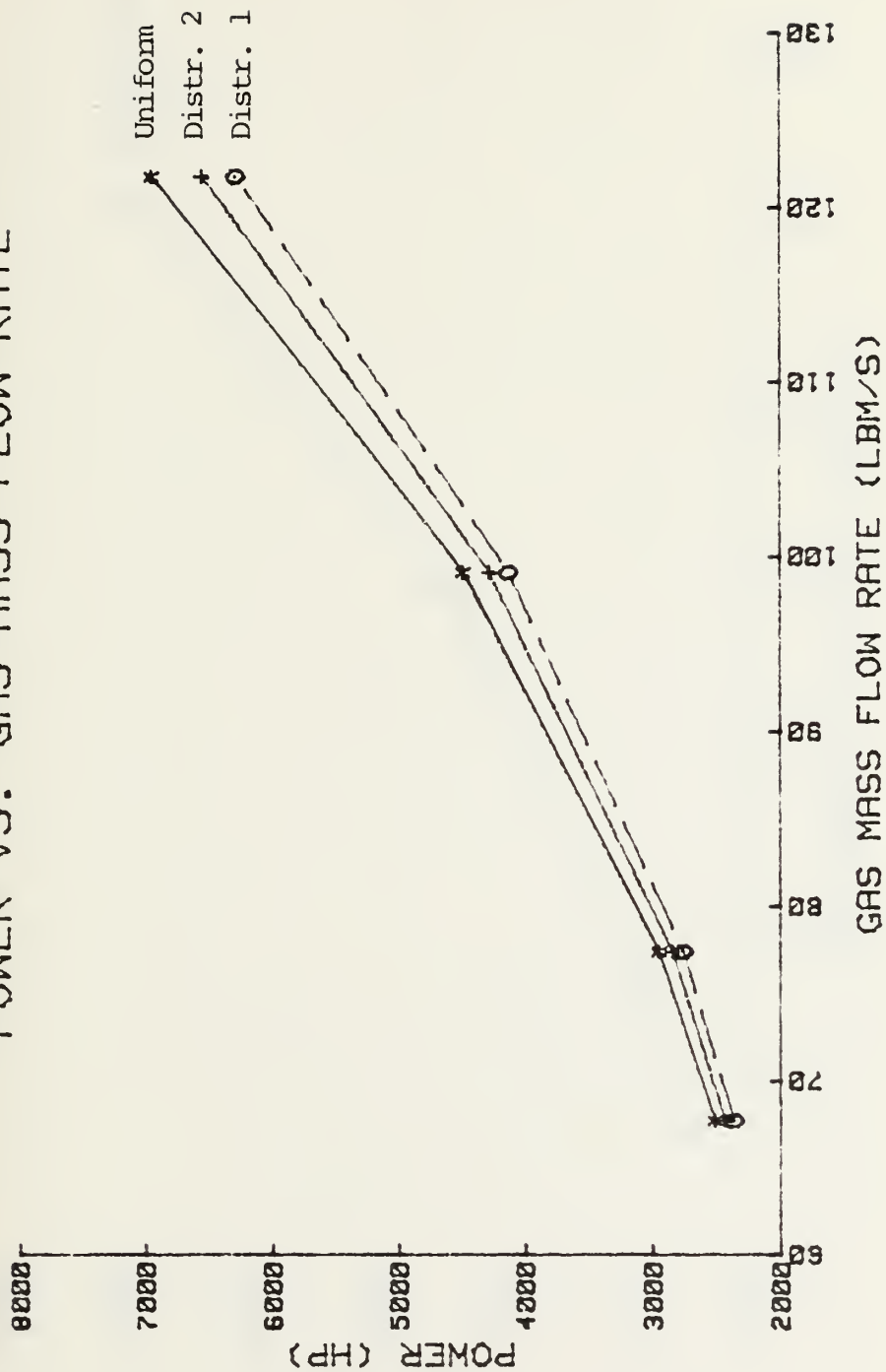


Figure 9-A. Power vs. Gas Flow Rate (Distr.'s U,1,2)

POWER VS. GAS MASS FLOW RATE

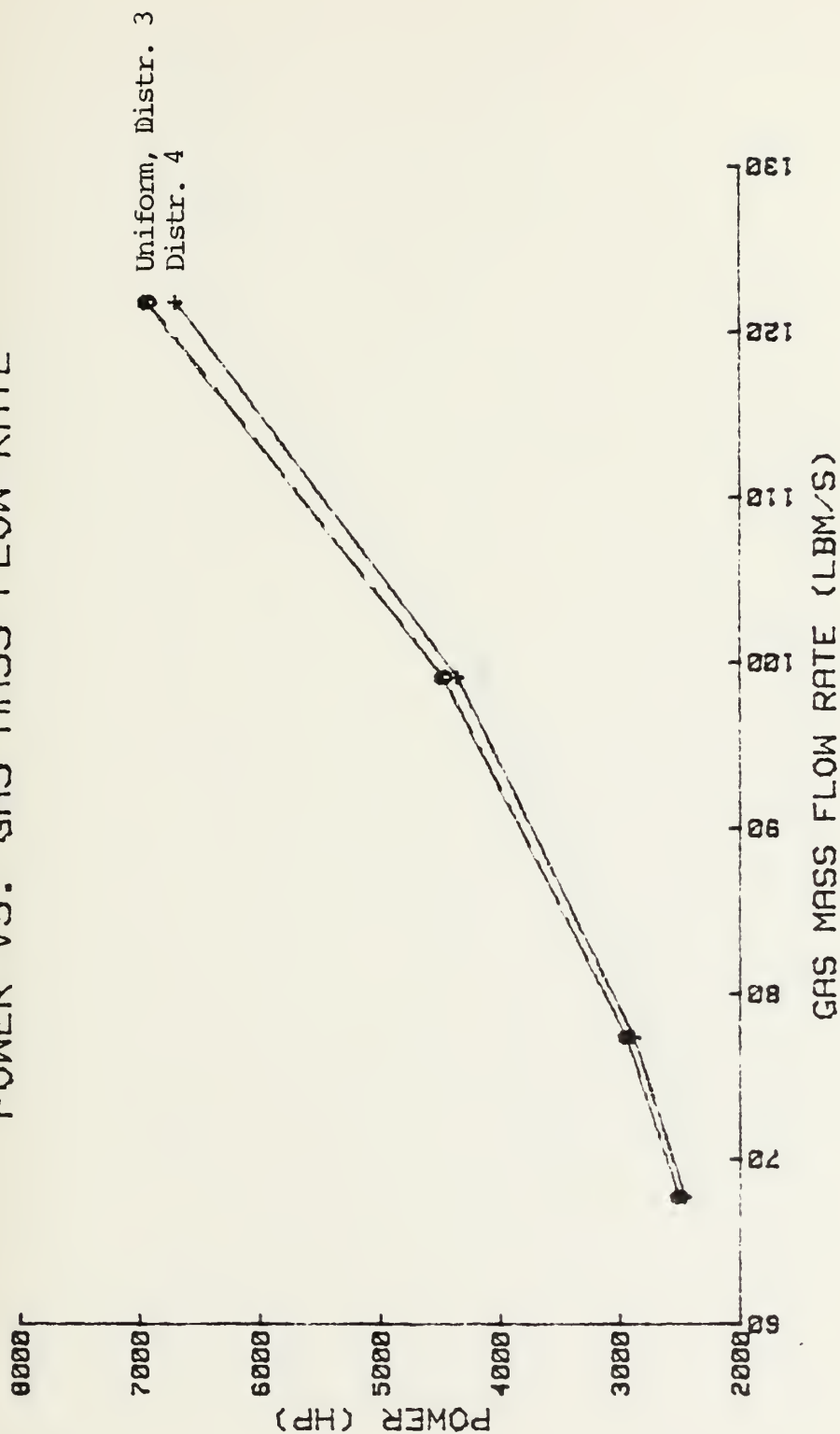


Figure 9-B. Power vs. Gas Flow Rate (Distr.'s U,3,4)

POWER VS. GAS MASS FLOW RATE

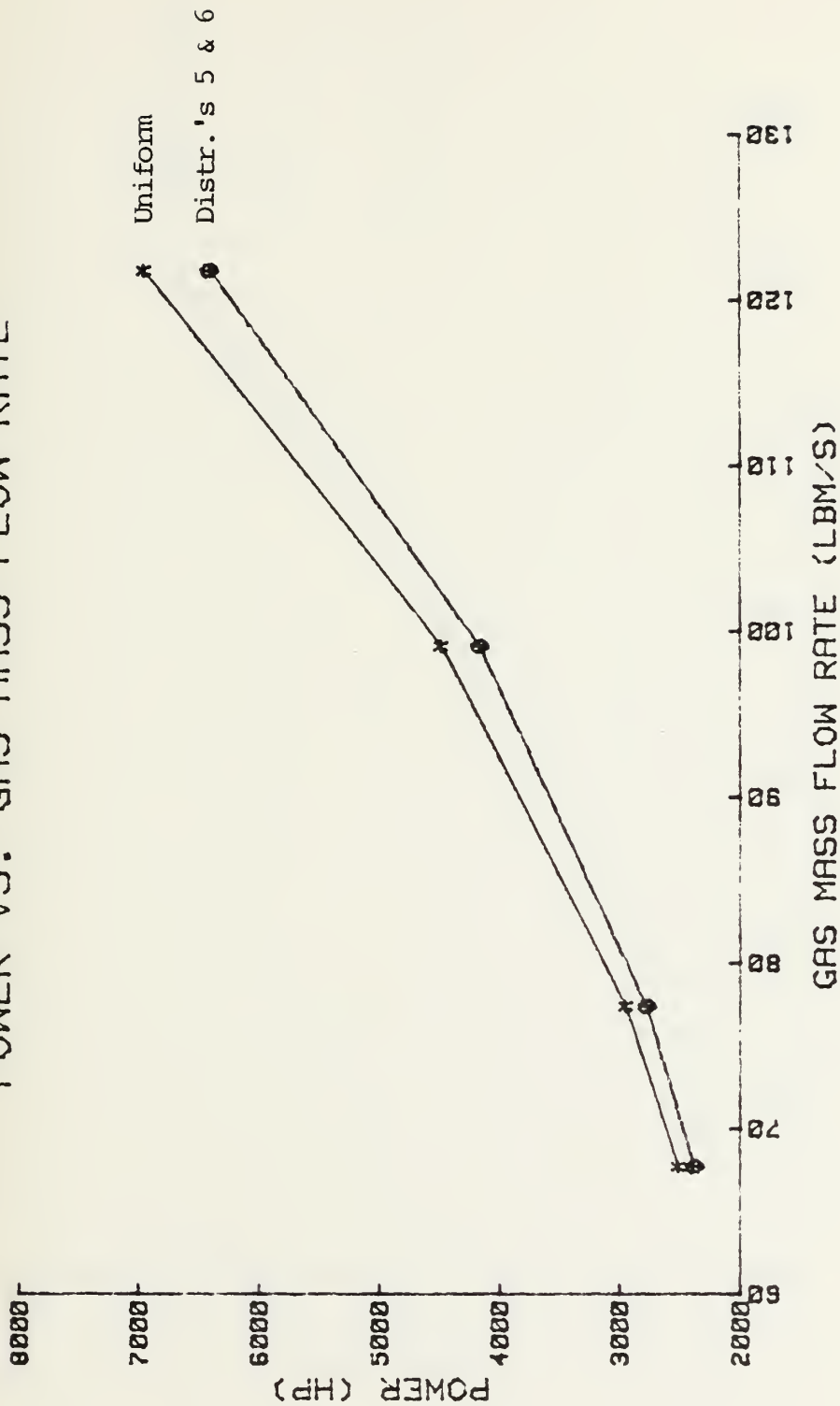


Figure 9-C. Power vs. Gas Flow Rate (Distr.'s U,5,6)

POWER VS. GAS MASS FLOW RATE

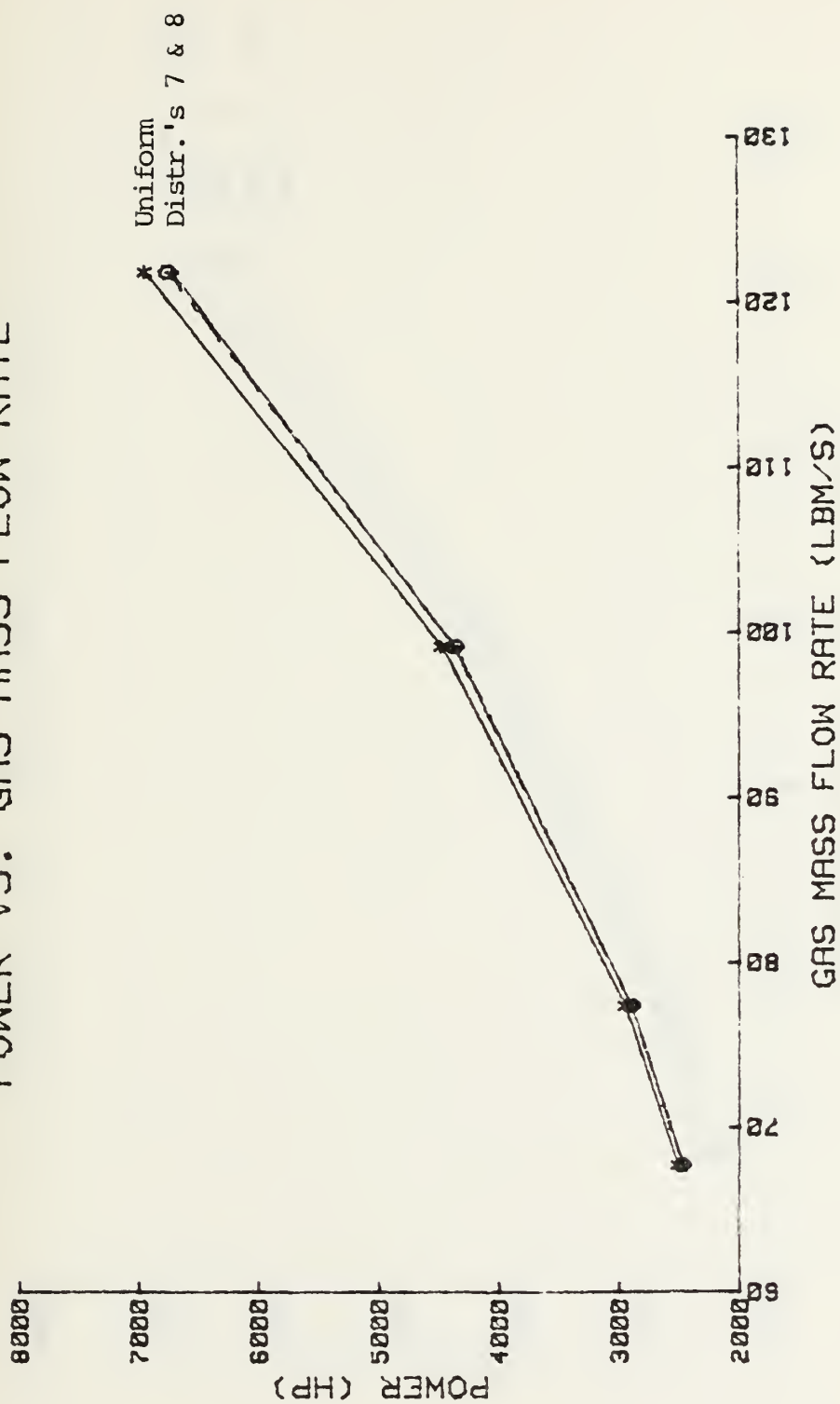


Figure 9-D. Power vs. Gas Flow Rate (Distr. 's U,7,8)

POWER VS. GAS MASS FLOW RATE

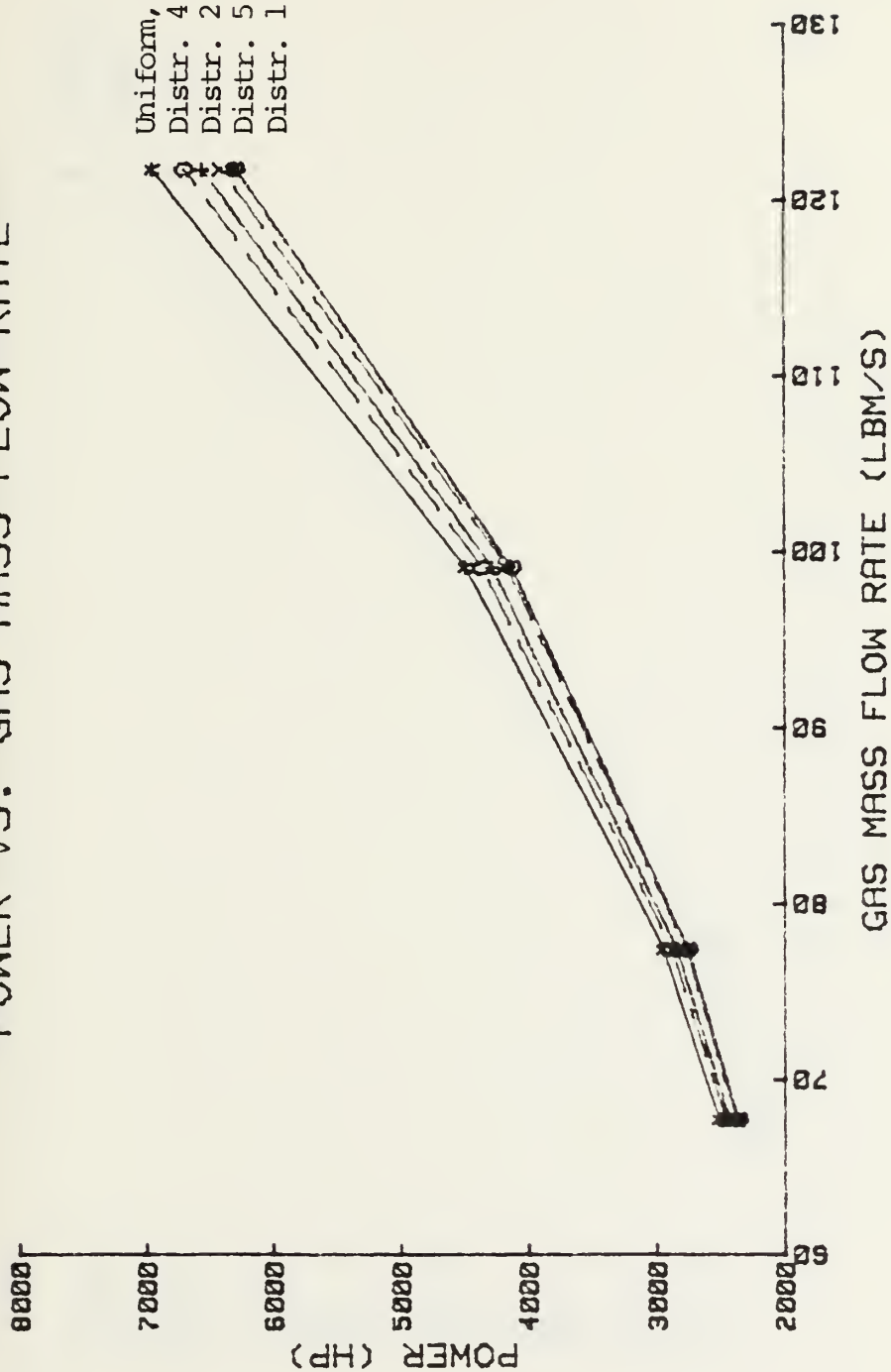


Figure 9-E. Power vs. Gas Flow Rate (Composite)

FLUID FLOW RATE VS. GAS FLOW RATE

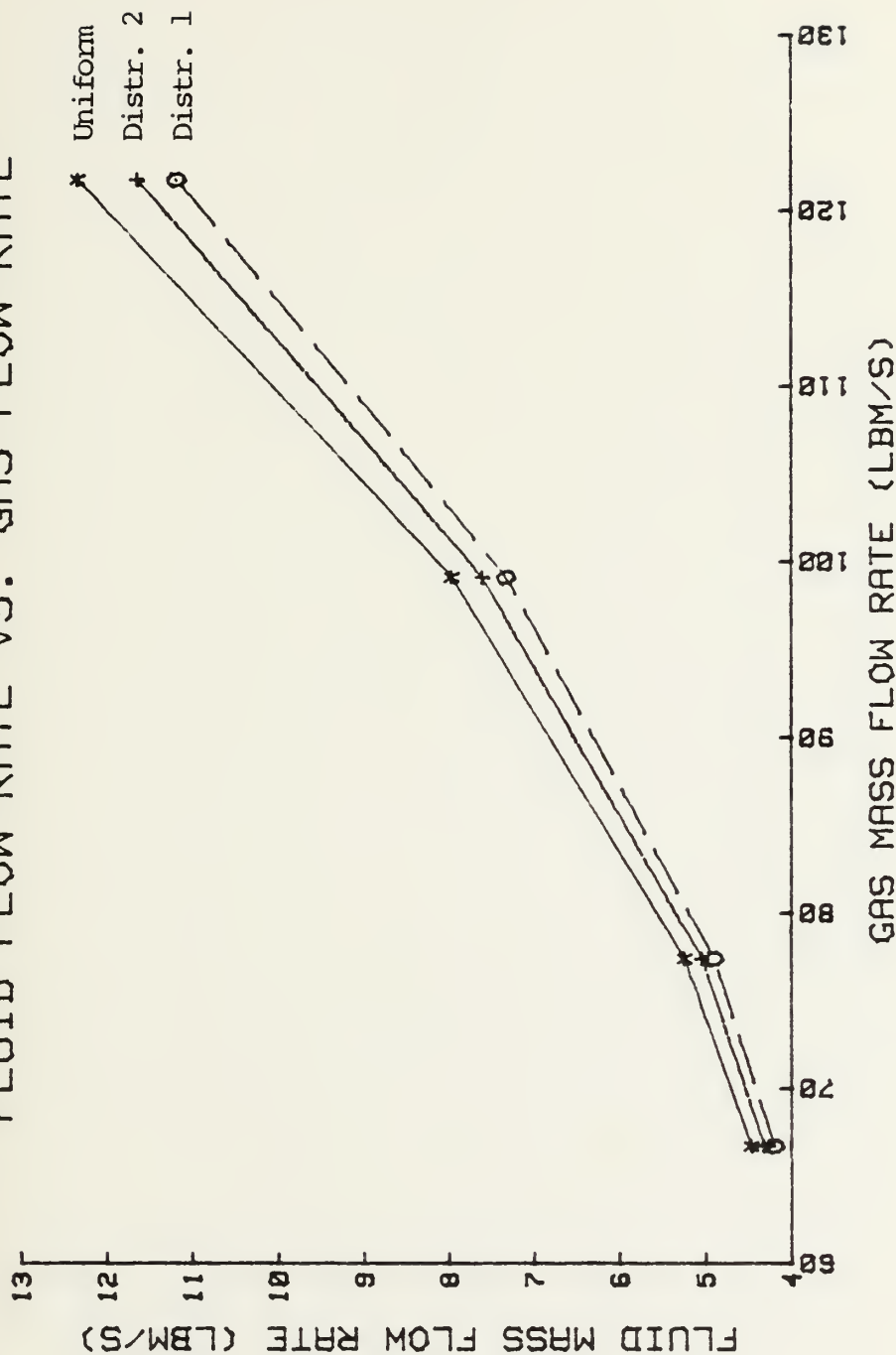


Figure 10-A. Fluid Flow Rate vs. Gas Flow Rate (Distr.'s U,1,2)

FLUID FLOW RATE VS. GAS FLOW RATE

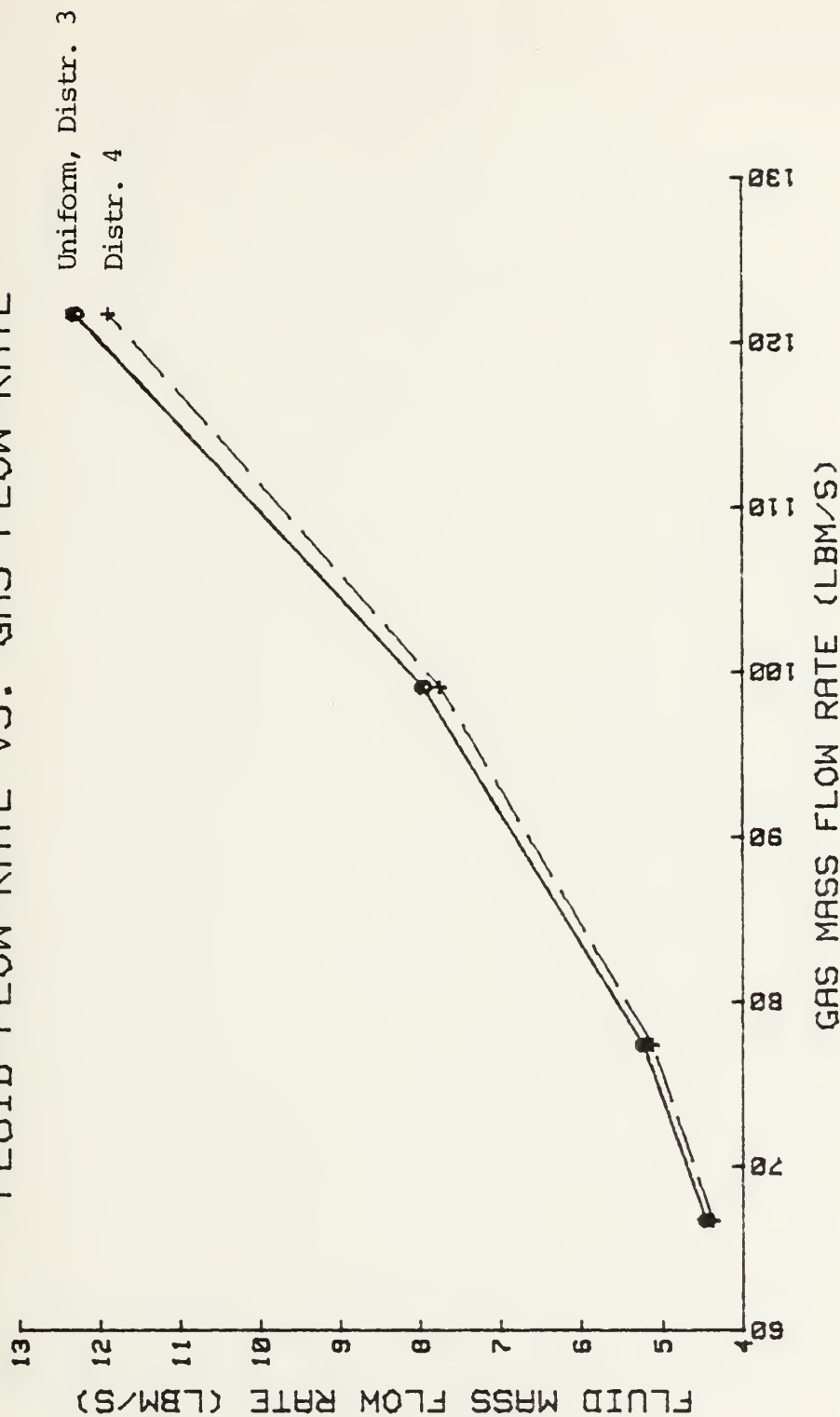


Figure 10-B. Fluid Flow Rate vs. Gas Flow Rate (Distr.'s U,3,4)

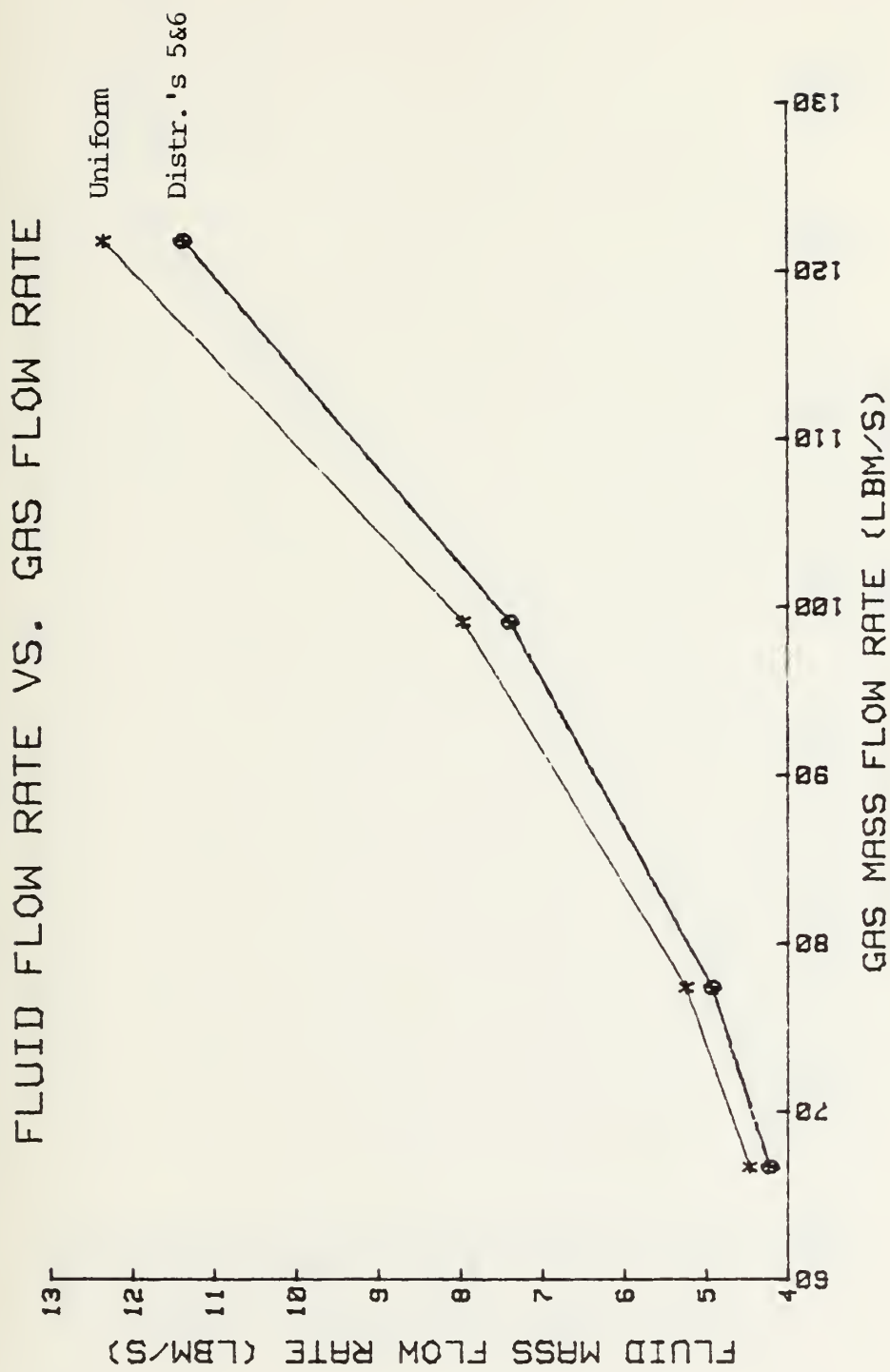


Figure 10-C. Fluid Flow Rate vs. Gas Flow Rate (Distr.'s U,5,6)

FLUID FLOW RATE VS. GAS FLOW RATE

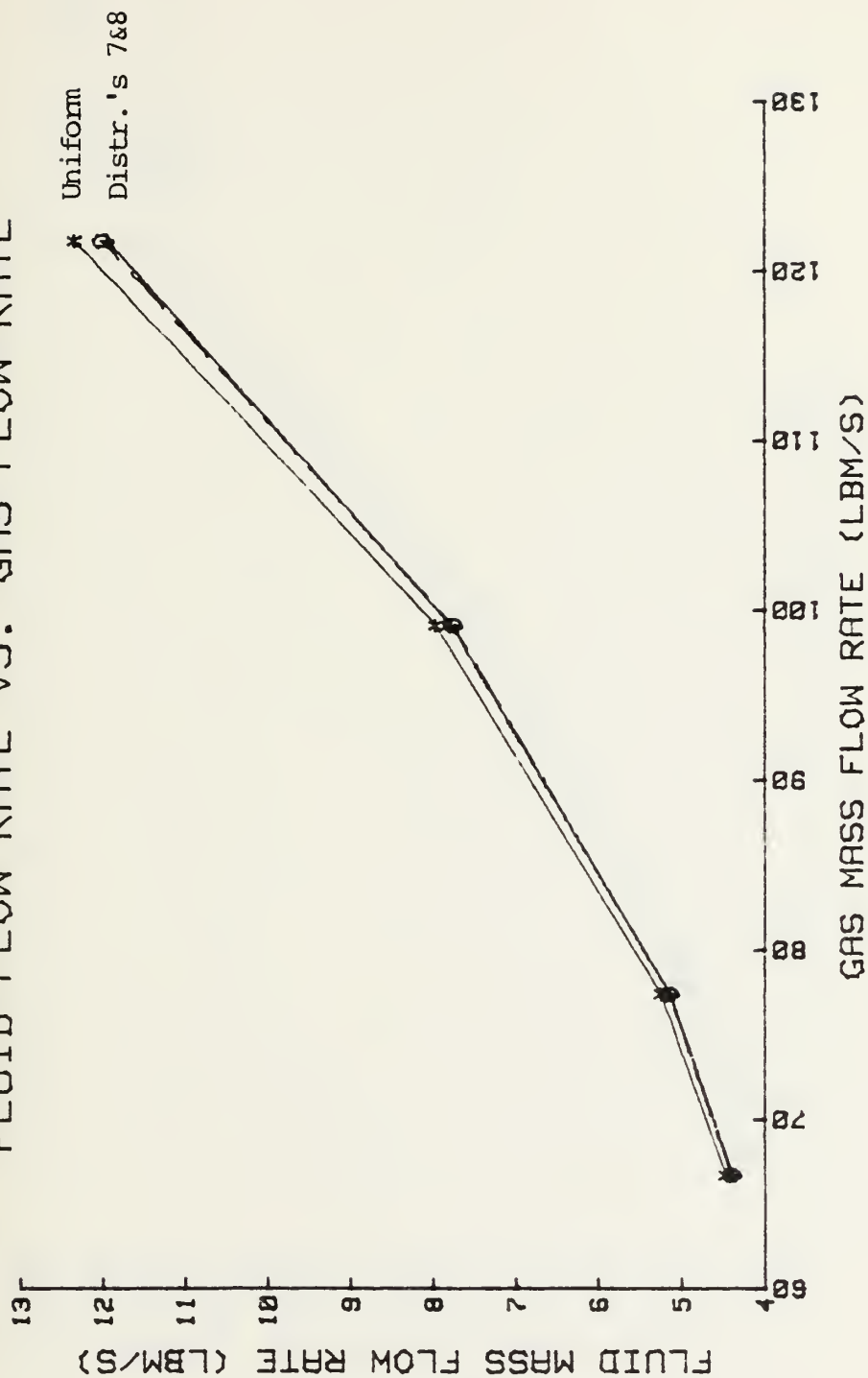


Figure 10-D. Fluid Flow Rate vs. Gas Flow Rate (Distr.'s U,7,8)

FLUID FLOW RATE VS. GAS FLOW RATE

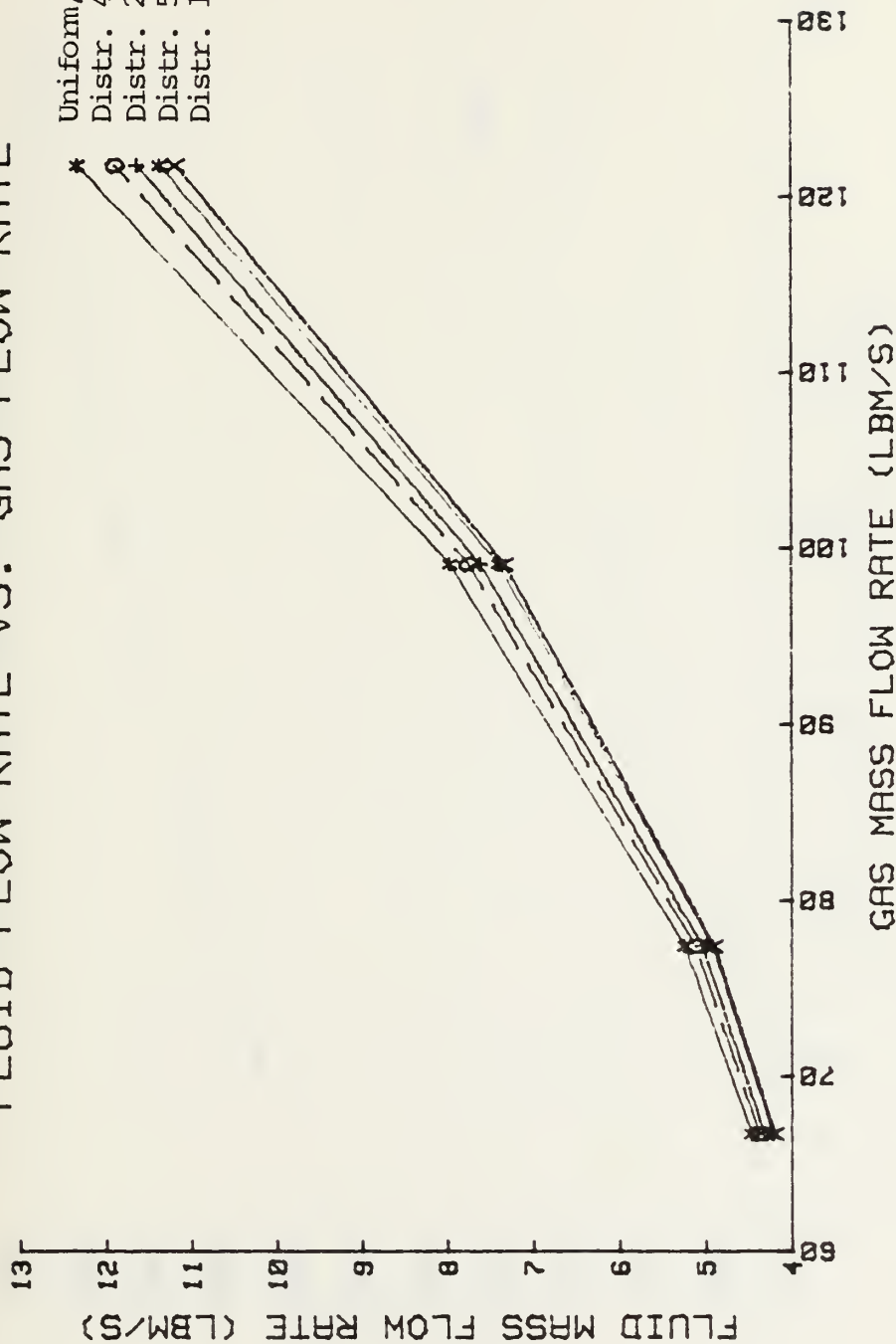


Figure 10-E. Fluid Flow Rate vs. Gas Flow Rate (Composite)

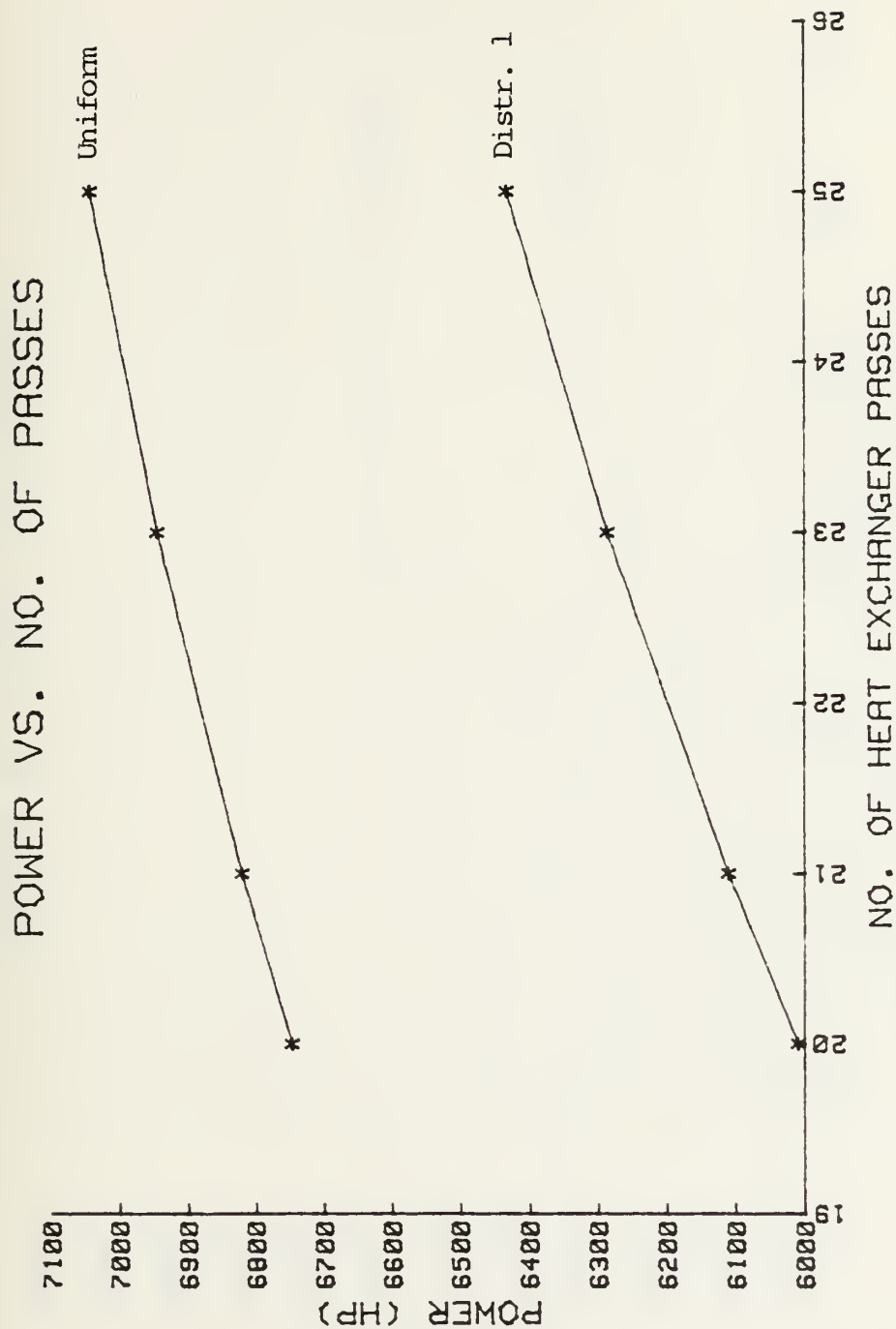


Figure 11-A. Power vs. No. of Heat Exchanger Passes
($m_g = 121.8 \text{ lbm/s}$)

POWER VS. NO. OF PASSES

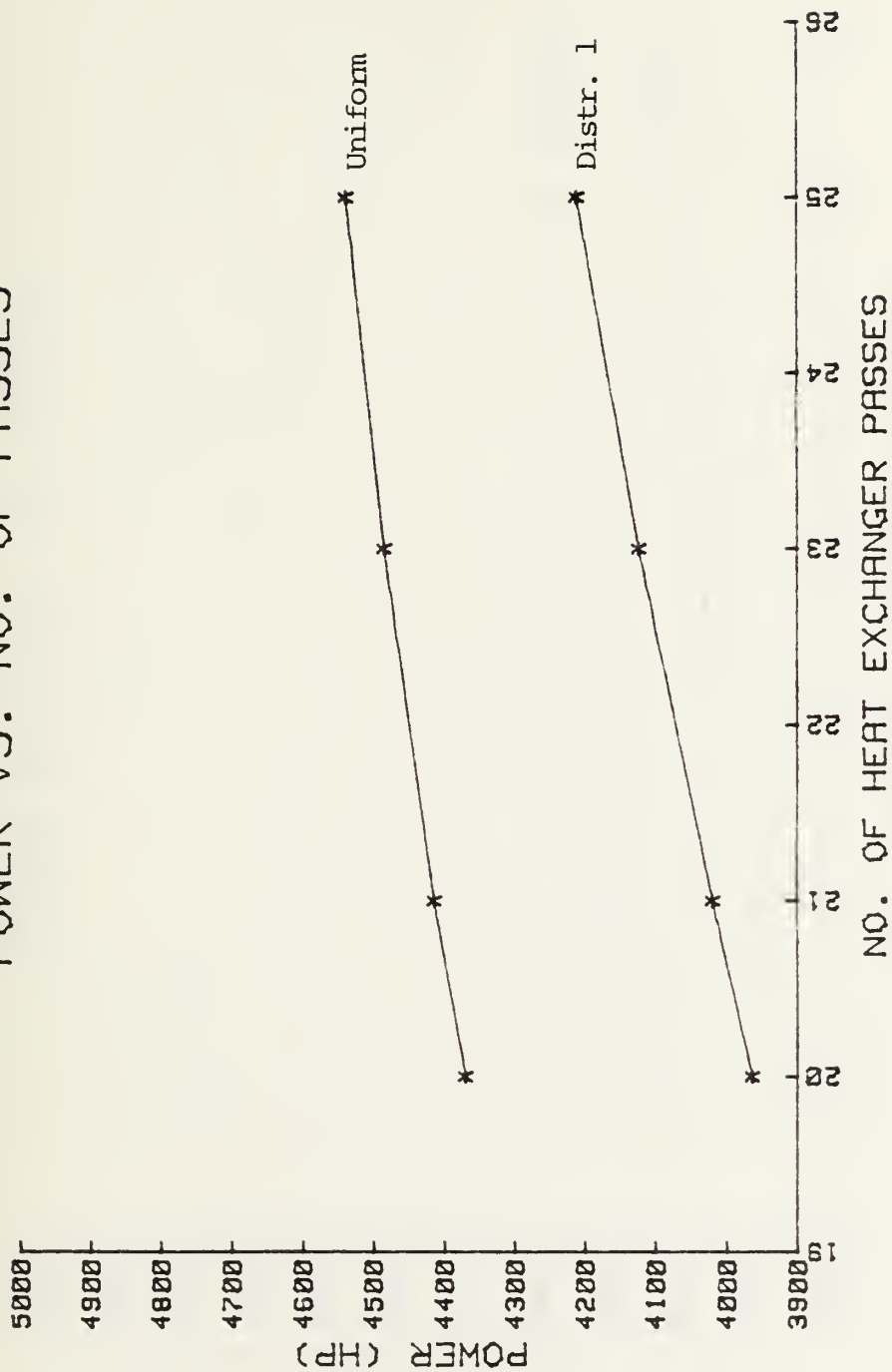


Figure 11-B. Power vs. No. of Heat Exchanger Passes ($m_g = 99.1 \text{ lbm/s}$)

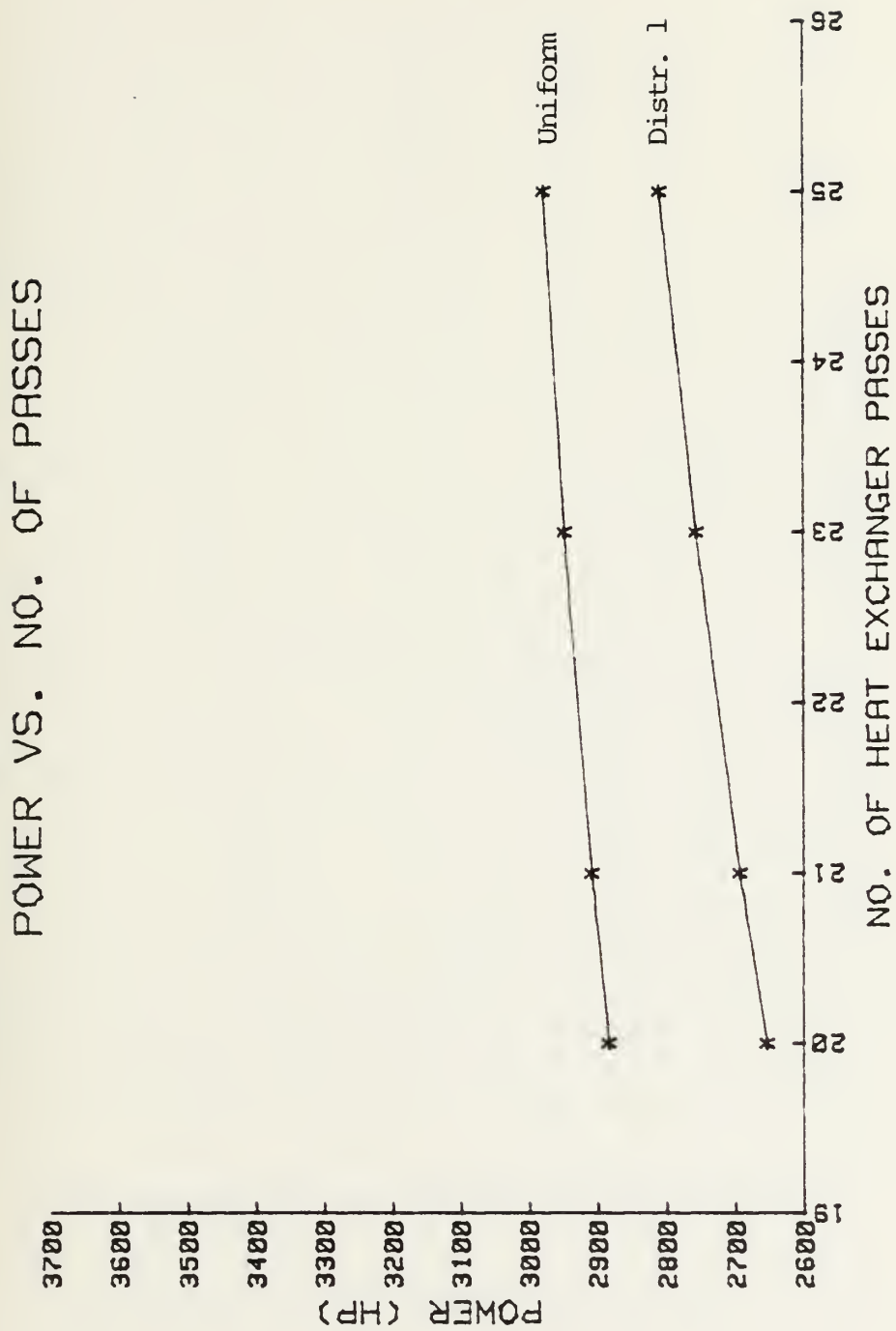


Figure 11-C. Power vs. No. of Heat Exchanger Passes ($m_g = 77.4 \text{ lbm/s}$)

POWER VS. NO. OF PASSES

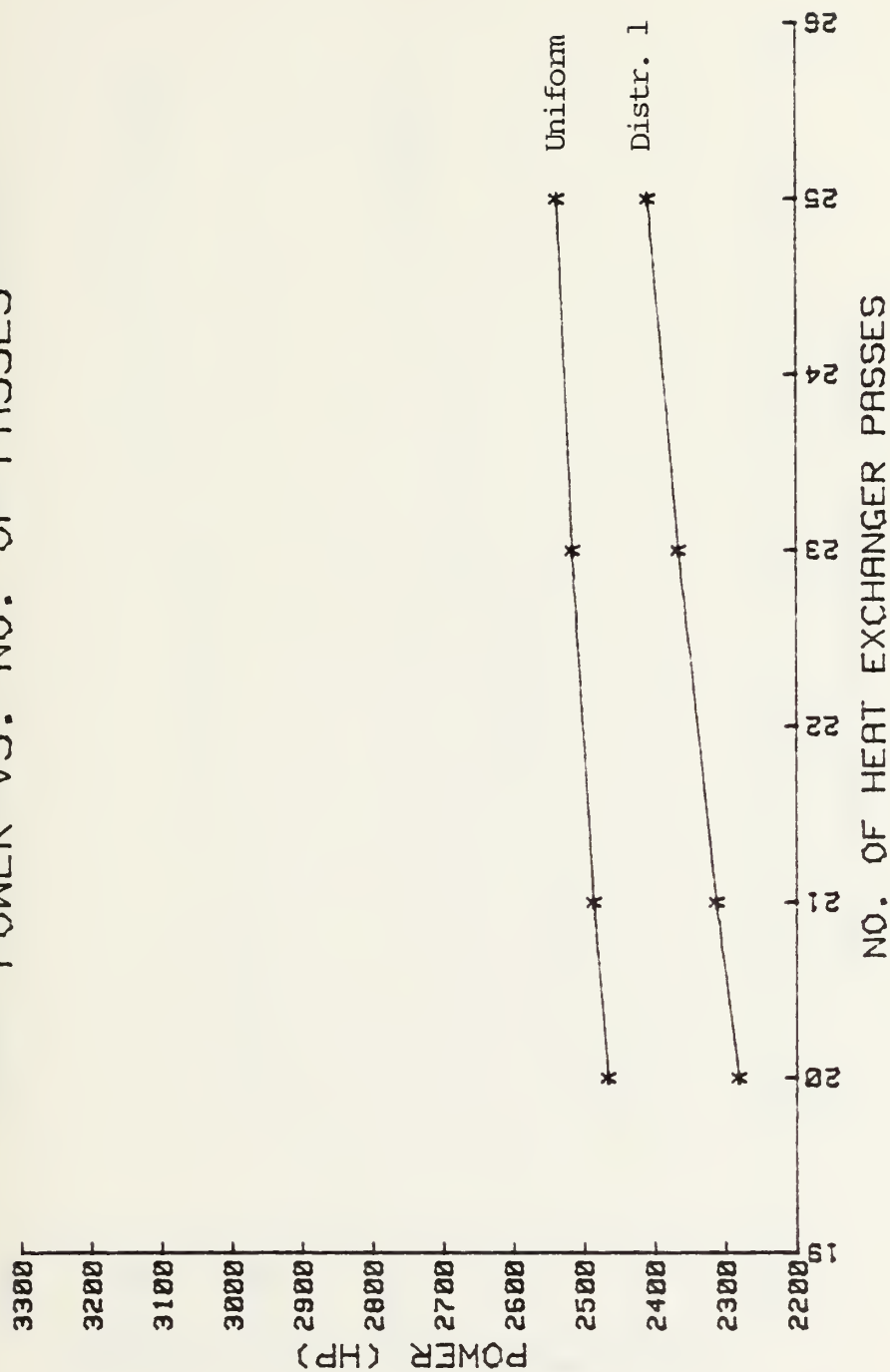


Figure 11-D. Power vs. No. of Heat Exchanger Passes ($m_g = 66.7 \text{ lbm/s}$)

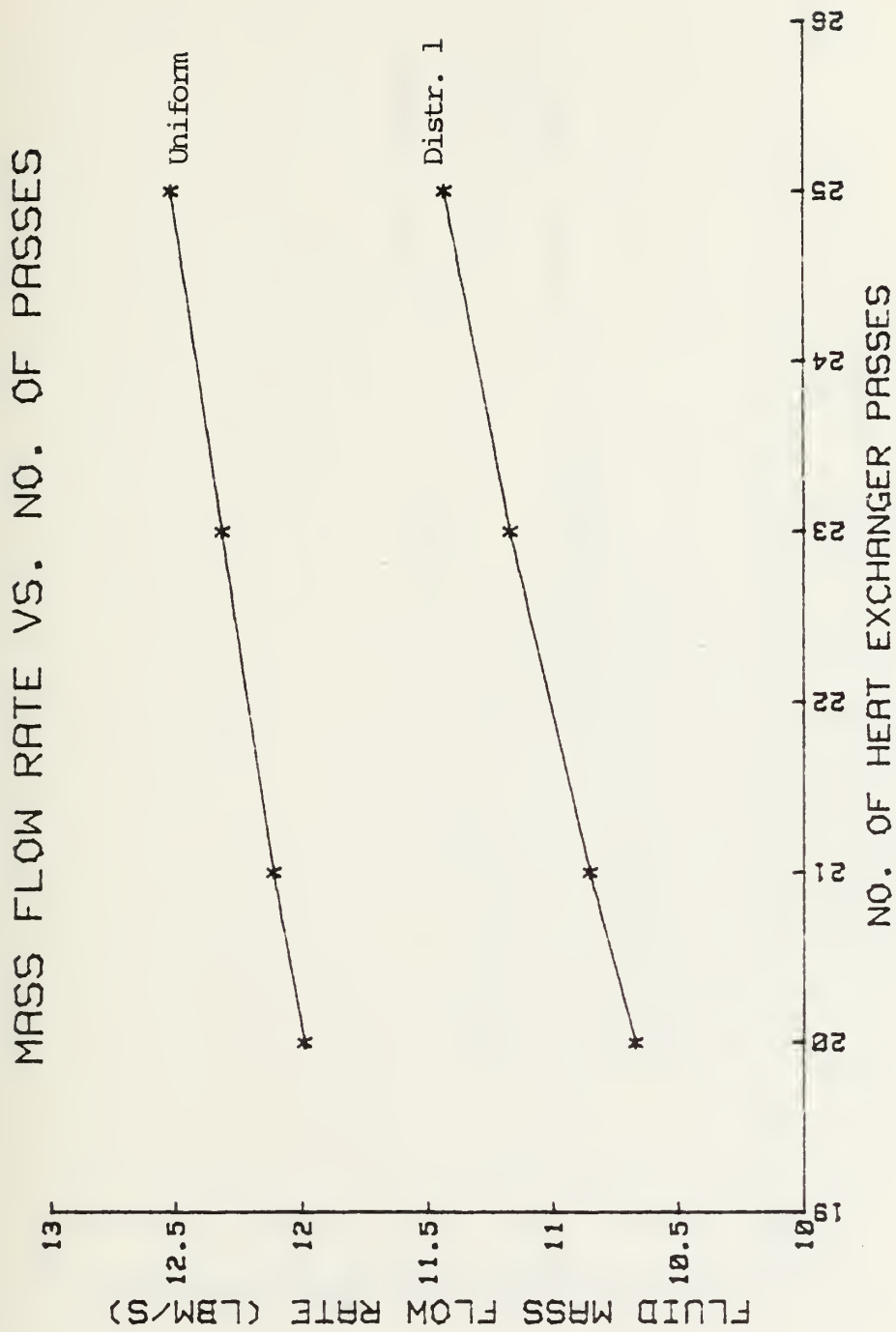


Figure 11-E. Fluid Flow Rate vs. No. of Heat Exchanger Passes
 $(m_g = 121.8 \text{ lbm/s})$

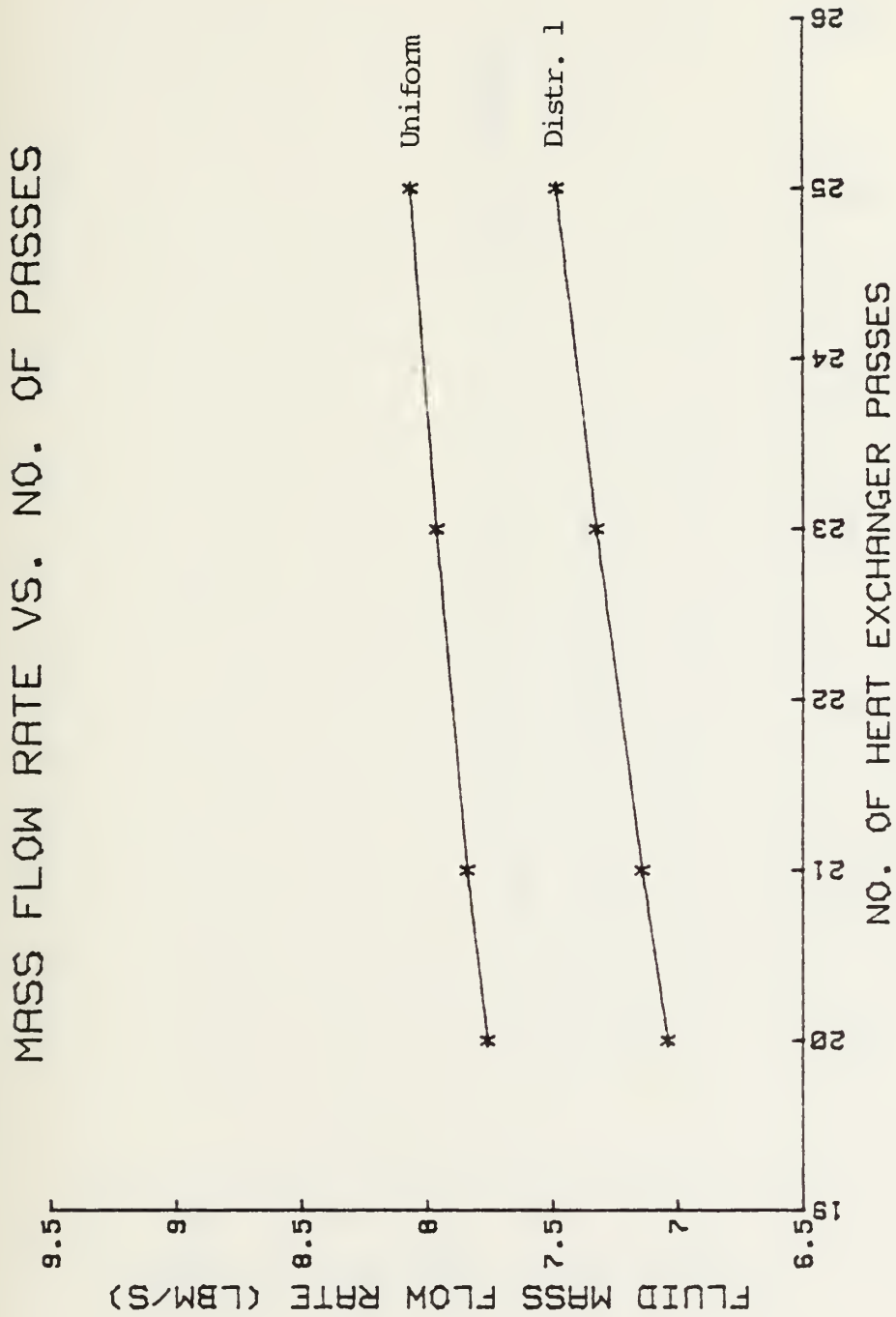


Figure 11-F. Fluid Flow Rate vs. No. of Heat Exchanger Passes
($m_g = 99.1 \text{ lbm/s}$)

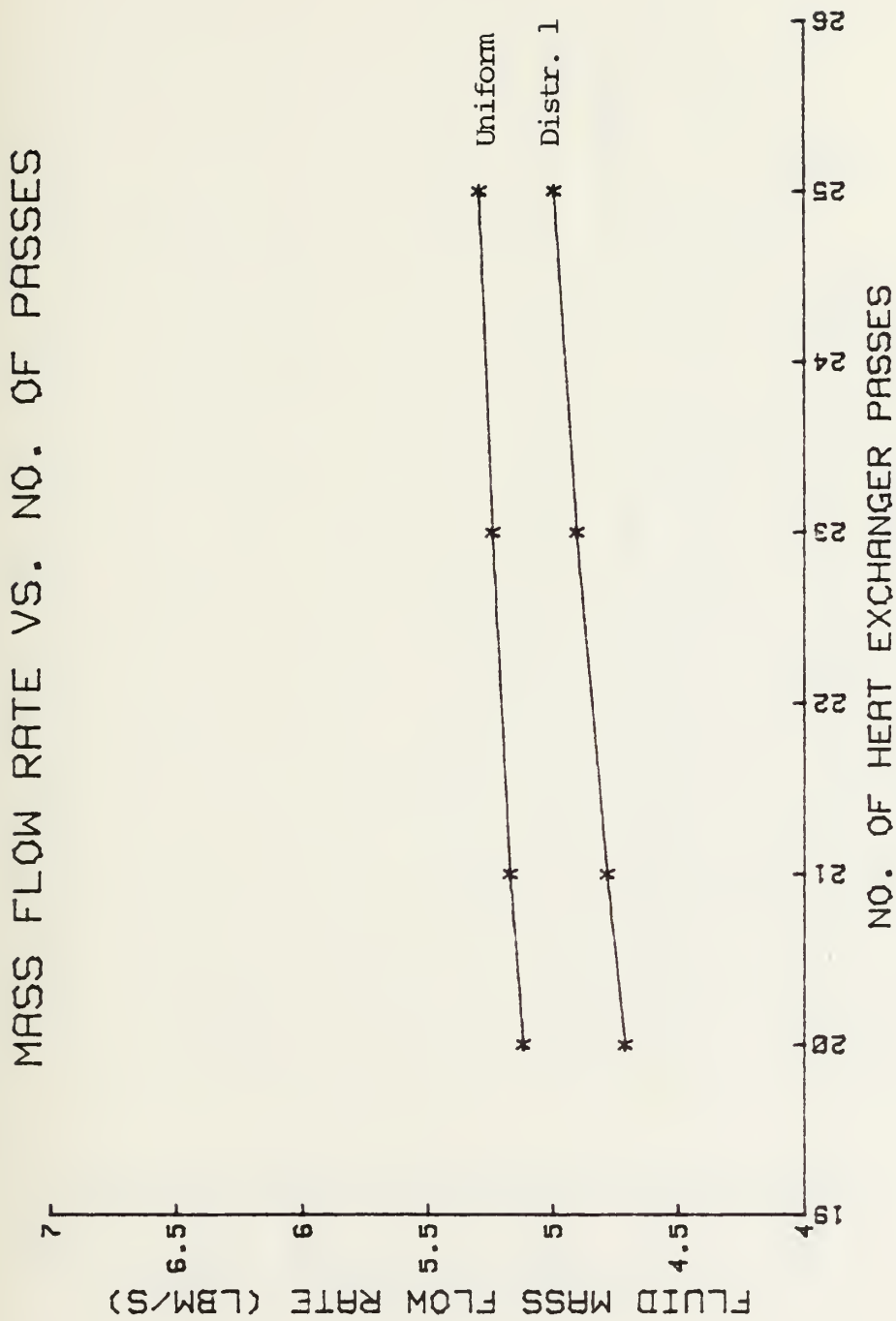


Figure 11-G. Fluid Flow Rate vs. No. of Heat Exchanger Passes
($m_g = 77.4 \text{ lbm/s}$)

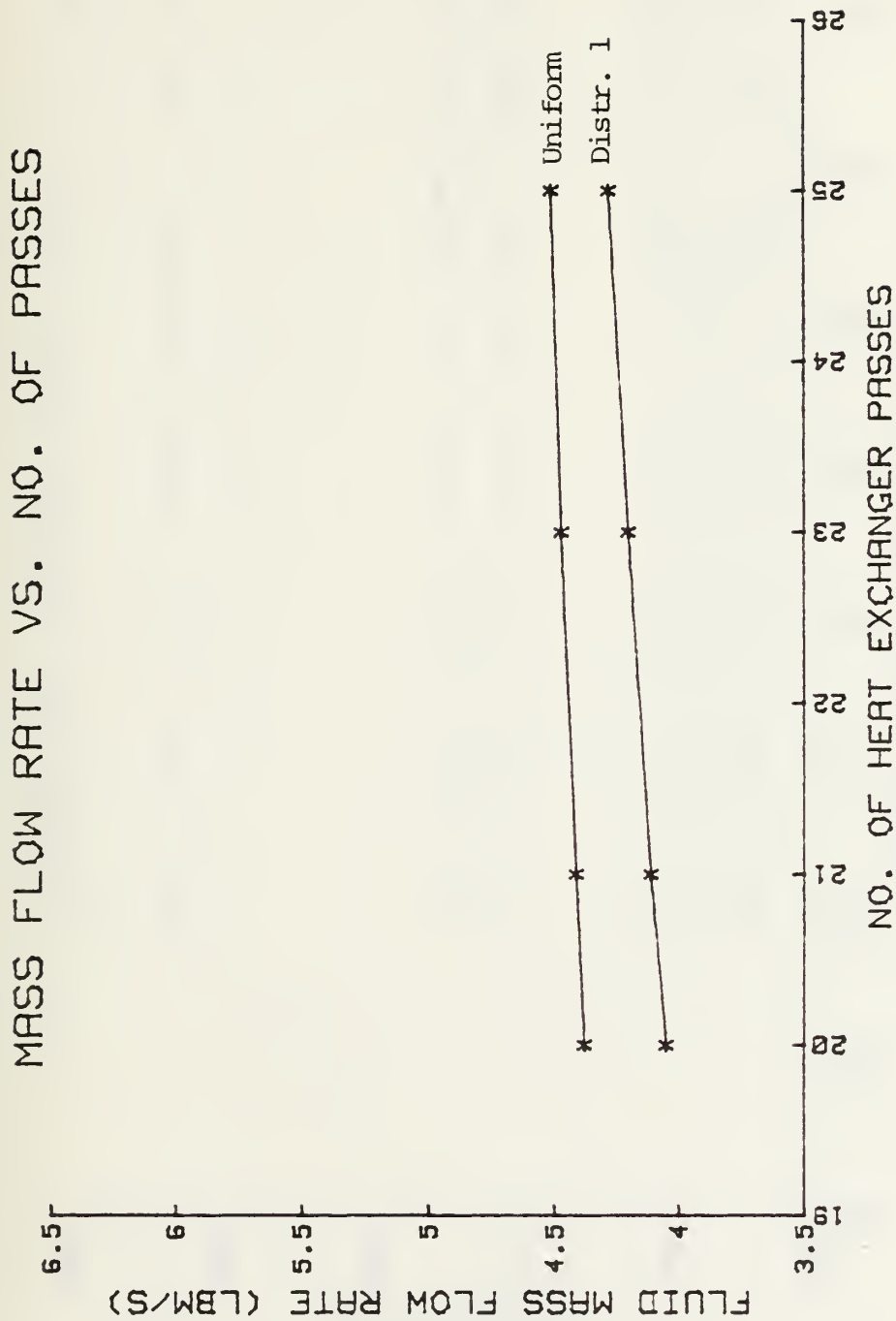


Figure 11-H. Fluid Flow Rate vs. No. of Heat Exchanger Passes
($m_g = 66.7 \text{ lbm/s}$)

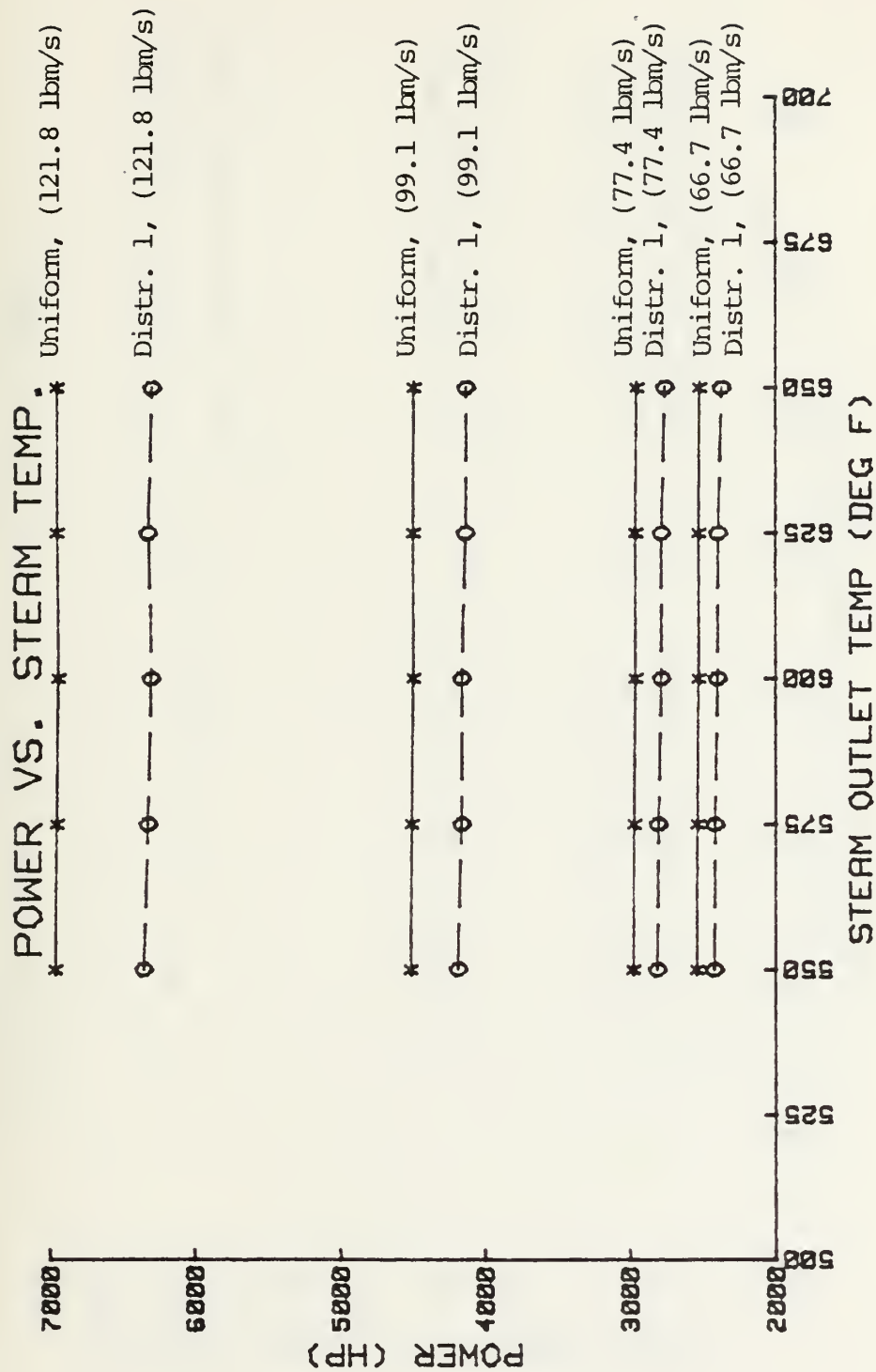


Figure 12-A. Power vs. Steam Outlet Temperature

FLUID FLOW RATE VS. STEAM TEMP.

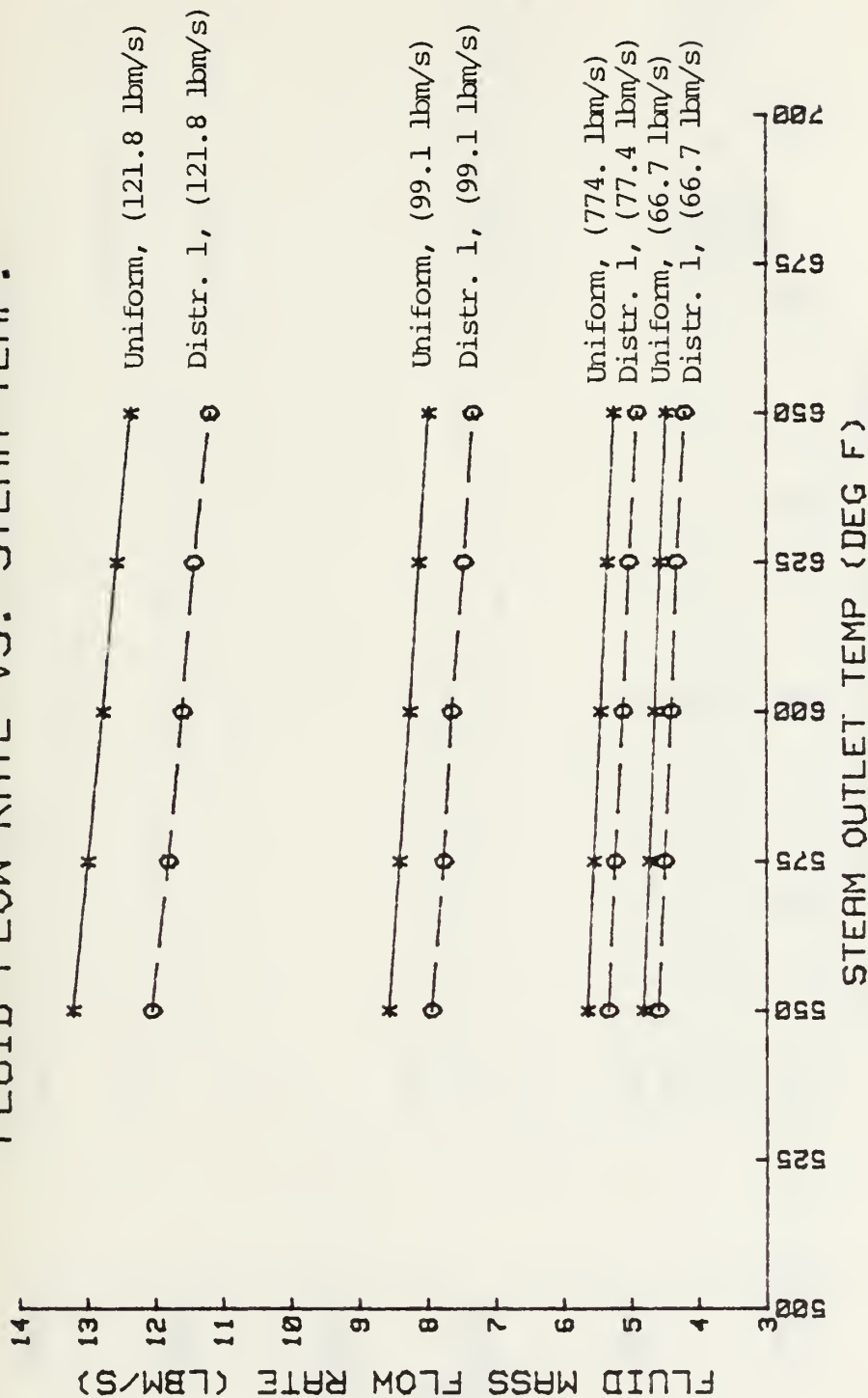


Figure 12-B. Fluid Mass Flow Rate vs. Steam Outlet Temperature

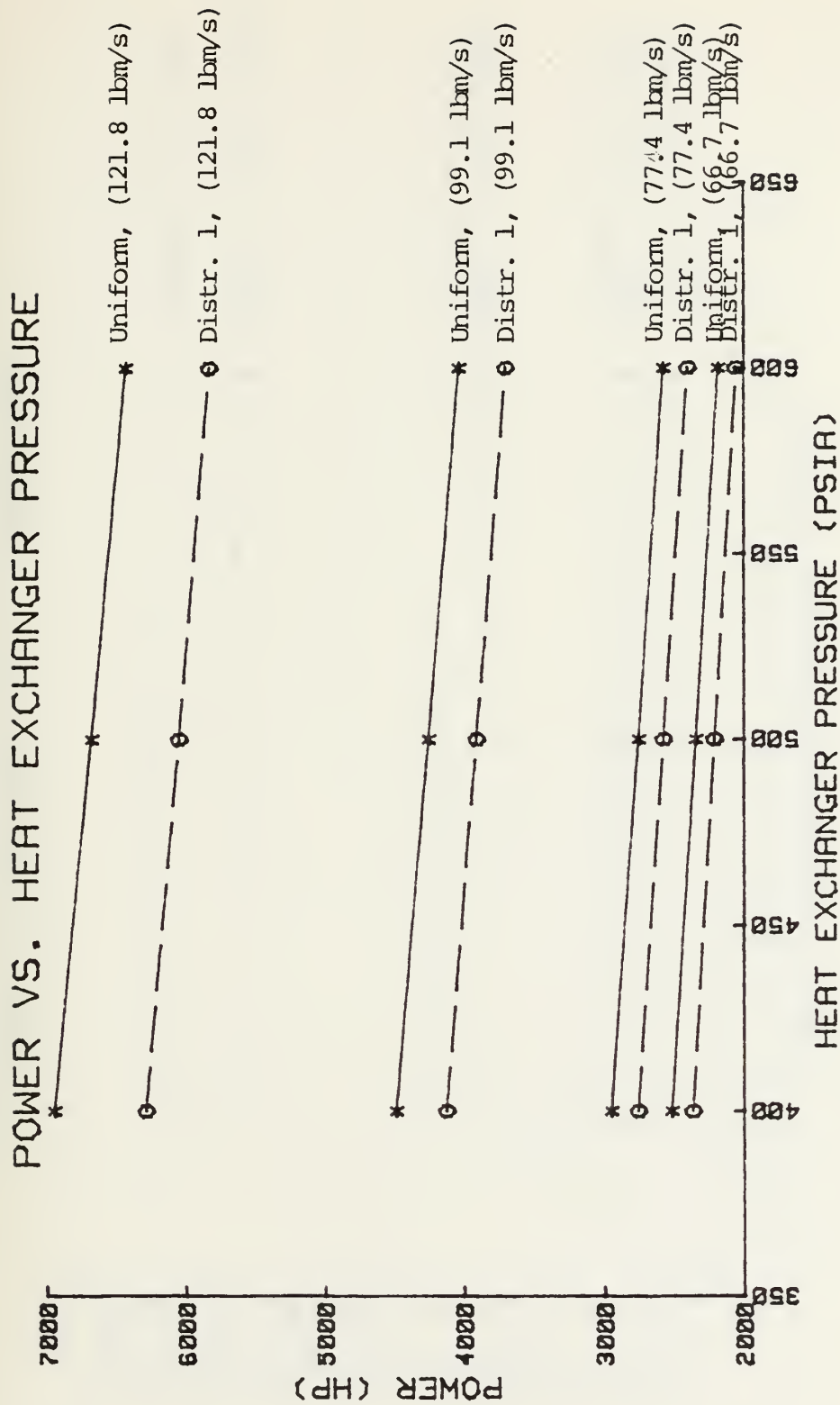


Figure 13-A. Power vs. Heat Exchanger Operating Pressure

FLUID FLOW RATE VS. PRESSURE

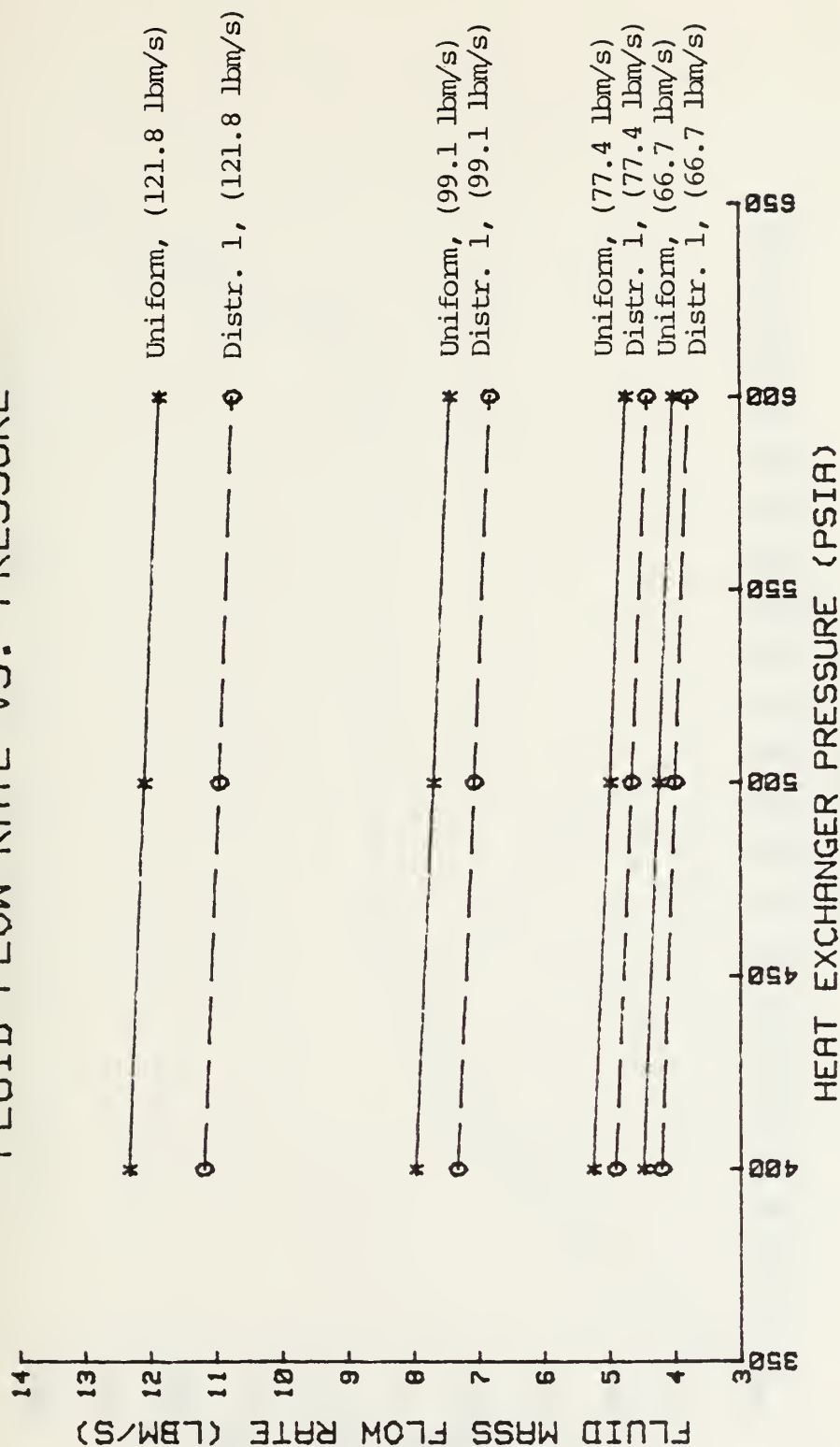


Figure 13-B. Fluid Mass Flow Rate vs. Heat Exchanger Operating Pressure

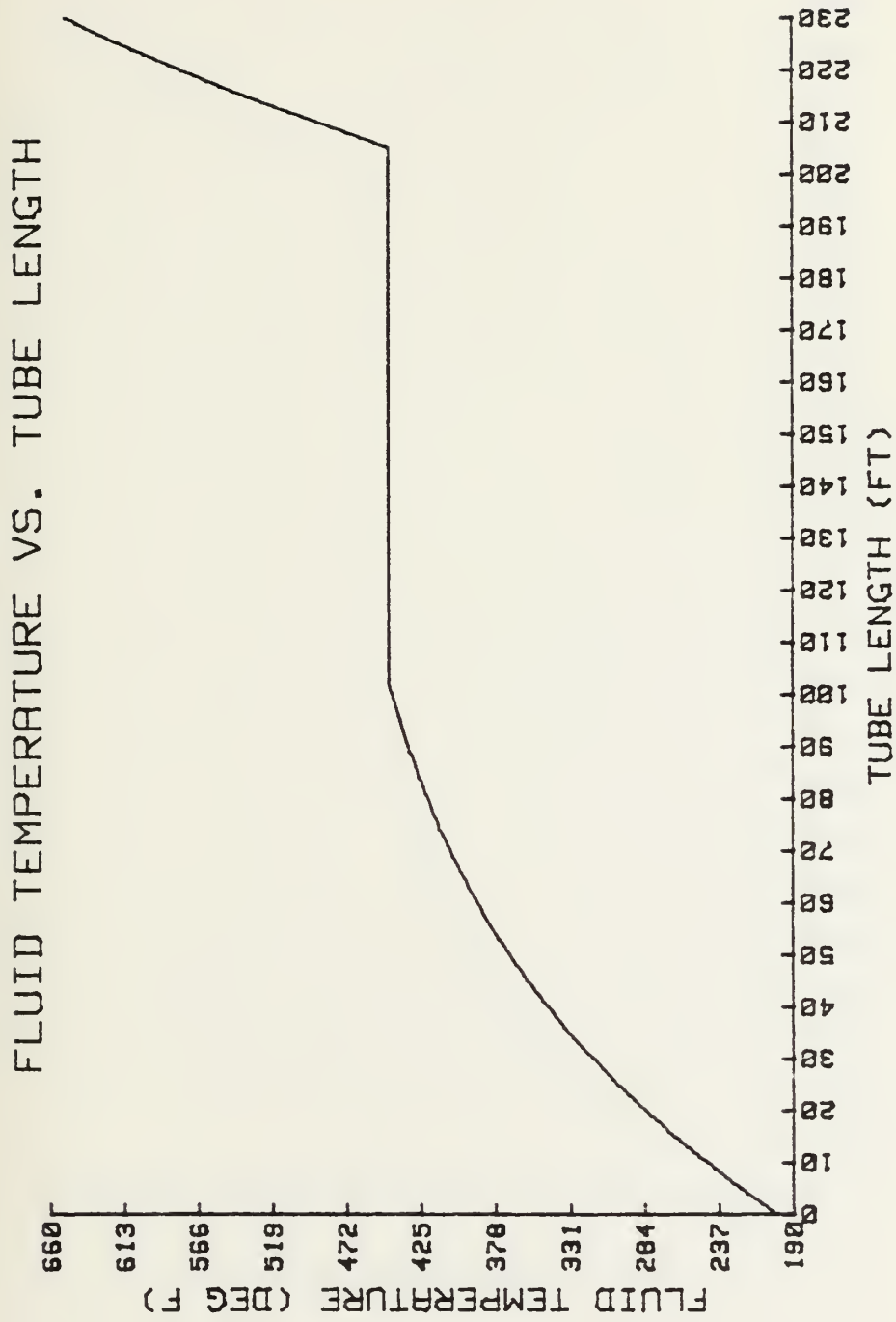


Figure 14-A. Fluid Temperature vs. Tube Length ($m_g = 121.8 \text{ lbm/s}$)

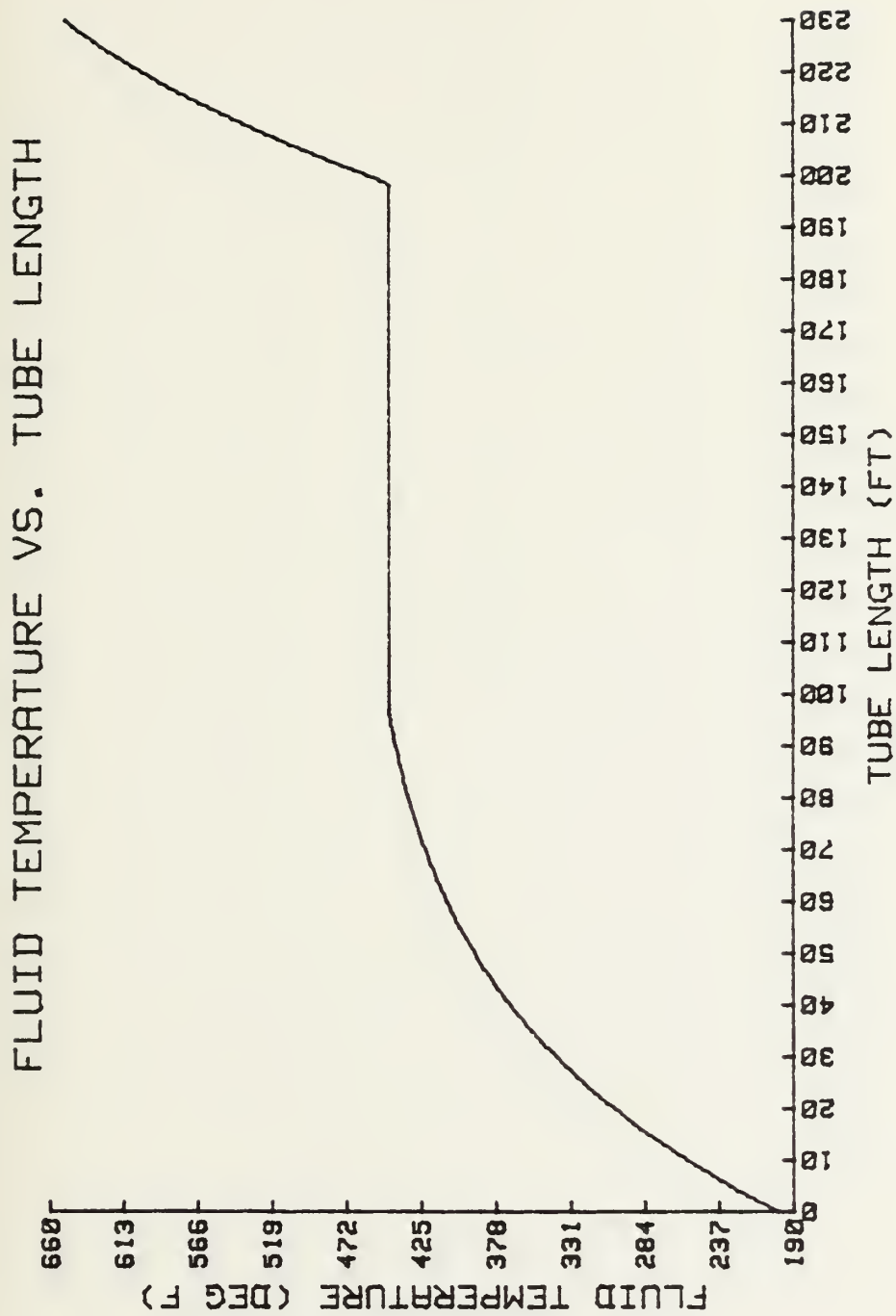


Figure 14-B. Fluid Temperature vs. Tube Length ($m_g = 99.1 \text{ lbm/s}$)

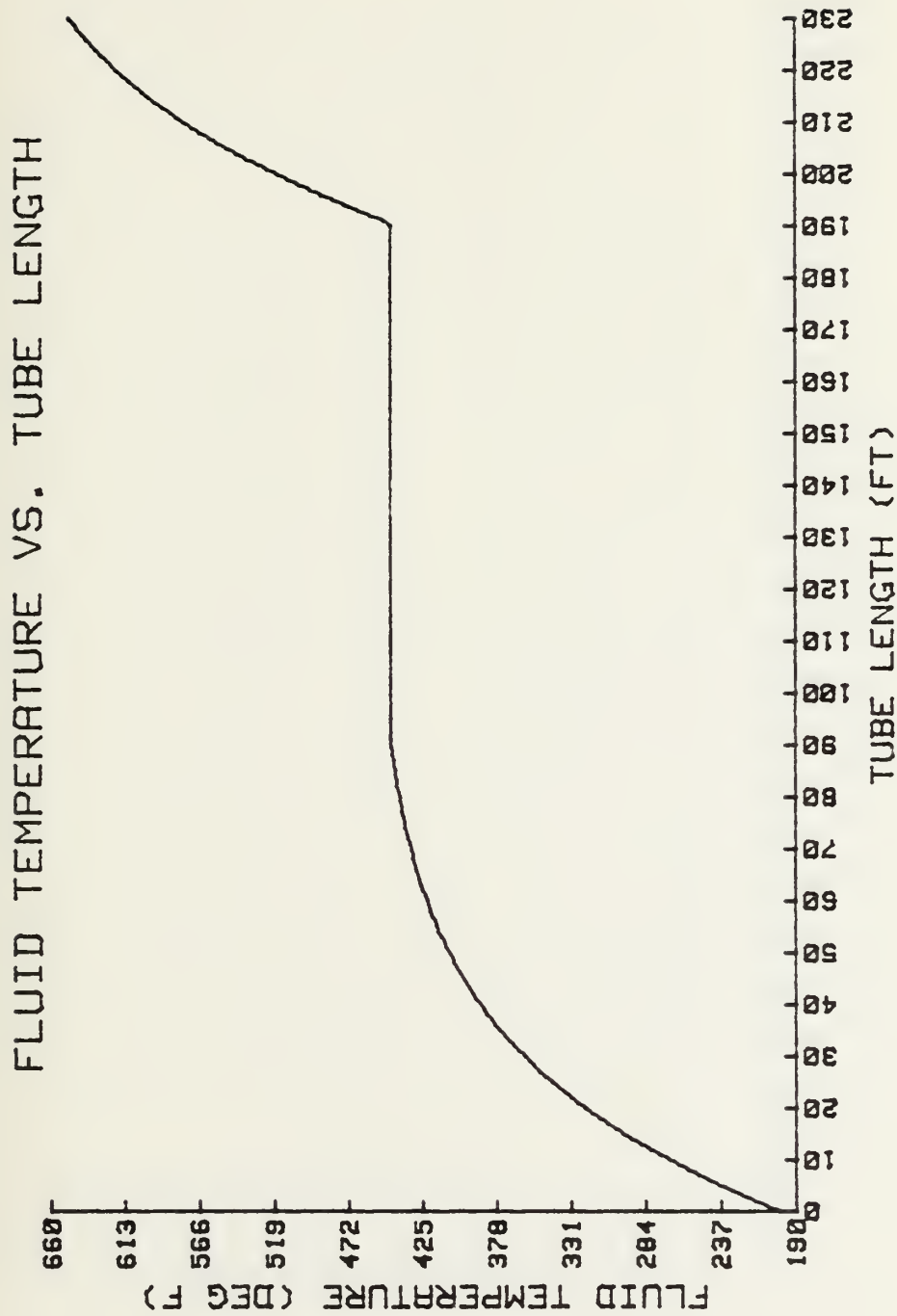


Figure 14-C. Fluid Temperature vs. Tube Length ($m_g = 77.4 \text{ lbm/s}$)

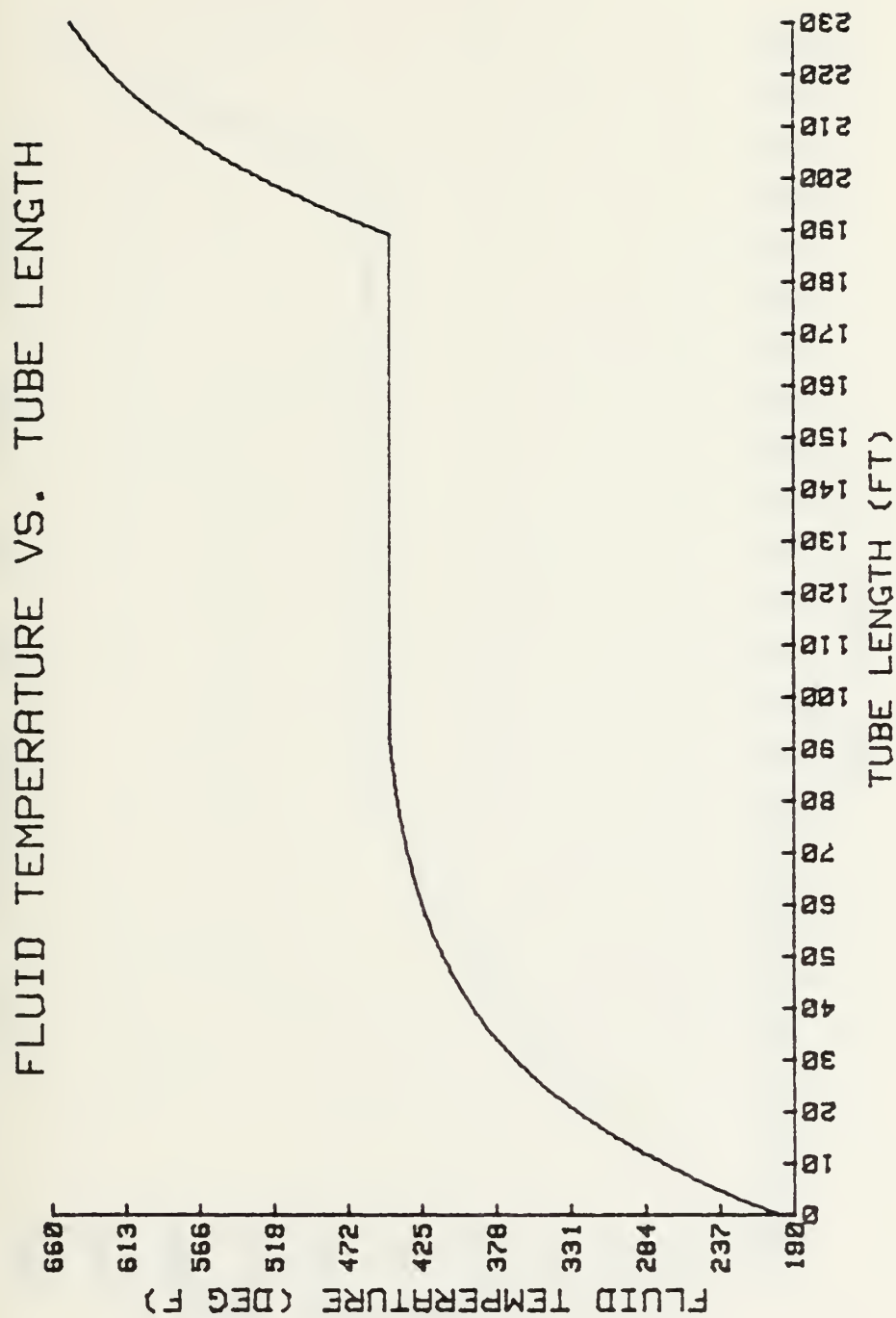


Figure 14-D. Fluid Temperature vs. Tube Length ($m_g = 66.7 \text{ lbm/s}$)

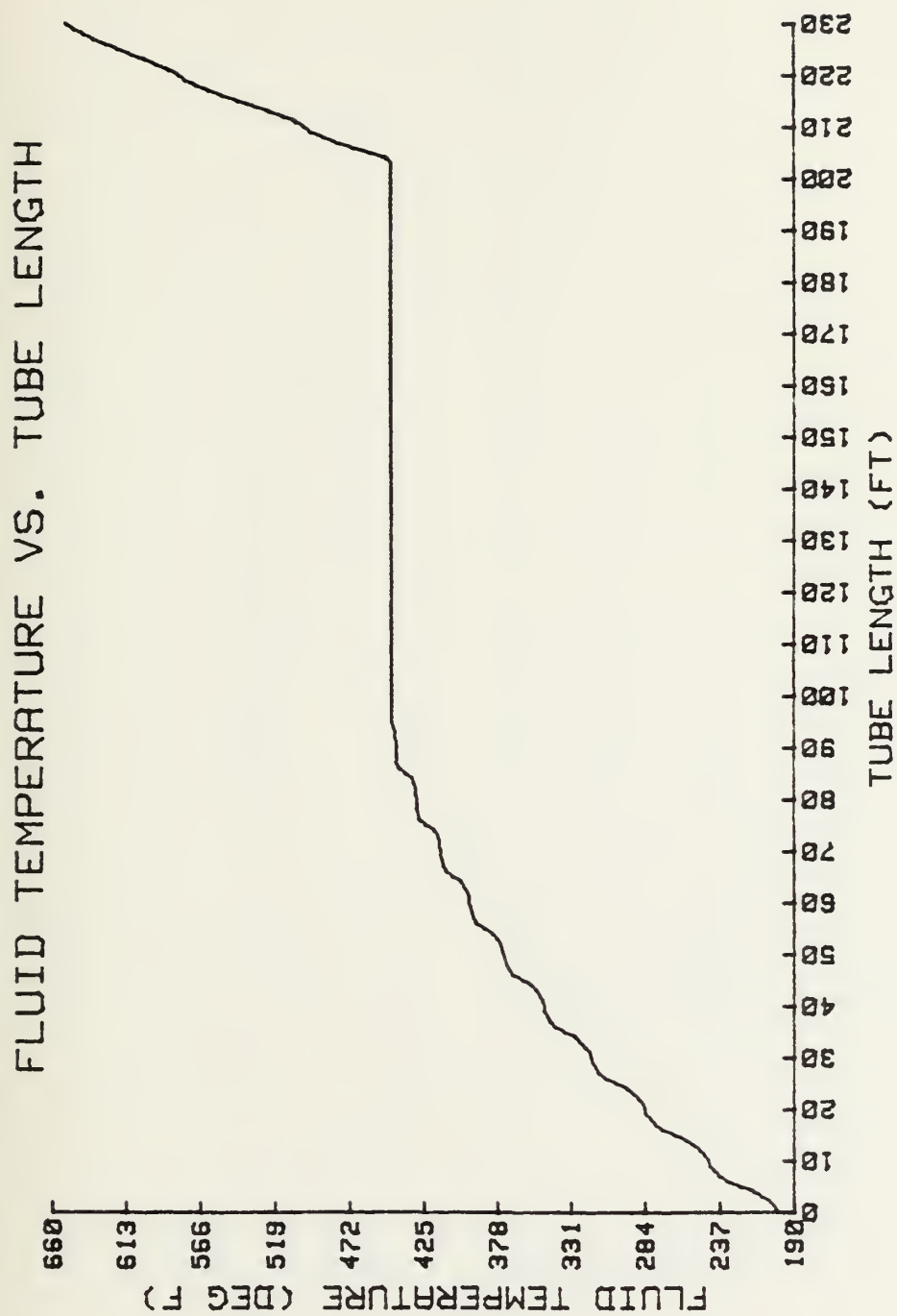


Figure 14-E. Fluid Temperature vs. Tube Length (Distr. 1,
 $m_g = 121.8 \text{ lbm/s}$)

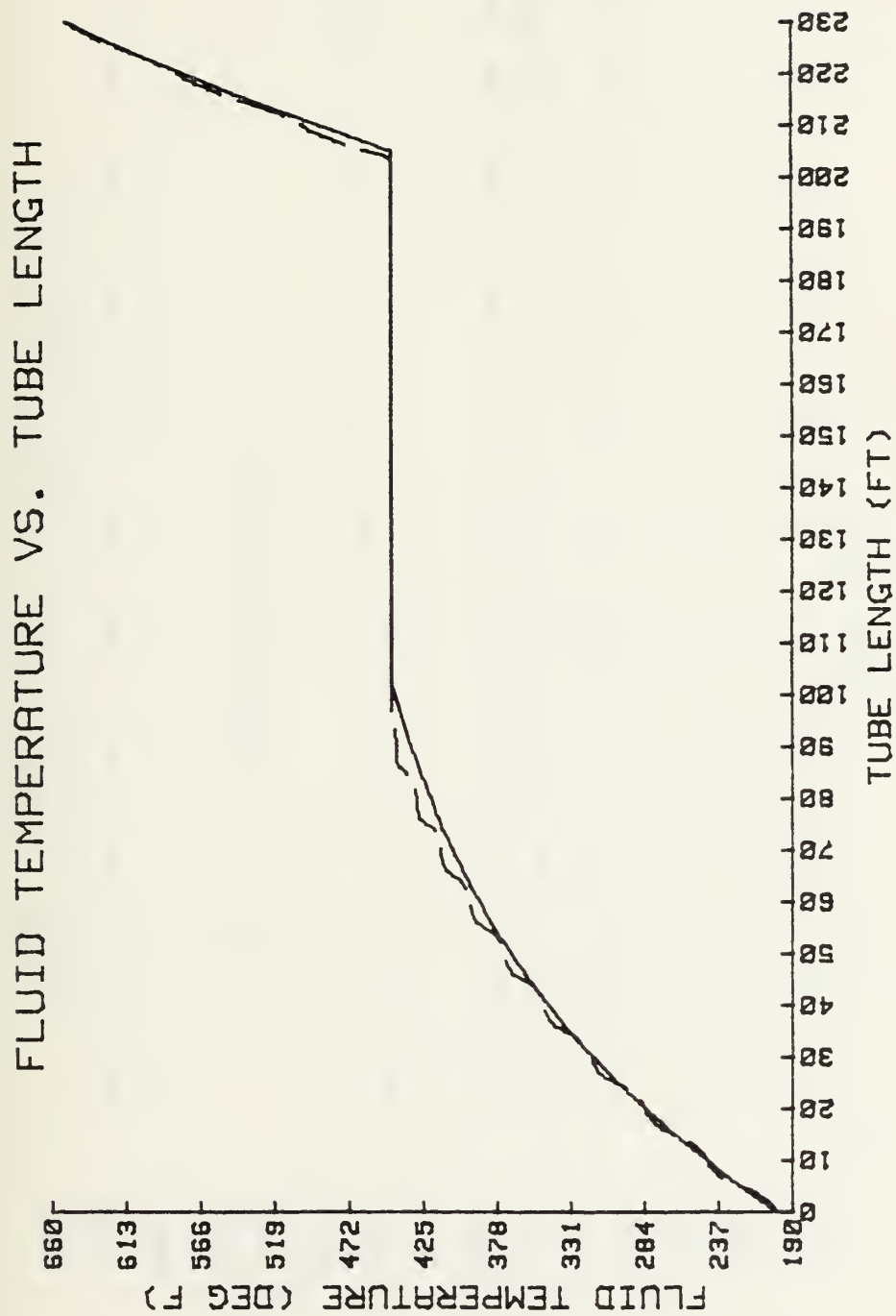
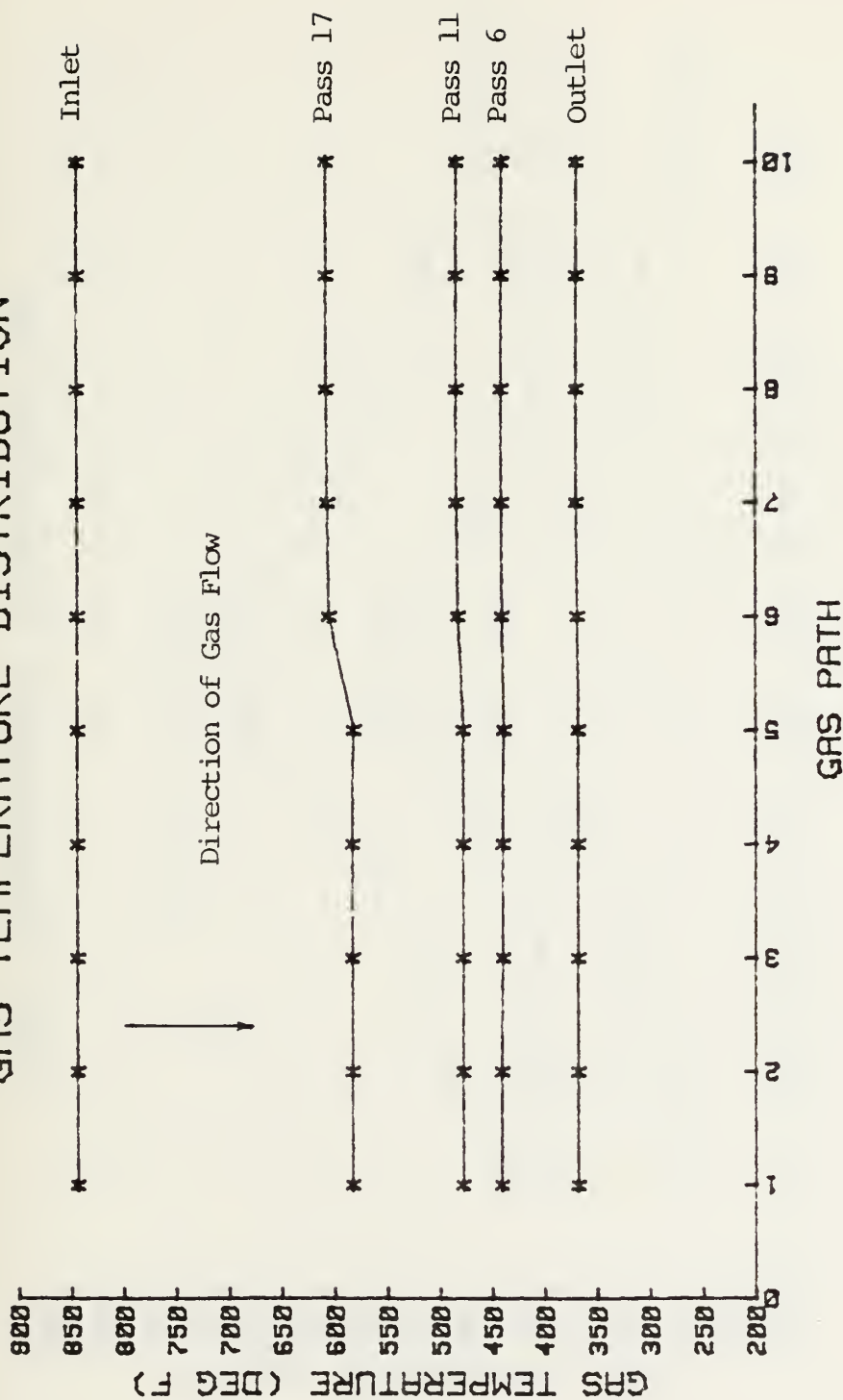


Figure 14-F. Fluid Temperature vs. Tube Length
(Distr.'s $U, 1; \dot{m}_g = 121.8 \text{ lbm/s}$)

GAS TEMPERATURE DISTRIBUTION



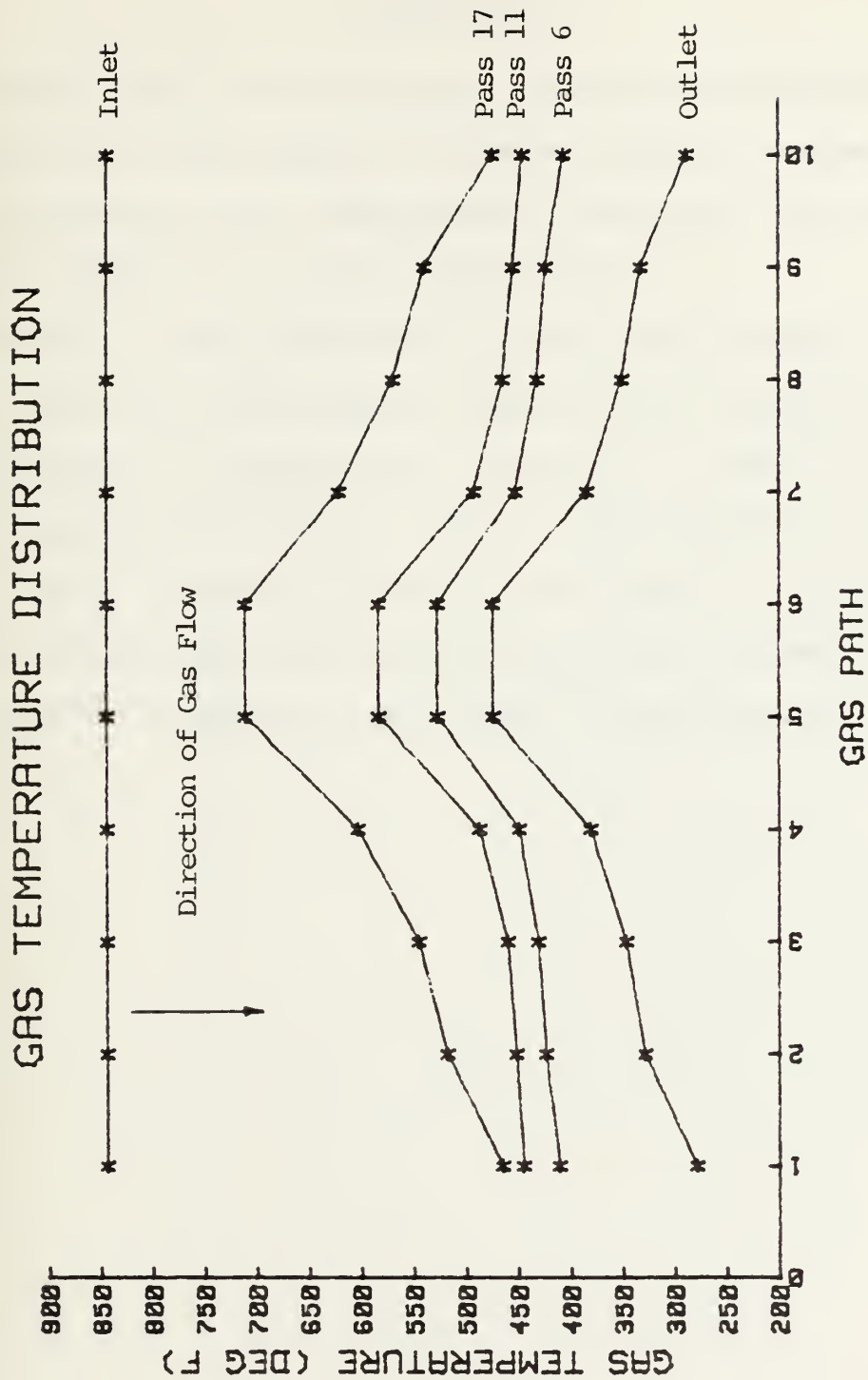


Figure 15-B. Gas Temperature Distribution (Distr. 1, $\dot{m}_g = 121.8 \text{ lbm/s}$)

APPENDIX A

Sample runs of the computer output are provided for a comparison of the effects of the non-uniform gas mass distributions on the temperatures within the heat exchanger and the effect on overall performance.

Runs 1, 2 and 6 utilized a total gas flow rate of 121.8 lbm/s with the uniform distribution, distribution 1 and distribution 5, respectively. Runs 10, 11 and 15 utilized the same distributions but with a total gas flow rate of 99.1 lbm/s. Runs 19, 20 and 24; and runs 28, 29 and 33 also utilized the same distributions but with mass flow rates of 77.4 lbm/s and 66.7 lbm/s, respectively.


```

RUN NUMBER = 1
ENTER NUMBER OF HEAT EXCHANGER PASSES DESIRED
23
ENTER EXHAUST GAS MASS FLOW RATE (LBM/S) FOR GAS PATHS 1 THROUGH 10
12.14 12.18 12.18 12.18 12.13 12.18 12.18 12.18 12.18 12.18
ENTER GAS TEMPERATURE AT INLET (DEG F) FOR GAS PATHS 1 THROUGH 10
844. 844. 844. 844. 844. 844. 844. 844. 844. 844.
ENTER FEEDWATER INLET TEMPERATURE (DEG F)
200.0
ENTER DESIRED STEAM TEMPERATURE AT OUTLET
650.0
ENTER DESIRED STEAM PRESSURE
400.0
ENTER MINIMUM EXHAUST GAS TEMPERATURE ALLOWED AT HEAT EXCHANGER EXIT
300.0
ENTER TUBE LENGTH (FT) PER NODE
1.0
ENTER NUMBER OF TUBES PER ROW
32.0
ENTER GEOMETRIC SCALING FACTOR
1.0

```


[illegible]

MATRIX OF EXHAUST GAS TEMPERATURES

368.	368.	368.	368.	369.	370.	370.	370.	370.
388.	388.	387.	387.	388.	388.	387.	387.	387.
403.	403.	402.	403.	403.	405.	405.	405.	405.
419.	418.	417.	417.	419.	418.	418.	418.	418.
429.	429.	429.	429.	431.	431.	431.	431.	431.
441.	441.	440.	440.	441.	441.	441.	441.	441.
449.	449.	448.	448.	451.	451.	451.	451.	451.
457.	457.	456.	456.	455.	458.	458.	458.	458.
463.	463.	461.	461.	461.	465.	465.	465.	465.
469.	469.	467.	467.	470.	470.	470.	470.	470.
473.	473.	471.	471.	475.	475.	475.	475.	475.
478.	478.	478.	478.	483.	484.	484.	484.	484.
487.	487.	487.	487.	494.	494.	494.	494.	494.
498.	498.	498.	498.	507.	507.	507.	507.	507.
512.	512.	512.	512.	523.	524.	524.	524.	524.
530.	530.	530.	530.	544.	545.	545.	545.	546.
553.	553.	553.	553.	571.	572.	572.	572.	573.
583.	583.	583.	583.	605.	606.	607.	607.	607.
620.	620.	620.	620.	649.	650.	651.	651.	651.
667.	667.	667.	667.	705.	706.	707.	707.	708.
728.	728.	728.	728.	776.	778.	778.	779.	780.
806.	806.	806.	806.	835.	805.	805.	804.	804.
825.	825.	826.	826.	827.	828.	829.	829.	830.
844.	844.	844.	844.	844.	844.	844.	844.	844.

MATRIX OF OVERALL HEAT TRANSFER COEFFICIENTS

80.	81.	82.	82.	83.	83.	84.	84.	84.
88.	88.	87.	87.	87.	86.	86.	85.	85.
88.	89.	89.	89.	89.	90.	90.	90.	90.
92.	92.	92.	92.	91.	91.	91.	91.	91.
92.	93.	93.	93.	93.	93.	93.	94.	94.
95.	95.	95.	95.	94.	94.	94.	94.	94.
95.	95.	95.	95.	95.	96.	96.	96.	96.
97.	96.	96.	96.	96.	96.	96.	96.	96.
97.	97.	97.	97.	97.	97.	97.	97.	97.
97.	97.	97.	97.	97.	97.	97.	97.	97.
98.	106.	160.	160.	150.	160.	160.	160.	160.
160.	160.	160.	160.	151.	161.	161.	161.	161.
161.	161.	161.	161.	161.	161.	161.	161.	161.
161.	161.	161.	161.	151.	161.	161.	161.	161.
162.	162.	162.	162.	162.	162.	162.	162.	162.
162.	162.	162.	162.	152.	162.	162.	162.	162.
163.	163.	163.	163.	163.	163.	163.	163.	163.
164.	164.	164.	164.	154.	164.	164.	164.	164.
165.	165.	165.	165.	165.	165.	165.	165.	165.
166.	166.	166.	166.	157.	167.	167.	167.	167.
168.	168.	168.	168.	62.	59.	59.	58.	58.
56.	56.	56.	56.	56.	57.	57.	57.	58.
56.	55.	55.	55.	55.	55.	55.	55.	55.

MATRIX OF HEAT TRANSFER (Q) PER NODE

61.	59.	58.	57.	55.	55.	53.	52.	51.	49.
43.	44.	45.	46.	48.	49.	51.	52.	53.	55.
48.	46.	45.	44.	43.	42.	41.	40.	38.	37.
32.	33.	33.	34.	35.	37.	38.	39.	40.	41.
35.	34.	33.	32.	31.	31.	30.	29.	28.	27.
23.	24.	24.	25.	25.	27.	28.	29.	30.	31.
26.	25.	24.	23.	22.	23.	22.	21.	21.	20.
17.	17.	17.	18.	18.	20.	21.	21.	22.	22.
19.	18.	17.	16.	16.	17.	16.	16.	15.	15.
12.	12.	12.	12.	13.	15.	15.	16.	16.	17.
14.	14.	21.	21.	21.	24.	25.	25.	25.	25.
27.	27.	27.	27.	27.	31.	31.	31.	31.	31.
34.	34.	34.	34.	34.	39.	40.	40.	40.	40.
43.	43.	43.	43.	43.	50.	50.	50.	50.	51.
54.	54.	54.	54.	54.	54.	64.	64.	64.	64.
69.	69.	69.	69.	69.	81.	81.	82.	82.	82.
88.	88.	88.	88.	88.	103.	104.	104.	104.	104.
113.	113.	113.	113.	113.	132.	133.	133.	133.	133.
144.	144.	144.	144.	144.	159.	170.	170.	171.	171.
185.	185.	185.	185.	185.	217.	218.	219.	219.	219.
238.	238.	238.	237.	237.	92.	85.	82.	79.	76.
58.	60.	62.	64.	67.	59.	72.	74.	77.	80.
60.	59.	57.	55.	53.	51.	50.	48.	46.	45.

FLUID MASS FLOW RATE = 44399.3 LBM/HR
 TOTAL Q (BTU/HR) BASED ON THE Q MATRIX = 51786611.5
 Q (BTU/HR) BASED ON THE WATER/STEAM MATRIX = 51765645.2
 Q (BTU/HR) BASED ON THE GAS MATRIX = 52197071.0
 THE MINIMUM PINCH POINT = 39.8 DEGREES
 BOILING BEGINS AT 10.3 INCHES INTO NODE 11 2
 SUPERHEATING BEGINS AT 0.3 INCHES INTO NODE 21 6
 THE ISENTROPIC POWER OF THE STEAM TURBINE = 6944. HORSEPOWER


```

RUN NUMBER =      2
ENTER NUMBER OF HEAT EXCHANGER PASSES DESIRED
23
ENTER EXHAUST GAS MASS FLOW RATE (LBM/S) FOR GAS PATHS 1 THROUGH 10
2.07  5.97  8.28  13.64  30.94  30.94  30.94  13.64  8.28  5.97  2.07
ENTER GAS TEMPERATURE AT INLET (DEG F) FOR GAS PATHS 1 THROUGH 10
844.  844.  844.  844.  844.  844.  844.  844.  844.  844.  844.
ENTER FEEDWATER INLET TEMPERATURE (DEG F)
200.0
ENTER DESIRED STEAM TEMPERATURE AT OUTLET
650.0
ENTER DESIRED STEAM PRESSURE
400.0
ENTER MINIMUM EXHAUST GAS TEMPERATURE ALLOWED AT HEAT EXCHANGER EXIT
300.0
ENTER TUBE LENGTH (FT) PER NODE
1.0
ENTER NUMBER OF TUBES PER ROW
32.0
ENTER GEOMETRIC SCALING FACTOR
1.0

```


MATRIX OF WATER/STEAM TEMPERATURES

[illegible]

MATRIX OF EXHAUST GAS TEMPERATURES

279.	329.	347.	381.	474.	474.	384.	350.	332.	288.
320.	357.	371.	399.	486.	487.	400.	370.	354.	312.
341.	375.	388.	413.	498.	498.	417.	391.	379.	349.
373.	396.	406.	428.	508.	509.	430.	406.	394.	366.
388.	409.	418.	438.	518.	519.	443.	421.	413.	394.
411.	424.	431.	449.	527.	527.	452.	431.	423.	406.
421.	432.	438.	456.	535.	536.	461.	442.	435.	425.
435.	441.	446.	463.	543.	543.	468.	447.	441.	432.
439.	444.	449.	468.	550.	550.	474.	454.	448.	443.
445.	448.	453.	472.	556.	557.	478.	456.	449.	444.
445.	450.	456.	479.	569.	569.	483.	459.	451.	445.
445.	452.	460.	487.	583.	583.	492.	464.	454.	445.
445.	456.	466.	498.	599.	599.	504.	471.	459.	446.
446.	461.	474.	511.	617.	617.	518.	481.	465.	447.
448.	468.	485.	527.	636.	637.	536.	494.	475.	449.
450.	479.	499.	547.	659.	659.	558.	512.	489.	453.
455.	495.	519.	572.	683.	684.	586.	536.	509.	460.
465.	518.	545.	603.	711.	711.	621.	569.	539.	474.
484.	552.	582.	643.	742.	743.	665.	614.	583.	501.
519.	601.	632.	692.	777.	778.	720.	677.	646.	552.
588.	674.	701.	753.	817.	817.	789.	762.	740.	651.
720.	781.	795.	812.	829.	829.	811.	794.	778.	711.
773.	812.	820.	829.	837.	837.	831.	824.	819.	791.
844.	844.	844.	844.	844.	844.	844.	844.	844.	844.

MATRIX OF OVERALL HEAT TRANSFER COEFFICIENTS

49.	68.	73.	80.	86.	87.	82.	76.	71.	50.
52.	73.	79.	86.	91.	90.	84.	77.	71.	51.
52.	74.	80.	87.	94.	94.	89.	81.	75.	53.
54.	77.	83.	91.	97.	95.	90.	82.	76.	53.
54.	77.	93.	91.	99.	99.	92.	84.	78.	55.
55.	79.	85.	94.	101.	100.	93.	85.	78.	55.
55.	79.	96.	94.	102.	102.	95.	86.	80.	56.
56.	80.	87.	96.	103.	103.	95.	87.	80.	56.
56.	80.	87.	96.	104.	104.	96.	87.	81.	56.
74.	125.	141.	165.	188.	181.	96.	88.	81.	56.
74.	125.	141.	165.	189.	189.	166.	141.	125.	74.
74.	125.	141.	166.	190.	190.	166.	142.	125.	74.
74.	125.	142.	166.	190.	190.	166.	142.	125.	74.
74.	125.	142.	167.	191.	191.	167.	142.	125.	74.
74.	125.	142.	167.	192.	192.	167.	142.	125.	75.
75.	125.	142.	168.	193.	193.	168.	143.	126.	75.
75.	126.	143.	168.	195.	195.	169.	143.	126.	75.
75.	126.	144.	169.	196.	196.	170.	144.	127.	75.
75.	127.	144.	171.	197.	197.	171.	145.	127.	75.
75.	128.	146.	172.	199.	199.	173.	147.	129.	76.
76.	129.	147.	137.	60.	53.	56.	53.	50.	39.
39.	48.	51.	53.	56.	55.	54.	52.	49.	39.
39.	48.	50.	53.	55.	55.	53.	50.	48.	39.

MATRIX OF HEAT TRANSFER (Q) PER NODE

20.	40.	48.	61.	95.	93.	56.	40.	31.	12.
10.	27.	34.	48.	87.	89.	56.	43.	36.	18.
16.	32.	37.	48.	82.	90.	43.	29.	23.	9.
8.	19.	24.	35.	73.	75.	42.	32.	27.	14.
12.	22.	26.	35.	69.	57.	31.	20.	15.	6.
5.	11.	15.	24.	61.	63.	31.	22.	18.	10.
8.	14.	16.	24.	59.	57.	22.	12.	8.	4.
2.	5.	7.	15.	53.	55.	22.	13.	10.	6.
3.	6.	8.	16.	53.	51.	14.	5.	2.	0.
0.	2.	6.	23.	97.	93.	15.	6.	3.	1.
0.	4.	9.	28.	108.	108.	31.	11.	5.	0.
0.	5.	12.	35.	121.	121.	39.	14.	7.	0.
0.	7.	16.	44.	136.	136.	48.	20.	10.	1.
1.	11.	22.	54.	152.	152.	60.	27.	14.	1.
1.	16.	29.	68.	170.	170.	76.	30.	20.	2.
3.	21.	40.	85.	191.	191.	94.	50.	30.	4.
5.	34.	55.	106.	215.	215.	118.	68.	44.	7.
10.	50.	75.	133.	241.	241.	148.	93.	64.	14.
18.	73.	103.	167.	272.	272.	187.	128.	95.	26.
35.	108.	142.	210.	306.	307.	235.	177.	140.	51.
68.	160.	196.	209.	94.	91.	78.	66.	57.	31.
28.	47.	53.	60.	69.	71.	68.	64.	61.	42.
38.	49.	51.	53.	54.	52.	47.	43.	39.	28.

FLUID MASS FLOW RATE = 40197.7 LBM/HR
 TOTAL Q (BTU/HR) BASED ON THE Q MATRIX = 46717911.3
 Q (BTU/HR) BASED ON THE WATER/STEAM MATRIX = 46863253.6
 Q (BTU/HR) BASED ON THE GAS MATRIX = 52730028.9
 THE MINIMUM PINCH POINT = 0.2 DEGREES
 BOILING BEGINS AT 1.1 INCHES INTO NODE 10 6
 SUPERHEATING BEGINS AT 8.2 INCHES INTO NODE 21 4
 THE ISENTROPIC POWER OF THE STEAM TURBINE = 6286. HORSEPOWER


```

RUN NUMBER =      6
ENTER NUMBER OF HEAT EXCHANGER PASSES DESIRED
23
ENTER EXHAUST GAS MASS FLOW RATE (LBM/S) FOR GAS PATHS 1 THROUGH 10
12.18  27.28  21.29  19.95  15.95  11.69  7.80  3.65  0.0  0.0
ENTER GAS TEMPERATURE AT INLET (DEG F) FOR GAS PATHS 1 THROUGH 10
844.   844.   844.   844.   844.   844.   844.   844.   844.
ENTER FEEDWATER INLET TEMPERATURE (DEG F)
200.0
ENTER DESIRED STEAM TEMPERATURE AT OUTLET
650.0
ENTER DESIRED STEAM PRESSURE
400.0
ENTER MINIMUM EXHAUST GAS TEMPERATURE ALLOWED AT HEAT EXCHANGER EXIT
300.0
ENTER TUBE LENGTH (FT) PER NODE
1.0
ENTER NUMBER OF TUBES PER ROW
32.0
ENTER GEOMETRIC SCALING FACTOR
1.0

```


MATRIX OF WATER/STEAM TEMPERATURES

[illegible]

MATRIX OF EXHAUST GAS TEMPERATURES

370.	453.	432.	415.	394.	369.	343.	305.	844.	844.
390.	466.	446.	430.	410.	386.	363.	328.	844.	844.
405.	478.	459.	444.	426.	404.	385.	358.	844.	844.
421.	490.	471.	457.	438.	418.	399.	375.	844.	844.
432.	500.	481.	468.	451.	432.	416.	398.	844.	844.
444.	509.	491.	478.	460.	442.	426.	410.	844.	844.
452.	517.	499.	486.	470.	452.	438.	427.	844.	844.
461.	526.	507.	494.	477.	458.	444.	434.	844.	844.
466.	532.	514.	501.	484.	465.	452.	443.	844.	844.
471.	539.	521.	507.	489.	459.	454.	445.	844.	844.
479.	552.	532.	515.	495.	474.	457.	446.	844.	844.
488.	566.	545.	527.	505.	482.	462.	448.	844.	844.
499.	581.	561.	541.	518.	492.	469.	450.	844.	844.
514.	599.	578.	558.	534.	505.	478.	453.	844.	844.
532.	619.	599.	579.	553.	522.	491.	458.	844.	844.
556.	642.	622.	602.	577.	544.	508.	467.	844.	844.
586.	668.	649.	631.	605.	571.	532.	481.	844.	844.
624.	698.	681.	664.	640.	606.	565.	504.	844.	844.
672.	732.	718.	703.	682.	652.	611.	542.	844.	844.
734.	770.	761.	750.	734.	710.	675.	605.	844.	844.
783.	814.	810.	806.	798.	785.	763.	710.	844.	844.
810.	827.	825.	822.	816.	808.	793.	754.	844.	844.
827.	836.	835.	834.	832.	829.	823.	808.	844.	844.
844.	844.	844.	844.	844.	844.	844.	844.	844.	844.

MATRIX OF OVERALL HEAT TRANSFER COEFFICIENTS

78.	85.	85.	85.	84.	31.	75.	52.	0.	0.
85.	92.	91.	89.	86.	82.	76.	62.	0.	0.
86.	93.	93.	92.	91.	37.	80.	65.	0.	0.
90.	97.	96.	95.	92.	88.	81.	66.	0.	0.
90.	98.	98.	97.	95.	93.	83.	58.	0.	0.
92.	101.	100.	98.	95.	91.	84.	68.	0.	0.
93.	101.	101.	100.	97.	93.	85.	59.	9.	0.
94.	103.	102.	100.	98.	93.	86.	69.	0.	0.
94.	104.	103.	101.	99.	94.	87.	70.	0.	0.
160.	187.	184.	123.	99.	94.	87.	70.	0.	0.
160.	188.	185.	180.	172.	158.	138.	100.	0.	0.
161.	189.	186.	181.	173.	159.	138.	100.	0.	0.
161.	189.	186.	181.	173.	159.	139.	100.	0.	0.
162.	190.	187.	182.	174.	159.	139.	100.	0.	0.
162.	191.	188.	183.	174.	150.	139.	100.	0.	0.
163.	192.	189.	184.	175.	161.	140.	100.	0.	0.
164.	193.	190.	185.	176.	151.	140.	101.	0.	0.
165.	195.	191.	186.	177.	162.	141.	101.	0.	0.
166.	196.	193.	187.	179.	154.	142.	102.	0.	0.
110.	198.	194.	189.	180.	155.	143.	103.	0.	0.
57.	60.	59.	58.	56.	54.	52.	45.	0.	0.
53.	56.	56.	55.	55.	53.	51.	45.	0.	0.
53.	56.	55.	55.	54.	53.	50.	44.	0.	0.

MATRIX OF HEAT TRANSFER (O) PER NODE

59.	91.	81.	73.	62.	50.	37.	20.	0.	0.
44.	78.	72.	68.	61.	52.	42.	27.	0.	0.
48.	78.	68.	60.	50.	39.	28.	15.	0.	0.
33.	65.	59.	55.	48.	40.	32.	21.	0.	0.
36.	65.	55.	47.	38.	28.	20.	11.	0.	0.
23.	55.	48.	44.	37.	29.	22.	14.	0.	0.
26.	55.	45.	37.	28.	19.	12.	6.	0.	0.
15.	47.	40.	35.	28.	20.	14.	9.	0.	0.
17.	47.	37.	30.	21.	12.	5.	1.	0.	0.
21.	83.	66.	35.	21.	13.	6.	2.	0.	0.
27.	94.	76.	60.	42.	23.	9.	1.	0.	0.
34.	106.	88.	71.	51.	30.	13.	2.	0.	0.
44.	121.	102.	84.	62.	38.	18.	3.	0.	0.
56.	137.	118.	99.	76.	48.	24.	5.	0.	0.
71.	156.	136.	117.	92.	52.	33.	8.	0.	0.
90.	177.	158.	139.	113.	80.	46.	13.	0.	0.
115.	202.	184.	164.	138.	102.	64.	21.	0.	0.
147.	230.	214.	195.	169.	132.	89.	34.	0.	0.
189.	263.	249.	232.	207.	170.	124.	57.	0.	0.
149.	301.	290.	277.	255.	220.	173.	95.	0.	0.
83.	91.	86.	81.	75.	58.	59.	41.	0.	0.
52.	60.	62.	63.	64.	53.	60.	50.	0.	0.
55.	56.	54.	51.	49.	45.	41.	34.	0.	0.

FLUID MASS FLOW RATE = 40876.6 LBM/HR
 TOTAL Q (BTU/HR) BASED ON THE Q MATRIX = 47614583.4
 Q (BTU/HR) BASED ON THE WATER/STEAM MATRIX = 47656302.3
 Q (BTU/HR) BASED ON THE GAS MATRIX = 40551687.8
 THE MINIMUM PINCH POINT = 3.1 DEGREES
 BOILING BEGINS AT 8.8 INCHES INTO NODE 10 4
 SUPERHEATING BEGINS AT 5.8 INCHES INTO NODE 20 1
 THE ISENTROPIC POWER OF THE STEAM TURBINE = 6393. HORSEPOWER


```

RUN NUMBER = 10
ENTER NUMBER OF HEAT EXCHANGER PASSES DESIRED
23
ENTER EXHAUST GAS MASS FLOW RATE (LBM/S) FOR GAS PATHS 1 THROUGH 10
9.91 9.91 9.91 9.91 9.91 9.91 9.91 9.91 9.91 9.91
ENTER GAS TEMPERATURE AT INLET (DEG F) FOR GAS PATHS 1 THROUGH 10
755. 755. 755. 755. 755. 755. 755. 755. 755. 755.
ENTER FEEDWATER INLET TEMPERATURE (DEG F)
200.0
ENTER DESIRED STEAM TEMPERATURE AT OUTLET
650.0
ENTER DESIRED STEAM PRESSURE
400.0
ENTER MINIMUM EXHAUST GAS TEMPERATURE ALLOWED AT HEAT EXCHANGER EXIT
300.0
ENTER TUBE LENGTH (FT) PER NODE
1.0
ENTER NUMBER OF TUBES PER ROW
32.0
ENTER GEOMETRIC SCALING FACTOR
1.0

```


[illegible]

MATRIX OF EXHAUST GAS TEMPERATURES

376.	376.	376.	377.	377.	378.	378.	378.	378.
397.	397.	396.	396.	396.	396.	395.	395.	394.
410.	411.	410.	411.	412.	412.	412.	412.	412.
425.	425.	424.	424.	424.	424.	424.	423.	423.
434.	433.	433.	433.	434.	434.	434.	435.	435.
443.	442.	441.	441.	441.	442.	442.	441.	441.
448.	448.	447.	447.	448.	448.	448.	448.	448.
454.	453.	452.	452.	453.	453.	453.	453.	452.
457.	457.	455.	455.	457.	457.	457.	457.	457.
461.	460.	458.	458.	459.	460.	460.	460.	459.
466.	465.	462.	462.	462.	462.	462.	462.	462.
472.	471.	468.	468.	468.	468.	468.	468.	468.
481.	479.	475.	475.	475.	475.	475.	475.	475.
493.	490.	484.	484.	484.	484.	485.	485.	485.
508.	505.	497.	497.	497.	497.	497.	497.	497.
528.	524.	513.	513.	513.	513.	514.	514.	514.
554.	549.	534.	535.	535.	535.	535.	535.	536.
588.	582.	563.	563.	564.	564.	564.	564.	564.
634.	625.	600.	601.	601.	602.	602.	602.	602.
695.	683.	650.	650.	651.	652.	652.	652.	652.
714.	715.	716.	716.	717.	718.	718.	719.	719.
734.	734.	734.	734.	734.	734.	734.	733.	733.
745.	745.	745.	746.	746.	747.	747.	747.	748.
755.	755.	755.	755.	755.	755.	755.	755.	755.

MATRIX OF OVERALL HEAT TRANSFER COEFFICIENTS

66.	66.	67.	67.	68.	58.	69.	59.	70.	70.
74.	73.	73.	73.	72.	72.	72.	71.	71.	71.
74.	74.	74.	75.	75.	75.	75.	75.	76.	76.
77.	77.	77.	77.	77.	77.	77.	76.	76.	76.
78.	78.	78.	78.	78.	78.	78.	78.	79.	79.
80.	79.	79.	79.	79.	79.	79.	79.	79.	79.
80.	80.	80.	80.	80.	80.	80.	80.	80.	80.
81.	81.	80.	80.	80.	80.	80.	80.	80.	80.
81.	81.	81.	81.	81.	81.	81.	81.	81.	81.
150.	150.	150.	150.	136.	81.	81.	81.	81.	81.
150.	150.	150.	150.	150.	150.	150.	150.	150.	150.
151.	151.	150.	150.	150.	150.	150.	150.	150.	150.
151.	151.	151.	151.	151.	151.	151.	151.	151.	151.
151.	151.	151.	151.	151.	151.	151.	151.	151.	151.
152.	152.	151.	151.	151.	151.	151.	151.	151.	151.
152.	152.	152.	152.	152.	152.	152.	152.	152.	152.
153.	153.	152.	152.	152.	152.	152.	152.	152.	152.
154.	154.	153.	153.	153.	153.	153.	153.	153.	153.
155.	155.	154.	154.	154.	154.	154.	154.	154.	154.
45.	74.	155.	155.	155.	155.	155.	155.	155.	155.
45.	45.	45.	44.	44.	44.	44.	43.	43.	43.
42.	42.	42.	42.	42.	42.	43.	43.	43.	43.
42.	42.	42.	42.	42.	42.	42.	42.	42.	42.

MATRIX OF HEAT TRANSFER (Q) PER NODE

51.	50.	49.	47.	46.	45.	44.	42.	41.	40.
32.	33.	34.	36.	37.	38.	40.	41.	42.	44.
36.	34.	33.	32.	31.	30.	29.	28.	27.	26.
20.	21.	22.	23.	23.	25.	25.	26.	27.	28.
23.	22.	21.	20.	19.	19.	18.	17.	17.	16.
13.	13.	13.	14.	14.	15.	16.	16.	17.	18.
14.	13.	12.	12.	12.	12.	11.	11.	10.	10.
8.	8.	8.	8.	9.	9.	10.	10.	11.	11.
9.	8.	7.	7.	7.	7.	7.	7.	6.	6.
12.	12.	10.	10.	9.	8.	6.	6.	7.	7.
16.	15.	13.	13.	13.	13.	13.	13.	13.	13.
21.	20.	18.	18.	18.	18.	18.	18.	18.	18.
28.	27.	23.	23.	23.	23.	23.	23.	23.	23.
37.	35.	30.	30.	30.	31.	31.	31.	31.	31.
49.	46.	40.	40.	40.	40.	40.	40.	40.	40.
64.	61.	53.	53.	53.	53.	53.	53.	53.	53.
85.	81.	70.	70.	70.	70.	70.	70.	70.	70.
113.	107.	92.	92.	93.	93.	93.	93.	93.	93.
150.	142.	122.	122.	123.	123.	123.	123.	124.	124.
49.	40.	162.	163.	163.	164.	164.	164.	164.	165.
51.	49.	47.	45.	43.	41.	40.	38.	37.	35.
25.	27.	28.	29.	30.	31.	32.	34.	35.	37.
26.	25.	24.	23.	23.	22.	21.	20.	19.	19.

FLUID MASS FLOW RATE = 28672.8 LB_M/HR
 TOTAL Q (BTU/HR) BASED ON THE Q MATRIX = 33438653.9
 Q (BTU/HR) BASED ON THE WATER/STEAM MATRIX = 33428012.0
 Q (BTU/HR) BASED ON THE GAS MATRIX = 33632787.5
 THE MINIMUM PINCH POINT = 17.5 DEGREES
 BOILING BEGINS AT 2.4 INCHES INTO NODE 10 5
 SUPERHEATING BEGINS AT 3.1 INCHES INTO NODE 20 2
 THE ISENTROPIC POWER OF THE STEAM TURBINE = 4484. HORSEPOWER


```

RUN NUMBER = 11
ENTER NUMBER OF HEAT EXCHANGER PASSES DESIRED
23
ENTER EXHAUST GAS MASS FLOW RATE (LBM/S) FOR GAS PATHS 1 THROUGH 10
1.68 4.86 6.74 11.10 25.17 25.17 25.17 11.10 6.74 4.86 1.68
ENTER GAS TEMPERATURE AT INLET (DEG F) FOR GAS PATHS 1 THROUGH 10
755. 755. 755. 755. 755. 755. 755. 755. 755. 755.
ENTER FEEDWATER INLET TEMPERATURE (DEG F)
200.0
ENTER DESIRED STEAM TEMPERATURE AT OUTLET
650.0
ENTER DESIRED STEAM PRESSURE
400.0
ENTER MINIMUM EXHAUST GAS TEMPERATURE ALLOWED AT HEAT EXCHANGER EXIT
300.0
ENTER TUBE LENGTH (FT) PER NODE
1.0
ENTER NUMBER OF TUBES PER ROW
32.0
ENTER GEOMETRIC SCALING FACTOR
1.0

```


MATRIX OF WATER/STEAM TEMPERATURES

[illegible]

MATRIX OF EXHAUST GAS TEMPERATURES

288.	338.	356.	386.	453.	450.	385.	358.	342.	299.
334.	368.	381.	404.	464.	451.	401.	378.	364.	324.
355.	386.	397.	418.	474.	471.	417.	399.	390.	364.
388.	407.	415.	431.	483.	479.	428.	412.	404.	381.
401.	418.	425.	440.	490.	487.	438.	426.	420.	407.
422.	431.	436.	448.	497.	493.	444.	433.	429.	417.
429.	437.	441.	454.	503.	499.	451.	441.	438.	433.
440.	444.	447.	459.	508.	503.	454.	445.	442.	437.
442.	446.	449.	462.	512.	508.	458.	449.	446.	445.
445.	448.	452.	465.	517.	513.	462.	450.	447.	445.
445.	449.	455.	471.	527.	523.	467.	452.	448.	445.
445.	452.	459.	479.	538.	534.	473.	456.	450.	445.
446.	456.	465.	489.	551.	546.	481.	460.	453.	445.
447.	462.	473.	501.	567.	551.	492.	467.	457.	446.
449.	470.	485.	517.	584.	577.	505.	477.	464.	447.
453.	484.	502.	538.	603.	595.	523.	490.	475.	450.
462.	505.	527.	566.	626.	617.	545.	509.	490.	456.
479.	537.	561.	601.	652.	642.	574.	536.	514.	468.
514.	586.	611.	646.	682.	670.	612.	575.	552.	493.
586.	662.	681.	705.	716.	703.	661.	630.	609.	542.
628.	690.	705.	723.	740.	740.	724.	709.	696.	643.
685.	721.	728.	738.	747.	747.	737.	727.	719.	679.
715.	737.	742.	747.	751.	752.	748.	745.	742.	727.
755.	755.	755.	755.	755.	755.	755.	755.	755.	755.

MATRIX OF OVERALL HEAT TRANSFER COEFFICIENTS

40.	56.	60.	65.	71.	72.	68.	63.	59.	42.
44.	61.	66.	72.	77.	76.	70.	64.	59.	42.
44.	62.	67.	73.	80.	30.	74.	68.	63.	45.
45.	65.	70.	76.	82.	32.	75.	69.	64.	45.
46.	65.	70.	77.	84.	34.	77.	71.	66.	46.
46.	66.	72.	78.	85.	95.	78.	71.	66.	46.
47.	66.	72.	79.	86.	35.	79.	72.	67.	47.
47.	67.	73.	80.	87.	37.	79.	72.	67.	47.
47.	67.	73.	80.	87.	120.	155.	130.	114.	66.
66.	114.	131.	156.	185.	185.	156.	131.	114.	66.
66.	114.	131.	156.	186.	146.	156.	131.	114.	66.
66.	114.	131.	156.	187.	186.	156.	131.	114.	66.
66.	114.	131.	156.	187.	137.	156.	131.	114.	66.
66.	115.	131.	157.	188.	188.	157.	131.	114.	66.
66.	115.	132.	157.	189.	138.	157.	131.	115.	66.
66.	115.	132.	158.	189.	189.	157.	132.	115.	66.
66.	115.	133.	159.	190.	190.	158.	132.	115.	66.
66.	116.	133.	160.	192.	191.	159.	133.	116.	66.
67.	117.	134.	161.	193.	192.	160.	134.	116.	67.
31.	39.	41.	44.	124.	194.	161.	135.	117.	67.
31.	39.	40.	42.	44.	44.	41.	39.	38.	30.
30.	37.	39.	41.	42.	43.	41.	39.	38.	31.
30.	37.	39.	40.	42.	42.	40.	39.	37.	30.

MATRIX OF HEAT TRANSFER (Q) PER NODE

19.	35.	41.	50.	71.	58.	44.	33.	26.	11.
9.	21.	27.	37.	61.	52.	42.	35.	30.	16.
13.	25.	29.	36.	55.	52.	30.	21.	17.	7.
5.	13.	17.	24.	46.	46.	28.	23.	20.	11.
8.	15.	18.	23.	41.	38.	18.	12.	10.	4.
3.	7.	9.	15.	35.	35.	17.	13.	11.	6.
5.	8.	10.	14.	32.	29.	10.	6.	4.	2.
1.	2.	4.	8.	28.	28.	10.	6.	5.	3.
1.	3.	4.	9.	27.	34.	10.	3.	1.	0.
0.	2.	5.	16.	63.	50.	13.	4.	1.	0.
0.	3.	7.	21.	72.	68.	17.	5.	2.	0.
0.	5.	10.	27.	82.	78.	22.	8.	3.	0.
0.	7.	14.	35.	94.	89.	29.	11.	5.	0.
1.	11.	20.	45.	107.	102.	37.	16.	8.	1.
2.	16.	28.	58.	123.	117.	48.	22.	12.	1.
4.	25.	40.	75.	141.	134.	62.	32.	19.	2.
7.	38.	58.	97.	162.	154.	80.	45.	29.	5.
15.	59.	83.	126.	186.	177.	104.	64.	45.	10.
30.	91.	119.	163.	215.	204.	135.	92.	69.	20.
18.	35.	41.	49.	151.	235.	176.	133.	106.	42.
24.	37.	39.	42.	44.	42.	36.	31.	27.	15.
13.	21.	24.	27.	31.	32.	31.	30.	29.	20.
17.	22.	22.	22.	23.	22.	20.	18.	16.	12.

FLUID MASS FLOW RATE = 26366.6 LBM/HR
 TOTAL Q (BTU/HR) BASED ON THE Q MATRIX = 30752819.5
 Q (BTU/HR) BASED ON THE WATER/STEAM MATRIX = 30740245.3
 Q (BTU/HR) BASED ON THE GAS MATRIX = 34621544.6
 THE MINIMUM PINCH POINT = 3.1 DEGREES
 BOILING BEGINS AT 7.9 INCHES INTO NODE 9 6
 SUPERHEATING BEGINS AT 6.3 INCHES INTO NODE 20 5
 THE ISENTROPIC POWER OF THE STEAM TURBINE = 4123. HORSEPOWER

RUN NUMBER = 15

ENTER NUMBER OF HEAT EXCHANGER PASSES DESIRED

23

ENTER EXHAUST GAS MASS FLOW RATE (LBM/S) FOR GAS PATHS 1 THROUGH 10
9.91 22.20 19.03 16.15 12.99 9.51 6.35 2.97 0.0 0.0

ENTER GAS TEMPERATURE AT INLET (DEG F) FOR GAS PATHS 1 THROUGH 10

755. 755. 755. 755. 755. 755. 755. 755. 755. 755.

ENTER FEEDWATER INLET TEMPERATURE (DEG F)

200.0

ENTER DESIRED STEAM TEMPERATURE AT OUTLET

650.0

ENTER DESIRED STEAM PRESSURE

400.0

ENTER MINIMUM EXHAUST GAS TEMPERATURE ALLOWED AT HEAT EXCHANGER EXIT

300.0

ENTER TUBE LENGTH (FT) PER NODE

1.0

ENTER NUMBER OF TUBES PER ROW

32.0

ENTER GEOMETRIC SCALING FACTOR

1.0

MATRIX OF WATER/STEAM TEMPERATURES

[illegible]

MATRIX OF EXHAUST GAS TEMPERATURES

375.	440.	425.	411.	394.	374.	352.	316.	755.	755.
396.	453.	439.	426.	410.	392.	372.	341.	755.	755.
410.	463.	450.	438.	424.	409.	395.	373.	755.	755.
425.	473.	461.	449.	435.	421.	408.	389.	755.	755.
434.	481.	469.	458.	445.	433.	423.	411.	755.	755.
444.	489.	476.	465.	452.	440.	431.	420.	755.	755.
449.	494.	482.	472.	459.	448.	440.	434.	755.	755.
455.	500.	488.	477.	464.	452.	444.	439.	755.	755.
458.	505.	492.	481.	468.	456.	449.	445.	755.	755.
461.	509.	497.	485.	473.	460.	451.	445.	755.	755.
467.	520.	506.	493.	480.	465.	454.	446.	755.	755.
474.	532.	517.	504.	488.	472.	458.	446.	755.	755.
483.	545.	531.	516.	500.	480.	463.	448.	755.	755.
495.	561.	546.	531.	513.	492.	471.	450.	755.	755.
510.	580.	565.	550.	531.	507.	483.	454.	755.	755.
531.	602.	587.	572.	553.	528.	500.	460.	755.	755.
559.	627.	614.	599.	581.	555.	524.	472.	755.	755.
595.	656.	645.	633.	616.	591.	559.	492.	755.	755.
643.	691.	682.	673.	660.	639.	609.	526.	755.	755.
706.	731.	727.	722.	715.	703.	683.	586.	755.	755.
721.	739.	737.	734.	730.	722.	710.	679.	755.	755.
737.	746.	745.	743.	740.	735.	727.	705.	755.	755.
746.	751.	750.	750.	749.	747.	744.	736.	755.	755.
755.	755.	755.	755.	755.	755.	755.	755.	755.	755.

MATRIX OF OVERALL HEAT TRANSFER COEFFICIENTS

63.	70.	70.	69.	66.	62.	51.	0.	0.
71.	77.	76.	72.	59.	63.	52.	0.	0.
71.	79.	78.	76.	72.	67.	55.	0.	0.
75.	82.	81.	79.	77.	68.	55.	0.	0.
75.	83.	82.	81.	79.	70.	57.	0.	0.
77.	85.	84.	82.	80.	75.	57.	0.	0.
77.	85.	85.	83.	81.	77.	58.	0.	0.
78.	87.	85.	84.	81.	77.	58.	0.	0.
78.	87.	86.	84.	128.	148.	127.	90.	0.
150.	183.	178.	172.	163.	148.	127.	90.	0.
150.	183.	179.	173.	163.	148.	128.	90.	0.
151.	184.	179.	173.	164.	149.	128.	90.	0.
151.	185.	180.	174.	164.	149.	128.	90.	0.
151.	185.	180.	174.	164.	149.	128.	90.	0.
152.	186.	181.	175.	165.	150.	129.	90.	0.
152.	187.	182.	175.	166.	150.	129.	91.	0.
153.	188.	183.	176.	166.	151.	129.	91.	0.
154.	189.	184.	177.	167.	152.	130.	91.	0.
155.	190.	185.	179.	169.	153.	131.	92.	0.
42.	44.	44.	44.	44.	43.	42.	86.	0.
42.	44.	43.	43.	42.	41.	39.	35.	0.
40.	42.	42.	42.	41.	40.	39.	35.	0.
40.	42.	42.	42.	41.	40.	38.	34.	0.

MATRIX OF HEAT TRANSFER (Q) PER NODE

50.	70.	63.	57.	49.	40.	31.	17.	0.	0.
33.	56.	53.	50.	46.	41.	34.	23.	0.	0.
37.	55.	48.	42.	35.	28.	21.	12.	0.	0.
22.	42.	39.	36.	32.	28.	23.	16.	0.	0.
24.	41.	35.	29.	23.	17.	13.	7.	0.	0.
13.	32.	28.	25.	21.	17.	14.	10.	0.	0.
15.	31.	26.	20.	15.	10.	6.	3.	0.	0.
7.	25.	22.	18.	14.	10.	7.	5.	0.	0.
8.	25.	20.	14.	14.	9.	3.	0.	0.	0.
13.	56.	44.	34.	23.	12.	4.	0.	0.	0.
17.	65.	53.	41.	28.	15.	6.	1.	0.	0.
22.	76.	62.	50.	36.	20.	9.	1.	0.	0.
29.	88.	74.	60.	45.	27.	13.	2.	0.	0.
39.	102.	88.	73.	56.	36.	18.	3.	0.	0.
51.	119.	105.	89.	71.	48.	26.	5.	0.	0.
67.	139.	124.	109.	89.	54.	38.	8.	0.	0.
89.	162.	148.	131.	112.	85.	55.	15.	0.	0.
118.	190.	177.	162.	142.	113.	80.	25.	0.	0.
156.	222.	212.	199.	180.	152.	116.	44.	0.	0.
38.	46.	47.	48.	48.	47.	44.	69.	0.	0.
39.	42.	39.	37.	35.	31.	27.	20.	0.	0.
23.	26.	27.	28.	28.	28.	27.	23.	0.	0.
23.	24.	23.	22.	20.	19.	17.	14.	0.	0.

FLUID MASS FLOW RATE = 26605.5 LBM/HR
 TOTAL Q (BTU/HR) BASED ON THE Q MATRIX = 31030556.4
 Q (BTU/HR) BASED ON THE WATER/STEAM MATRIX = 31017056.1
 Q (BTU/HR) BASED ON THE GAS MATRIX = 26377549.7
 THE MINIMUM PINCH POINT = 3.5 DEGREES
 BOILING BEGINS AT 5.2 INCHES INFO NODE 9 5
 SUPERHEATING BEGINS AT 10.5 INCHES INFO NODE 20 8
 THE ISENTROPIC POWER OF THE STEAM TURBINE = 4161. HORSEPOWER


```

RUN NUMBER = 19
ENTER NUMBER OF HEAT EXCHANGER PASSES DESIRED
23
ENTER EXHAUST GAS MASS FLOW RATE (LBM/S) FOR GAS PATHS 1 THROUGH 10
7.74 7.74 7.74 7.74 7.74 7.74 7.74 7.74 7.74 7.74
ENTER GAS TEMPERATURE AT INLET (DEG F) FOR GAS PATHS 1 THROUGH 10
702. 702. 702. 702. 702. 702. 702. 702. 702. 702.
ENTER FEEDWATER INLET TEMPERATURE (DEG F)
200.0
ENTER DESIRED STEAM TEMPERATURE AT OUTLET
650.0
ENTER DESIRED STEAM PRESSURE
400.0
ENTER MINIMUM EXHAUST GAS TEMPERATURE ALLOWED AT HEAT EXCHANGER EXIT
300.0
ENTER TUBE LENGTH (FT) PER NODE
1.0
ENTER NUMBER OF TUBES PER ROW
32.0
ENTER GEOMETRIC SCALING FACTOR
1.0

```


[illegible]

MATRIX OF EXHAUST GAS TEMPERATURES

381.	382.	383.	383.	384.	384.	384.	385.
404.	403.	403.	403.	402.	402.	401.	401.
416.	417.	417.	418.	418.	418.	418.	419.
429.	429.	429.	429.	428.	428.	428.	428.
436.	436.	437.	437.	437.	437.	437.	438.
443.	443.	443.	443.	442.	442.	442.	443.
446.	447.	447.	447.	447.	447.	447.	448.
450.	450.	450.	450.	450.	450.	450.	451.
452.	452.	452.	452.	452.	452.	452.	454.
454.	454.	454.	454.	454.	454.	453.	455.
457.	457.	457.	457.	457.	457.	457.	459.
462.	462.	462.	462.	462.	461.	461.	464.
468.	468.	468.	468.	468.	468.	468.	472.
477.	477.	477.	477.	477.	477.	477.	482.
489.	489.	489.	489.	489.	489.	489.	496.
506.	506.	506.	506.	506.	506.	505.	516.
529.	529.	529.	529.	529.	529.	529.	543.
562.	562.	562.	562.	561.	561.	561.	580.
607.	607.	606.	606.	606.	605.	605.	632.
669.	669.	669.	668.	668.	667.	667.	666.
680.	681.	681.	682.	682.	683.	683.	683.
692.	691.	691.	691.	691.	691.	691.	691.
697.	697.	697.	698.	698.	698.	698.	698.
702.	702.	702.	702.	702.	702.	702.	702.

MATRIX OF OVERALL HEAT TRANSFER COEFFICIENTS

52.	53.	54.	54.	55.	55.	56.	57.	57.
60.	60.	60.	60.	59.	59.	58.	58.	58.
61.	61.	61.	61.	61.	62.	62.	62.	62.
64.	63.	63.	63.	63.	63.	63.	63.	62.
64.	64.	64.	64.	64.	64.	64.	64.	64.
65.	65.	65.	65.	65.	65.	65.	65.	64.
65.	65.	65.	65.	65.	65.	65.	65.	65.
66.	66.	65.	65.	65.	65.	65.	65.	65.
66.	66.	66.	66.	66.	66.	66.	66.	66.
138.	138.	138.	138.	138.	138.	138.	137.	136.
138.	138.	138.	138.	138.	138.	138.	138.	138.
138.	138.	138.	138.	138.	138.	138.	138.	138.
138.	138.	138.	138.	138.	138.	138.	138.	138.
139.	139.	139.	139.	139.	139.	139.	139.	139.
139.	139.	139.	139.	139.	139.	139.	139.	139.
140.	140.	140.	140.	140.	140.	140.	140.	140.
140.	140.	140.	140.	140.	140.	140.	140.	141.
142.	142.	141.	141.	141.	141.	141.	141.	77.
33.	33.	33.	33.	33.	34.	34.	34.	35.
33.	33.	33.	32.	32.	32.	32.	32.	32.
32.	32.	32.	32.	32.	32.	32.	32.	32.
32.	32.	32.	32.	32.	32.	32.	32.	32.

MATRIX OF HEAT TRANSFER (O) PER NODE

42.	41.	40.	38.	37.	35.	35.	33.	32.	31.
23.	24.	25.	27.	28.	29.	30.	31.	33.	34.
25.	24.	23.	22.	21.	21.	20.	19.	18.	17.
12.	13.	14.	14.	15.	15.	16.	17.	18.	19.
14.	13.	12.	12.	11.	11.	10.	10.	9.	9.
6.	7.	7.	7.	8.	8.	9.	9.	9.	10.
7.	7.	6.	6.	6.	6.	5.	5.	5.	5.
3.	3.	4.	4.	4.	4.	4.	5.	5.	5.
4.	3.	3.	3.	3.	3.	3.	3.	3.	3.
6.	6.	6.	6.	6.	6.	6.	6.	6.	7.
9.	9.	9.	9.	9.	9.	9.	9.	9.	10.
12.	12.	12.	12.	12.	12.	12.	12.	12.	14.
17.	17.	17.	17.	17.	17.	17.	17.	17.	20.
23.	23.	23.	23.	23.	23.	23.	23.	23.	27.
32.	32.	32.	32.	32.	32.	32.	32.	32.	37.
45.	45.	45.	45.	45.	44.	44.	44.	44.	52.
62.	62.	62.	62.	62.	62.	62.	61.	61.	72.
86.	86.	86.	86.	86.	86.	86.	85.	85.	100.
120.	120.	120.	120.	120.	119.	119.	119.	119.	66.
22.	23.	24.	25.	26.	27.	29.	30.	31.	33.
22.	21.	20.	20.	19.	18.	17.	16.	16.	15.
10.	11.	11.	12.	12.	13.	13.	14.	15.	15.
10.	10.	10.	9.	9.	8.	8.	8.	7.	7.

FLUID MASS FLOW RATE = 18853.1 LBM/HR
 TOTAL Q (BTU/HR) BASED ON THE Q MATRIX = 21987181.0
 Q (BTU/HR) BASED ON THE WATER/STEAM MATRIX = 21981805.8
 Q (BTU/HR) BASED ON THE GAS MATRIX = 22088931.7
 THE MINIMUM PINCH POINT = 9.4 DEGREES
 BOILING BEGINS AT 0.2 INCHES INTO NODE 10 10
 SUPERHEATING BEGINS AT 4.7 INCHES INTO NODE 19 10
 THE ISENTROPIC POWER OF THE STEAM TURBINE = 2948. HORSEPOWER


```

RUN NUMBER = 20
ENTER NUMBER OF HEAT EXCHANGER PASSES DESIRED
23
ENTER EXHAUST GAS MASS FLOW RATE (LBM/S) FOR GAS PATHS 1 THROUGH 10
1.31 3.80 5.26 8.67 19.66 19.66 8.67 5.26 3.80 1.31
ENTER GAS TEMPERATURE AT INLET (DEG F) FOR GAS PATHS 1 THROUGH 10
702. 702. 702. 702. 702. 702. 702. 702. 702. 702.
ENTER FEEDWATER INLET TEMPERATURE (DEG F)
200.0
ENTER DESIRED STEAM TEMPERATURE AT OUTLET
650.0
ENTER DESIRED STEAM PRESSURE
400.0
ENTER MINIMUM EXHAUST GAS TEMPERATURE ALLOWED AT HEAT EXCHANGER EXIT
300.0
ENTER TUBE LENGTH (FT) PER NODE
1.0
ENTER NUMBER OF TUBES PER ROW
32.0
ENTER GEOMETRIC SCALING FACTOR
1.0

```


[illegible]

MATRIX OF EXHAUST GAS TEMPERATURES

295.	345.	362.	388.	439.	440.	389.	365.	350.	308.
347.	378.	388.	407.	450.	450.	406.	386.	373.	335.
367.	395.	404.	420.	459.	459.	421.	407.	399.	377.
400.	415.	421.	432.	466.	455.	431.	419.	412.	392.
411.	424.	429.	439.	472.	473.	440.	431.	427.	417.
429.	435.	438.	446.	477.	477.	445.	437.	433.	425.
434.	440.	442.	449.	481.	481.	450.	443.	441.	437.
443.	445.	446.	453.	484.	485.	451.	446.	443.	440.
444.	445.	447.	455.	487.	488.	455.	448.	446.	445.
445.	446.	448.	456.	492.	495.	459.	450.	447.	445.
445.	447.	450.	460.	500.	504.	464.	452.	448.	445.
445.	449.	453.	466.	510.	515.	471.	456.	451.	445.
445.	452.	457.	473.	522.	527.	480.	462.	454.	446.
446.	456.	463.	483.	535.	542.	493.	470.	460.	447.
448.	463.	473.	496.	551.	559.	509.	483.	470.	450.
452.	474.	487.	514.	571.	580.	532.	502.	486.	456.
460.	492.	508.	538.	593.	604.	562.	531.	512.	469.
479.	522.	540.	570.	620.	632.	604.	574.	555.	498.
518.	571.	589.	615.	651.	666.	660.	640.	624.	561.
605.	650.	661.	675.	689.	699.	674.	659.	647.	595.
631.	667.	675.	685.	694.	694.	686.	677.	671.	641.
666.	684.	698.	693.	698.	699.	693.	688.	683.	661.
681.	693.	695.	698.	700.	700.	699.	697.	695.	688.
702.	702.	702.	702.	702.	702.	702.	702.	702.	702.

MATRIX OF OVERALL HEAT TRANSFER COEFFICIENTS

32.	45.	48.	53.	58.	59.	55.	51.	48.	34.
36.	50.	54.	59.	63.	63.	57.	52.	48.	35.
36.	51.	55.	60.	66.	66.	61.	56.	52.	37.
37.	53.	57.	62.	68.	68.	62.	56.	52.	37.
37.	53.	57.	63.	69.	59.	63.	58.	54.	38.
38.	54.	59.	64.	70.	70.	64.	58.	54.	38.
38.	54.	59.	64.	71.	71.	65.	59.	55.	38.
38.	55.	59.	65.	71.	71.	65.	59.	55.	38.
38.	55.	59.	65.	117.	179.	143.	118.	102.	57.
57.	102.	118.	144.	179.	179.	144.	118.	102.	57.
57.	102.	118.	144.	180.	133.	144.	118.	102.	57.
57.	102.	118.	144.	180.	180.	144.	118.	102.	57.
57.	102.	118.	144.	180.	131.	144.	118.	102.	57.
57.	102.	119.	144.	181.	181.	145.	119.	102.	57.
57.	102.	119.	145.	182.	132.	145.	119.	102.	57.
57.	103.	119.	145.	182.	183.	146.	119.	103.	57.
57.	103.	119.	146.	183.	134.	146.	120.	103.	57.
57.	103.	120.	146.	184.	185.	147.	121.	104.	57.
58.	104.	121.	148.	185.	139.	34.	32.	30.	24.
24.	29.	30.	32.	33.	34.	32.	31.	30.	24.
24.	29.	30.	31.	33.	32.	31.	30.	29.	23.
23.	28.	29.	31.	32.	32.	31.	30.	29.	24.
23.	28.	29.	31.	32.	32.	31.	29.	28.	23.

MATRIX OF HEAT TRANSFER (Q) PER NODE

16.	30.	34.	40.	53.	51.	35.	26.	21.	9.
7.	16.	20.	28.	42.	44.	33.	27.	24.	13.
10.	19.	21.	25.	36.	34.	21.	15.	12.	5.
4.	9.	11.	16.	28.	29.	19.	16.	14.	8.
6.	10.	11.	14.	24.	23.	11.	8.	6.	3.
2.	4.	5.	8.	19.	20.	10.	8.	7.	4.
3.	5.	5.	7.	17.	16.	5.	3.	2.	1.
0.	1.	1.	3.	14.	15.	5.	3.	3.	1.
0.	1.	1.	3.	23.	37.	8.	2.	1.	0.
0.	1.	2.	9.	40.	43.	11.	3.	1.	0.
0.	2.	4.	12.	48.	51.	15.	5.	2.	0.
0.	2.	5.	16.	56.	60.	20.	7.	4.	0.
0.	4.	8.	21.	66.	71.	26.	11.	6.	0.
1.	7.	12.	28.	78.	84.	36.	17.	9.	1.
1.	11.	18.	38.	93.	100.	48.	25.	15.	2.
3.	17.	28.	52.	110.	118.	66.	37.	24.	4.
6.	28.	42.	70.	130.	140.	89.	57.	40.	9.
13.	46.	63.	95.	154.	166.	121.	86.	65.	20.
28.	75.	95.	130.	183.	199.	31.	26.	22.	11.
9.	16.	19.	22.	26.	27.	25.	24.	23.	15.
11.	16.	17.	18.	19.	19.	16.	13.	12.	7.
5.	8.	10.	11.	13.	13.	13.	12.	12.	9.
7.	9.	9.	9.	9.	9.	8.	7.	6.	5.

FLUID MASS FLOW RATE = 17625.2 LBM/HR
 TOTAL Q (BTU/HR) BASED ON THE Q MATRIX = 20557382.4
 Q (BTU/HR) BASED ON THE WATER/STEAM MATRIX = 20549047.7
 Q (BTU/HR) BASED ON THE GAS MATRIX = 23107185.0
 THE MINIMUM PINCH POINT = 0.1 DEGREES
 BOILING BEGINS AT 6.9 INCHES INTO NODE 9 5
 SUPERHEATING BEGINS AT 5.9 INCHES INTO NODE 19 6
 THE ISENTROPIC POWER OF THE STEAM TURBINE = 2756. HORSEPOWER


```

RUN NUMBER = 24
ENTER NUMBER OF HEAT EXCHANGER PASSES DESIRED
23
ENTER EXHAUST GAS MASS FLOW RATE (LBM/S) FOR GAS PATHS 1 THROUGH 10
7.74 17.34 14.86 12.61 10.15 7.43 4.96 2.32 0.0 0.0
ENTER GAS TEMPERATURE AT INLET (DEG F) FOR GAS PATHS 1 THROUGH 10
702. 702. 702. 702. 702. 702. 702. 702. 702.
ENTER FEEDWATER INLET TEMPERATURE (DEG F)
200.0
ENTER DESIRED STEAM TEMPERATURE AT OUTLET
650.0
ENTER DESIRED STEAM PRESSURE
400.0
ENTER MINIMUM EXHAUST GAS TEMPERATURE ALLOWED AT HEAT EXCHANGER EXIT
300.0
ENTER TUBE LENGTH (FT) PER NODE
1.0
ENTER NUMBER OF TUBES PER ROW
32.0
ENTER GEOMETRIC SCALING FACTOR
1.0

```


200.	208.	219.	229.	238.	245.	252.	257.	260.	260.	260.	260.
310.	305.	297.	289.	282.	275.	269.	263.	260.	260.	260.	260.
310.	315.	323.	329.	335.	339.	343.	346.	348.	348.	348.	348.
338.	376.	370.	366.	361.	357.	353.	350.	348.	348.	348.	348.
378.	381.	386.	390.	394.	396.	398.	400.	401.	401.	401.	401.
418.	417.	413.	410.	408.	405.	403.	402.	401.	401.	401.	401.
418.	420.	423.	426.	428.	429.	430.	431.	431.	431.	431.	431.
441.	441.	438.	436.	434.	433.	432.	431.	431.	431.	431.	431.
441.	442.	445.	445.	445.	445.	445.	445.	445.	445.	445.	445.
445.	445.	445.	445.	445.	445.	445.	445.	445.	445.	445.	445.
445.	445.	445.	445.	445.	445.	445.	445.	445.	445.	445.	445.
445.	445.	445.	445.	445.	445.	445.	445.	445.	445.	445.	445.
445.	445.	445.	445.	445.	445.	445.	445.	445.	445.	445.	445.
449.	445.	445.	445.	445.	445.	445.	445.	445.	445.	445.	445.
449.	458.	467.	475.	484.	491.	498.	504.	508.	508.	508.	508.
558.	553.	546.	540.	533.	526.	520.	513.	508.	508.	508.	508.
558.	564.	570.	575.	581.	586.	590.	594.	597.	597.	597.	597.
627.	624.	620.	616.	612.	608.	604.	600.	597.	597.	597.	597.
627.	611.	634.	637.	640.	643.	646.	648.	650.	650.	650.	650.

MATRIX OF EXHAUST GAS TEMPERATURES

380.	432.	419.	408.	395.	379.	359.	325.	702.	702.
402.	445.	432.	422.	411.	397.	380.	350.	702.	702.
415.	454.	442.	434.	425.	414.	402.	384.	702.	702.
429.	463.	451.	443.	435.	425.	415.	399.	702.	702.
437.	470.	458.	451.	443.	435.	428.	419.	702.	702.
445.	476.	464.	457.	449.	441.	435.	427.	702.	702.
450.	480.	468.	461.	454.	447.	442.	438.	702.	702.
454.	484.	472.	465.	457.	450.	445.	441.	702.	702.
456.	487.	475.	467.	460.	453.	448.	445.	702.	702.
458.	491.	482.	473.	465.	455.	449.	445.	702.	702.
464.	500.	490.	481.	471.	460.	452.	446.	702.	702.
471.	511.	500.	490.	479.	466.	455.	447.	702.	702.
481.	524.	513.	502.	489.	474.	461.	449.	702.	702.
495.	539.	528.	517.	503.	496.	469.	452.	702.	702.
514.	558.	547.	535.	521.	502.	482.	459.	702.	702.
540.	581.	570.	559.	545.	525.	502.	471.	702.	702.
577.	608.	599.	589.	576.	556.	531.	493.	702.	702.
627.	641.	635.	627.	616.	600.	577.	534.	702.	702.
660.	681.	679.	675.	670.	661.	646.	611.	702.	702.
676.	689.	687.	684.	681.	674.	663.	634.	702.	702.
684.	693.	692.	691.	689.	685.	679.	662.	702.	702.
693.	697.	697.	696.	695.	692.	688.	676.	702.	702.
697.	700.	700.	699.	699.	698.	697.	693.	702.	702.
702.	702.	702.	702.	702.	702.	702.	702.	702.	702.

MATRIX OF OVERALL HEAT TRANSFER COEFFICIENTS

51.	56.	56.	56.	56.	54.	50.	42.	0.	0.
58.	63.	62.	61.	59.	56.	51.	42.	0.	0.
58.	65.	64.	63.	62.	59.	55.	45.	0.	0.
61.	68.	66.	65.	63.	60.	55.	45.	0.	0.
62.	68.	68.	67.	65.	62.	57.	47.	0.	0.
63.	70.	69.	67.	65.	62.	57.	47.	0.	0.
63.	70.	69.	68.	66.	63.	58.	47.	0.	0.
64.	71.	70.	68.	66.	63.	58.	47.	0.	0.
64.	71.	166.	162.	151.	135.	115.	79.	0.	0.
138.	175.	169.	162.	151.	136.	115.	79.	0.	0.
138.	176.	169.	162.	152.	136.	115.	79.	0.	0.
138.	176.	170.	162.	152.	136.	115.	79.	0.	0.
139.	176.	170.	163.	152.	136.	115.	79.	0.	0.
139.	177.	171.	163.	153.	137.	116.	79.	0.	0.
139.	178.	171.	164.	153.	137.	116.	79.	0.	0.
140.	178.	172.	164.	154.	138.	116.	80.	0.	0.
141.	179.	173.	165.	155.	138.	117.	80.	0.	0.
76.	180.	174.	166.	156.	139.	118.	81.	0.	0.
33.	35.	34.	34.	33.	32.	31.	27.	0.	0.
31.	33.	33.	32.	32.	31.	30.	27.	0.	0.
31.	32.	32.	32.	31.	31.	29.	26.	0.	0.
31.	32.	32.	32.	31.	31.	29.	27.	0.	0.
31.	32.	32.	32.	31.	30.	29.	26.	0.	0.

MATRIX OF HEAT TRANSFER (Q) PER NODE

40.	54.	48.	44.	38.	32.	25.	14.	0.	0.
25.	40.	38.	37.	35.	32.	27.	19.	0.	0.
27.	38.	33.	29.	24.	20.	15.	8.	0.	0.
15.	27.	25.	23.	21.	19.	17.	12.	0.	0.
16.	26.	21.	17.	14.	11.	8.	5.	0.	0.
8.	19.	16.	14.	12.	11.	9.	6.	0.	0.
9.	18.	13.	10.	8.	5.	3.	2.	0.	0.
4.	14.	11.	9.	7.	5.	4.	2.	0.	0.
4.	14.	25.	18.	12.	5.	2.	0.	0.	0.
10.	39.	31.	23.	15.	8.	3.	0.	0.	0.
14.	47.	38.	29.	20.	11.	4.	1.	0.	0.
19.	56.	46.	37.	26.	15.	7.	1.	0.	0.
26.	67.	57.	46.	34.	21.	10.	2.	0.	0.
36.	81.	70.	58.	45.	30.	16.	4.	0.	0.
50.	98.	86.	74.	59.	41.	24.	7.	0.	0.
70.	118.	106.	94.	78.	58.	36.	13.	0.	0.
97.	142.	131.	119.	103.	81.	56.	24.	0.	0.
63.	172.	162.	151.	136.	113.	86.	44.	0.	0.
31.	33.	31.	29.	26.	24.	20.	14.	0.	0.
16.	20.	20.	21.	21.	21.	20.	16.	0.	0.
17.	18.	17.	16.	14.	13.	11.	8.	0.	0.
9.	10.	11.	11.	11.	12.	11.	10.	0.	0.
9.	9.	9.	8.	8.	7.	7.	5.	0.	0.

FLUID MASS FLOW RATE = 17714.1 LBM/HR
 TOTAL Q (BTU/HR) BASED ON THE Q MATRIX = 20659747.1
 Q (BTU/HR) BASED ON THE WATER/STEAM MATRIX = 20652083.5
 Q (BTU/HR) BASED ON THE GAS MATRIX = 17521945.0
 THE MINIMUM PINCH POINT = 0.7 DEGREES
 BOILING BEGINS AT 0.3 INCHES INTO NODE 9 3
 SUPERHEATING BEGINS AT 4.7 INCHES INTO NODE 18 1
 THE ISENTROPIC POWER OF THE STEAM TURBINE = 2770. HORSEPOWER


```

RUN NUMBER = 28
ENTER NUMBER OF HEAT EXCHANGER PASSES DESIRED
23
ENTER EXHAUST GAS MASS FLOW RATE (LBM/S) FOR GAS PATHS 1 THROUGH 10
6.77 6.77 6.77 6.77 6.77 6.77 6.77 6.77 6.77 6.77
ENTER GAS TEMPERATURE AT INLET (DEG F) FOR GAS PATHS 1 THROUGH 10
694. 694. 694. 694. 594. 694. 694. 694. 694. 694.
ENTER FEEDWATER INLET TEMPERATURE (DEG F)
200.0
ENTER DESIRED STEAM TEMPERATURE AT OUTLET
650.0
ENTER DESIRED STEAM PRESSURE
400.0
ENTER MINIMUM EXHAUST GAS TEMPERATURE ALLOWED AT HEAT EXCHANGER EXIT
300.0
ENTER TUBE LENGTH (FT) PER NODE
1.0
ENTER NUMBER OF TUBES PER ROW
32.0
ENTER GEOMETRIC SCALING FACTOR
1.0

```


[illegible]

MATRIX OF EXHAUST GAS TEMPERATURES

381.	381.	382.	383.	383.	384.	384.	385.
404.	404.	403.	403.	403.	402.	402.	401.
416.	416.	417.	418.	418.	418.	419.	420.
429.	429.	429.	429.	429.	428.	429.	428.
435.	436.	436.	436.	436.	437.	437.	438.
442.	442.	442.	442.	442.	442.	442.	442.
445.	445.	445.	445.	446.	446.	447.	447.
448.	448.	448.	448.	448.	448.	449.	450.
450.	450.	450.	450.	450.	450.	452.	452.
451.	451.	451.	451.	451.	451.	453.	454.
454.	454.	454.	454.	454.	454.	457.	457.
458.	458.	458.	458.	458.	458.	462.	462.
463.	463.	463.	463.	463.	464.	469.	469.
471.	471.	471.	471.	471.	472.	479.	479.
483.	483.	482.	482.	482.	483.	494.	494.
498.	498.	498.	498.	498.	499.	515.	515.
521.	521.	521.	521.	521.	522.	544.	544.
553.	553.	553.	553.	553.	555.	586.	586.
599.	599.	598.	598.	598.	601.	646.	646.
664.	664.	664.	663.	663.	662.	662.	661.
674.	675.	675.	676.	676.	677.	677.	677.
685.	685.	685.	685.	684.	684.	684.	684.
689.	690.	690.	690.	690.	691.	691.	691.
694.	694.	694.	694.	694.	694.	694.	694.

MATRIX OF OVERALL HEAT TRANSFER COEFFICIENTS

47.	48.	49.	49.	50.	50.	51.	51.	52.	52.
55.	55.	55.	54.	54.	54.	54.	53.	53.	53.
55.	56.	56.	56.	56.	56.	57.	57.	57.	57.
58.	58.	58.	58.	58.	58.	58.	57.	57.	57.
58.	58.	58.	58.	59.	59.	59.	59.	59.	59.
59.	59.	59.	59.	59.	59.	59.	59.	59.	59.
59.	59.	59.	59.	60.	60.	60.	60.	60.	60.
60.	60.	60.	60.	60.	60.	60.	60.	60.	60.
60.	60.	60.	60.	60.	60.	60.	60.	60.	60.
131.	131.	131.	131.	131.	131.	131.	131.	131.	118.
131.	131.	131.	131.	131.	131.	131.	131.	131.	131.
131.	131.	131.	131.	131.	131.	131.	131.	131.	131.
131.	131.	131.	131.	131.	131.	131.	131.	131.	131.
132.	132.	132.	132.	132.	131.	131.	132.	132.	132.
132.	132.	132.	132.	132.	132.	132.	132.	132.	132.
132.	132.	132.	132.	132.	132.	132.	132.	133.	133.
133.	133.	133.	133.	133.	133.	133.	133.	133.	133.
133.	133.	133.	133.	133.	133.	133.	133.	134.	134.
134.	134.	134.	134.	134.	134.	134.	127.	31.	31.
29.	29.	29.	30.	30.	30.	30.	30.	30.	31.
29.	29.	29.	29.	29.	29.	29.	29.	29.	29.
28.	28.	28.	28.	29.	29.	29.	29.	29.	29.
28.	28.	28.	28.	28.	28.	28.	28.	28.	28.

MATRIX OF HEAT TRANSFER (Q) PER NODE

38.	37.	36.	35.	33.	32.	31.	30.	29.	27.
20.	21.	22.	23.	24.	25.	27.	28.	29.	30.
22.	21.	20.	19.	18.	18.	17.	16.	15.	15.
10.	11.	11.	12.	12.	13.	14.	14.	15.	16.
11.	11.	10.	10.	9.	9.	8.	8.	8.	7.
5.	5.	5.	6.	6.	6.	7.	7.	8.	8.
5.	5.	5.	5.	4.	4.	4.	4.	4.	4.
2.	2.	3.	3.	3.	3.	3.	3.	4.	4.
3.	2.	2.	2.	2.	2.	2.	2.	2.	2.
5.	5.	5.	5.	5.	5.	5.	5.	6.	5.
7.	7.	7.	7.	7.	7.	6.	7.	8.	9.
9.	9.	9.	9.	9.	9.	9.	9.	12.	12.
13.	13.	13.	13.	13.	13.	13.	13.	17.	17.
19.	19.	19.	19.	19.	19.	19.	19.	24.	24.
26.	26.	26.	26.	26.	25.	26.	27.	35.	35.
38.	38.	38.	38.	38.	38.	37.	38.	49.	49.
54.	54.	54.	54.	54.	53.	53.	54.	70.	70.
77.	77.	77.	77.	76.	76.	76.	78.	101.	101.
110.	110.	110.	110.	110.	109.	109.	103.	27.	26.
17.	18.	19.	20.	21.	22.	23.	24.	26.	27.
18.	17.	16.	16.	15.	14.	14.	13.	12.	12.
8.	8.	9.	9.	10.	10.	10.	11.	12.	12.
8.	8.	7.	7.	7.	5.	6.	6.	6.	5.

FLUID MASS FLOW RATE = 16083.8 LBM/HR
 TOTAL Q (BTU/HR) BASED ON THE Q MATRIX = 18758450.6
 Q (BTU/HR) BASED ON THE WATER/STEAM MATRIX = 18752465.6
 Q (BTU/HR) BASED ON THE GAS MATRIX = 18941260.0
 THE MINIMUM PINCH POINT = 7.8 DEGREES
 BOILING BEGINS AT 2.1 INCHES INTO NODE 10 10
 SUPERHEATING BEGINS AT 11.1 INCHES INTO NODE 19 8
 THE ISENTROPIC POWER OF THE STEAM TURBINE = 2515. HORSEPOWER


```

RUN NUMBER = 29
ENTER NUMBER OF HEAT EXCHANGER PASSES DESIRED
23
ENTER EXHAUST GAS MASS FLOW RATE (LBM/S) FOR GAS PATHS 1 THROUGH 10
1.15 3.32 4.60 7.58 17.20 17.20 7.58 4.60 3.32 1.15
ENTER GAS TEMPERATURE AT INLET (DEG F) FOR GAS PATHS 1 THROUGH 10
694. 694. 694. 694. 594. 694. 694. 694. 694. 694.
ENTER FEEDWATER INLET TEMPERATURE (DEG F)
200.0
ENTER DESIRED STEAM TEMPERATURE AT OUTLET
650.0
ENTER DESIRED STEAM PRESSURE
400.0
ENTER MINIMUM EXHAUST GAS TEMPERATURE ALLOWED AT HEAT EXCHANGER EXIT
300.0
ENTER TUBE LENGTH (FT) PER NODE
1.0
ENTER NUMBER OF TUBES PER ROW
32.0
ENTER GEOMETRIC SCALING FACTOR
1.0

```


[illegible]

MATRIX OF EXHAUST GAS TEMPERATURES

295.	345.	362.	387.	435.	435.	388.	365.	350.	309.
349.	379.	389.	406.	447.	445.	405.	386.	373.	336.
370.	396.	405.	419.	455.	455.	421.	408.	400.	380.
402.	416.	421.	431.	463.	452.	430.	419.	413.	395.
413.	425.	430.	438.	468.	468.	439.	431.	428.	419.
430.	436.	438.	444.	473.	472.	444.	437.	434.	426.
435.	440.	442.	448.	477.	476.	448.	443.	441.	438.
443.	444.	446.	451.	480.	479.	451.	445.	443.	441.
444.	445.	446.	452.	483.	482.	453.	447.	446.	445.
445.	446.	447.	453.	488.	439.	456.	448.	446.	445.
445.	446.	449.	457.	496.	498.	460.	450.	447.	445.
445.	448.	451.	461.	506.	508.	466.	454.	449.	445.
445.	450.	455.	467.	519.	521.	474.	459.	452.	446.
446.	454.	460.	476.	534.	535.	486.	466.	458.	447.
447.	460.	468.	488.	552.	555.	502.	478.	467.	449.
451.	470.	481.	505.	573.	577.	523.	496.	482.	455.
459.	487.	501.	529.	599.	604.	554.	525.	507.	468.
476.	516.	533.	561.	630.	536.	596.	569.	550.	498.
516.	565.	581.	606.	668.	675.	656.	537.	623.	566.
607.	647.	657.	669.	682.	632.	609.	655.	644.	597.
631.	663.	670.	679.	687.	687.	679.	672.	666.	640.
662.	678.	682.	686.	690.	593.	686.	681.	677.	658.
676.	686.	688.	690.	692.	693.	691.	690.	688.	682.
694.	694.	694.	694.	694.	594.	694.	694.	694.	694.

MATRIX OF OVERALL HEAT TRANSFER COEFFICIENTS

29.	41.	44.	48.	53.	54.	50.	47.	44.	31.
33.	46.	49.	54.	58.	58.	52.	48.	44.	32.
33.	46.	50.	55.	61.	61.	56.	51.	47.	33.
34.	48.	52.	57.	63.	52.	57.	52.	48.	34.
34.	49.	53.	58.	64.	64.	58.	53.	49.	34.
35.	50.	54.	59.	65.	55.	58.	53.	49.	34.
35.	50.	54.	59.	65.	65.	59.	54.	50.	35.
35.	50.	54.	59.	66.	55.	59.	54.	50.	35.
35.	50.	54.	59.	123.	174.	137.	111.	95.	52.
52.	95.	111.	137.	175.	175.	137.	111.	95.	52.
52.	95.	111.	137.	175.	175.	137.	111.	96.	52.
52.	96.	111.	137.	175.	176.	137.	112.	96.	52.
52.	96.	112.	137.	176.	176.	137.	112.	96.	52.
52.	96.	112.	137.	176.	177.	138.	112.	96.	52.
52.	96.	112.	138.	177.	177.	138.	112.	96.	52.
52.	96.	112.	138.	178.	178.	139.	112.	96.	52.
52.	96.	113.	139.	179.	179.	139.	113.	97.	53.
53.	97.	113.	139.	180.	180.	140.	114.	97.	53.
53.	98.	114.	140.	62.	32.	30.	28.	27.	22.
21.	26.	27.	28.	30.	30.	29.	28.	27.	22.
21.	26.	27.	28.	29.	29.	28.	27.	26.	21.
21.	25.	26.	28.	29.	29.	28.	27.	26.	21.
21.	25.	26.	28.	29.	29.	28.	26.	25.	21.

MATRIX OF HEAT TRANSFER (Q) PER NODE

15.	27.	30.	36.	47.	45.	31.	24.	19.	8.
6.	14.	18.	24.	37.	39.	29.	24.	22.	12.
9.	17.	19.	22.	31.	29.	18.	13.	10.	4.
3.	7.	9.	13.	23.	25.	16.	14.	12.	7.
5.	9.	10.	12.	20.	19.	9.	6.	5.	2.
1.	3.	4.	6.	15.	15.	8.	7.	6.	3.
2.	4.	4.	6.	14.	13.	4.	2.	2.	1.
0.	0.	1.	2.	11.	12.	4.	2.	2.	1.
0.	1.	1.	2.	22.	31.	6.	2.	1.	0.
0.	1.	2.	6.	36.	37.	8.	2.	1.	0.
0.	1.	3.	9.	44.	45.	11.	4.	2.	0.
0.	2.	4.	12.	52.	54.	15.	5.	3.	0.
0.	3.	6.	16.	63.	65.	21.	9.	4.	0.
0.	5.	10.	23.	76.	78.	30.	13.	7.	1.
1.	8.	15.	32.	92.	94.	41.	21.	12.	2.
2.	14.	23.	44.	111.	114.	57.	32.	21.	4.
5.	24.	36.	61.	114.	138.	80.	50.	35.	8.
11.	40.	55.	85.	162.	157.	112.	78.	60.	19.
26.	68.	87.	119.	60.	30.	25.	21.	18.	9.
7.	13.	15.	17.	21.	22.	20.	19.	19.	12.
9.	13.	14.	14.	15.	14.	12.	11.	9.	5.
4.	7.	7.	8.	10.	10.	10.	10.	9.	7.
5.	7.	7.	7.	7.	7.	6.	5.	5.	3.

FLUID MASS FLOW RATE = 15119.8 LBM/HR
 TOTAL Q (BTU/HR) BASED ON THE Q MATRIX = 17635891.5
 Q (BTU/HR) BASED ON THE WATER/STEAM MATRIX = 17628689.5
 Q (BTU/HR) BASED ON THE GAS MATRIX = 19775397.3
 THE MINIMUM PINCH POINT = 0.1 DEGREES
 BOILING BEGINS AT 5.7 INCHES INTO NODE 9 5
 SUPERHEATING BEGINS AT 2.4 INCHES INTO NODE 19 5
 THE ISENTROPIC POWER OF THE STEAM TURBINE = 2365. HORSEPOWER


```

RUN NUMBER = 33
ENTER NUMBER OF HEAT EXCHANGER PASSES DESIRED
23
ENTER EXHAUST GAS MASS FLOW RATE (LBM/S) FOR GAS PATHS 1 THROUGH 10
6.77 15.17 13.00 11.03 8.88 6.50 4.34 2.03 0.0 0.0
ENTER GAS TEMPERATURE AT INLET (DEG F) FOR GAS PATHS 1 THROUGH 10
694. 694. 694. 694. 694. 694. 694. 694. 694.
ENTER FEEDWATER INLET TEMPERATURE (DEG F)
200.0
ENTER DESIRED STEAM TEMPERATURE AT OUTLET
650.0
ENTER DESIRED STEAM PRESSURE
400.0
ENTER MINIMUM EXHAUST GAS TEMPERATURE ALLOWED AT HEAT EXCHANGER EXIT
300.0
ENTER TUBE LENGTH (FT) PER NODE
1.0
ENTER NUMBER OF TUBES PER ROW
32.0
ENTER GEOMETRIC SCALING FACTOR
1.0

```


[illegible]

MATRIX OF EXHAUST GAS TEMPERATURES

379.	430.	414.	405.	393.	378.	359.	325.	694.	694.
401.	443.	428.	419.	409.	396.	380.	351.	694.	694.
414.	452.	438.	431.	423.	414.	403.	385.	694.	694.
429.	461.	447.	440.	433.	424.	415.	400.	694.	694.
436.	468.	454.	447.	441.	435.	429.	420.	694.	694.
444.	473.	459.	453.	447.	440.	435.	428.	694.	694.
448.	478.	463.	457.	451.	446.	442.	438.	694.	694.
453.	482.	466.	460.	454.	448.	444.	441.	694.	694.
455.	485.	468.	462.	456.	450.	447.	445.	694.	694.
457.	489.	474.	467.	460.	453.	448.	445.	694.	694.
462.	499.	482.	474.	465.	457.	450.	446.	694.	694.
469.	511.	491.	482.	473.	462.	453.	446.	694.	694.
479.	525.	503.	493.	482.	469.	458.	448.	694.	694.
493.	543.	518.	507.	495.	480.	465.	451.	694.	694.
513.	566.	537.	525.	512.	495.	477.	457.	694.	694.
542.	593.	560.	549.	535.	517.	496.	468.	694.	694.
583.	626.	590.	579.	566.	548.	525.	490.	694.	694.
641.	667.	627.	619.	608.	592.	571.	531.	694.	694.
656.	675.	673.	670.	665.	657.	644.	611.	694.	694.
670.	682.	680.	678.	675.	669.	658.	633.	694.	694.
678.	686.	685.	684.	682.	679.	673.	658.	694.	694.
686.	690.	689.	689.	687.	685.	681.	671.	694.	694.
690.	692.	692.	692.	691.	691.	689.	686.	694.	694.
694.	694.	694.	694.	694.	694.	694.	694.	694.	694.

MATRIX OF OVERALL HEAT TRANSFER COEFFICIENTS

46.	51.	52.	51.	51.	49.	46.	38.	0.	0.
53.	58.	57.	55.	54.	51.	47.	38.	0.	0.
53.	59.	59.	58.	57.	54.	50.	41.	0.	0.
56.	62.	61.	60.	58.	55.	51.	41.	0.	0.
56.	63.	62.	61.	59.	57.	52.	43.	0.	0.
58.	64.	63.	62.	60.	57.	52.	43.	0.	0.
58.	64.	64.	62.	61.	58.	53.	43.	0.	0.
58.	65.	64.	63.	61.	58.	53.	43.	0.	0.
58.	77.	163.	155.	145.	129.	108.	74.	0.	0.
131.	170.	163.	155.	145.	129.	108.	74.	0.	0.
131.	170.	163.	156.	145.	129.	109.	74.	0.	0.
131.	171.	164.	156.	145.	129.	109.	74.	0.	0.
132.	171.	164.	156.	145.	129.	109.	74.	0.	0.
132.	172.	165.	157.	146.	130.	109.	74.	0.	0.
132.	173.	165.	157.	146.	130.	109.	74.	0.	0.
133.	174.	166.	158.	147.	130.	109.	74.	0.	0.
134.	175.	167.	159.	148.	131.	110.	74.	0.	0.
30.	32.	165.	160.	149.	132.	111.	75.	0.	0.
30.	31.	30.	30.	29.	29.	27.	24.	0.	0.
28.	29.	29.	29.	29.	29.	27.	24.	0.	0.
28.	29.	29.	29.	28.	27.	26.	24.	0.	0.
27.	29.	29.	28.	28.	27.	26.	24.	0.	0.
27.	29.	29.	28.	28.	27.	26.	24.	0.	0.

MATRIX OF HEAT TRANSFER (Q) PER NODE

37.	48.	43.	39.	34.	29.	22.	13.	0.	0.
22.	35.	33.	32.	31.	28.	25.	17.	0.	0.
24.	34.	28.	25.	21.	17.	13.	7.	0.	0.
12.	23.	20.	19.	18.	15.	14.	10.	0.	0.
14.	22.	17.	14.	12.	9.	7.	4.	0.	0.
7.	16.	12.	11.	10.	9.	7.	5.	0.	0.
7.	15.	10.	8.	6.	4.	3.	1.	0.	0.
3.	12.	8.	7.	5.	4.	3.	2.	0.	0.
3.	14.	19.	14.	9.	4.	1.	0.	0.	0.
8.	37.	24.	18.	12.	6.	2.	0.	0.	0.
12.	45.	30.	23.	16.	8.	3.	0.	0.	0.
17.	55.	38.	30.	21.	12.	5.	1.	0.	0.
24.	68.	48.	38.	28.	17.	8.	2.	0.	0.
34.	83.	60.	49.	38.	24.	13.	3.	0.	0.
48.	102.	75.	64.	51.	35.	20.	6.	0.	0.
69.	126.	95.	83.	68.	50.	31.	11.	0.	0.
98.	155.	120.	108.	93.	72.	49.	21.	0.	0.
24.	30.	149.	140.	125.	104.	78.	40.	0.	0.
25.	27.	25.	21.	21.	19.	16.	11.	0.	0.
13.	16.	16.	17.	17.	17.	16.	13.	0.	0.
13.	14.	13.	12.	11.	10.	9.	7.	0.	0.
7.	8.	8.	9.	9.	9.	9.	8.	0.	0.
7.	7.	7.	6.	6.	6.	5.	4.	0.	0.

FLUID MASS FLOW RATE = 15200.8 LBM/HR
 TOTAL Q (BTU/HR) BASED ON THE Q MATRIX = 17727478.0
 Q (BTU/HR) BASED ON THE WATER/STEAM MATRIX = 17721859.0
 Q (BTU/HR) BASED ON THE GAS MATRIX = 15014392.6
 THE MINIMUM PINCH POINT = 0.5 DEGREES
 BOILING BEGINS AT 10.6 INCHES INTO NODE 9 2
 SUPERHEATING BEGINS AT 11.8 INCHES INTO NODE 18 3
 THE ISENTROPIC POWER OF THE STEAM TURBINE = 2377. HORSEPOWER

LIST OF REFERENCES

1. Halkola, J.T., Cambell, A.H. and Jung, D., "Racer Conceptual Design," ASME Paper No. 83-GT-50.
2. Mattson, W.S., "Designing Reliability and Maintainability into the Racer System," Naval Engineers Journal, v. 95, no. 3, May 1983.
3. Combs, R.M., Waste Heat Recovery Unit Design for Gas Turbine Propulsion Systems, Master's Thesis, Naval Postgraduate School, September 1979.
4. Shu, H.T. and Kuo, S.C., "Flow Distribution Control Characteristics in Marine Gas Turbine Waste-Heat Steam Generators," United Technologies Research Center, Annual Technical Report, No. R82-955750-4, July 1982.
5. Weirman, C., Taborak, J., and Marner, W.J., Comparison of Inline and Staggered Banks of Tubes with Segmented Fins, paper presented at the Fifteenth National Heat Transfer Conference AIChE-ASME, San Francisco, California, 1975.
6. Incropera, F.P. and DeWitt, D.P., Fundamentals of Heat Transfer, John Wiley and Sons, Inc., 1981.
7. Tong, L.C., Boiling Heat Transfer and Two-Phase Flow, John Wiley and Sons, Inc., 1965.
8. General Electric Company, Performance Data for the General Electric LM2500 Gas Turbine Engine, MID-TD-2500-8, Revised November 1978.

INITIAL DISTRIBUTION LIST

	No. Copies
1. Defense Technical Information Center Cameron Station Alexandria, Virginia 22314	2
2. Library, Code 0142 Naval Postgraduate School Monterey, California 93943	2
3. Department Chairman, Code 69 Department of Mechanical Engineering Naval Postgraduate School Monterey, California 93943	1
4. Professor Paul F. Pucci, Code 69Pc Department of Mechanical Engineering Naval Postgraduate School Monterey, California 93943	5
5. LCDR S.L. Wesco c/o Mike Smith 1383 Barnhart Road Troy, Ohio 45373	3
6. LCDR J.S. Pine Executive Officer U.S.S. Oldendorf DD-972 F.P.O. San Francisco, California 96674	1
7. Donald Tempesco Code SEA 56X3 Naval Sea Systems Command Washington, D.C. 20362	2
8. Dr. Keith Ellingsworth Office of Naval Research 800 Quincy St. Arlington, VA 22217	1

T Thesis
W W474
c c.1

202570

Wesco

An improved model for
a once-through counter-
cross-flow waste heat
recovery unit.

Thesis
W474
c.1

202570

Wesco

An improved model for
a once-through counter-
cross-flow waste heat
recovery unit.

thesW474

An improved model for a once-through cou



3 2768 001 95002 5

DUDLEY KNOX LIBRARY